Doctor Dissertation

Study of Group Combustion Excitation in Randomly Distributed Droplet Clouds Using Percolation Approach Based on Flame-spread Characteristics in Microgravity

(微小重力場における燃え広がり特性に基づいたパーコレーション手法によるランダム分散液滴群の群燃焼発現に関する研究)

September, 2015

HERMAN SAPUTRO

Graduate School of Science and Engineering
Yamaguchi University

Abstract

In this dissertation, a study of group combustion excitation in randomly distributed droplet clouds using percolation approach based on flame-spread characteristics in microgravity is presented.

One of the most important issues in spray combustion science is how to understanding the mechanism of the group combustion of liquid fuel spray, especially the excitation mechanism of the group combustion and the role of fuel droplets in it. The group combustion is required in stable spray combustion. Flame spread among fuel droplets plays an important role in excitation of the group combustion. The investigation on the flame-spread phenomenon has been performed in a simplified system of fuel droplets. Experiments of flame-spread of fuel droplets have been performed in microgravity actively. However, the experiment has limitation in the number of droplets due to relatively short microgravity durations in the ground based facilities. It is difficult to conduct flame spread experiments of large scale droplet clouds in microgravity.

This study has simulated the flame-spread behavior in randomly distributed large-scale droplet clouds with a low-volatility fuel equal size droplets and group combustion excitation by using a percolation approach. This study created a percolation model based on so-called "Mode 3" flame-spread with paying attention to the flame-spread limit distance $(S/d_0)_{limit}$ which was obtained in microgravity experiment of flame-spread droplet array and droplet cloud element with n-decane as a fuel. The simulation applies a simple flame-spread rule that the flame can spread to droplets existing within the flame-spread limit distance $(S/d_0)_{limit}$, which varies with the flame-spread direction and droplet interaction. Therefore, the study is classified as follows: 1) Simulating flame-spread behavior of randomly distributed droplet clouds without considering droplet interaction. These simulations were created based on microgravity experimental results of evenly spaced droplet array. 2) Simulating flame-spread behavior of randomly distributed droplet clouds considering two-droplet interaction. This simulation was created based on microgravity experiments of droplet-cloud elements.

The percolation theory describes macroscopic connection characteristics in randomly distributed particle cloud with near field connection rule. When the percolation theory is applied to fuel spray combustion, the droplet is characterized as the particle. The flame spread rule between droplets is characterized as the connection rule. Droplets are arranged at lattice points in two-dimensional (2D) lattice or three-dimensional (3D) lattice. The group combustion of droplet cloud is defined to appear if the flame starting from a side in 2D droplet arrangements and a face in 3D droplet arrangements reaches the other sides in 2D droplet arrangements and the other faces in 3D droplet arrangements.

Mean droplet spacing $(S/d_0)_m$ of droplet cloud, lattice size NL/d_0 and lattice point interval L/d_0 were varied in order to investigate their effects on the occurrence probability of group combustion (OPGC) and the flame-spread behavior in large-scale droplet clouds. $(S/d_0)_m$ for 0.5 OPGC is defined as the critical mean droplet spacing $(S/d_0)_{critical}$, which separates the droplet cloud into two groups if the lattice size becomes infinity; relatively dense droplet clouds in which the group combustion is excited through flame spread and dilute droplet clouds in which the group combustion is never excited.

The main conclusions of flame-spread simulation of randomly distributed droplet clouds without and with considering two-droplet interaction are as follows:

1. The occurrence probability of group combustion, OPGC, rapidly decreases around the critical mean droplet spacing $(S/d_0)_{critical}$ as the mean droplet spacing $(S/d_0)_m$ is increased. When the lattice size, NL/d_0, is increased, the OPGC graph approaches a step function in which OPGC is unity for $(S/d_0)_m$ less than the threshold value and zero for $(S/d_0)_m$ greater than the threshold value, and the critical mean droplet spacing $(S/d_0)_{critical}$ approaches the threshold value.
2. $(S/d_0)_{critical}$ is affected by the ambient temperature and pressure. $(S/d_0)_{critical}$ is greater at higher temperature and at lower pressure.
3. $(S/d_0)_{critical}$ in 3D droplet arrangement is greater than that in 2D droplet arrangement.

4. The $(S/d_0)_{critical}$ considering two-droplet interaction is higher than that without considering two-droplets interaction. The effect of two-droplet interaction on $(S/d_0)_{critical}$ in 2D droplet arrangements is almost similar to that in 3D droplet arrangements.
5. Even when the group combustion occurs, a portion of the droplets remains unburned. The number of unburned droplets attains maximum for the mean droplet spacing slightly greater than the critical mean droplet spacing.

The ignition time of the last burned droplet has a wide range of values, and the averaged ignition time attains maximum around the critical mean droplet spacing, showing the characteristic time of flame spread in randomly distributed droplet cloud attains maximum. Thus, the flame spread rate over the droplet cloud also has a wide range of values around the critical mean droplet spacing

CONTENTS

Chapter 1

Introduction

In this chapter, the background, related works, the motivation, the problem statement and target of the research about the simulating flame-spread behavior in large scale of randomly distributed droplet cloud by using percolation approach are introduced.

1.1 Background

Combustion of liquid fuels plays a significant part in providing major portion of world energy supply, such as in the spray combustion engine. The spray combustion technology has been widely used in direct-injection gasoline engines, diesel engines, gas turbine, jet engines, industrial furnace and boiler. Therefore, the consumptions of liquid fuel are predicted increases every year as shown in Fig 1.1. It is obvious that maximizing the efficiency of combustion processes and clean combustion system are important.

The spray combustion process may approach the non-premixed flame model or the premixed flame model, according to how much fuel-and-air mixing exists before burning. In most of spray combustion engine, liquid fuel is mixed with the oxidizer, ignition and burned in the form of droplet spray. Spray of fuel in the combustion chamber has two phase flow involving a liquid as a dispersed or discrete phase in the form of droplet and gas as the continuous phase. Spray combustion can be divided into three zones; the spray formation zone, the vaporization zone, and the combustion zone. When liquid fuel is injected into a combustion chamber, it undergoes atomization which causes the liquid to break up into a large number of droplets in various sizes and velocities. Therefore, in the combustion engine utilize liquid fuel spray in order to increase the fuel surface area and thus increase the vaporization and combustion rate. In order to design an efficient and clean combustion system is needed the knowledge about the flame spread of droplet combustion.

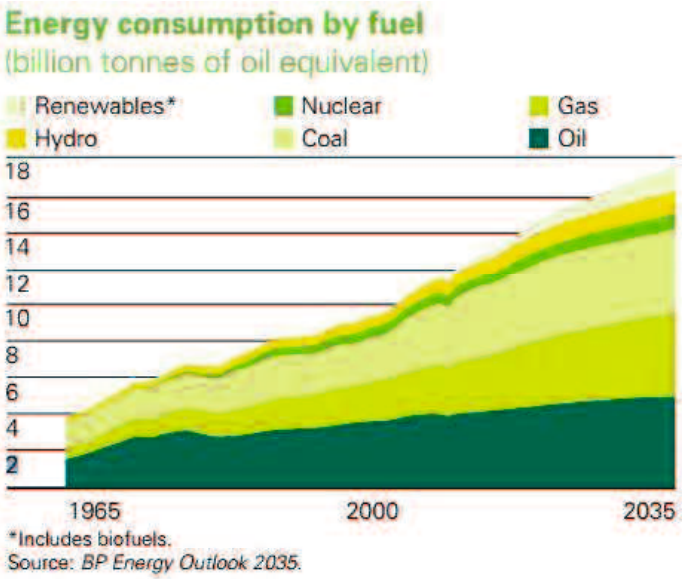

Figure 1.1 World energy consumption
(British Petroleum annual report and form 20-F 2014)

One of the most important issues in spray combustion science is how to understand the mechanism of the combustion of liquid fuel spray, especially in the flame-spread phenomenon. In spray combustion, the existence of group combustion is very important in order to obtain the stable combustion. The group combustion is burning state with a merged flame or group flame, wherein inside of flame surrounds many burned droplets. Therefore, the flame spread among fuel droplets affects the occurrence of stable combustion in the spray combustion engine.

Since the flame spread among fuel droplets plays an important role in the occurrence of stable combustion, some researchers have made efforts to study details of that phenomenon. The investigation into the flame spread phenomenon has been performed in a simplified system of fuel droplet. However, it is difficult to create the droplets size similar in the real sprays. The latest experiment in the suspended-droplet technique by Mikami et al., 2005 could generate droplets size 0.3 to 1.5 mm in normal gravity, whereas in practical combustion processes, fuel droplet sizes are very small (under 50 microns). When the droplet size is very

small, the gravitational effect and buoyancy effect on processes around each droplet are negligible and the flame shape is spheres even though in normal gravity. On the other hand, when the droplets size are larger than those in real sprays is burned in normal gravity, the gravitational effect and buoyancy effect influence to the processes around each droplet. The buoyancy effect destroyed the spherical symmetry of flame shape.

In order to understanding and prediction of spray combustion behavior, it is essential to clarify the flame spread mechanism of fuel droplets by using microgravity environment, which enables employment of relatively larger droplets than those in real sprays. The experiment of droplet combustion was conducted in the microgravity in order to avoid the influence of natural convection or buoyancy effect on the burning droplets (Fig 1.2 and 1.3). The microgravity environment is needed because with the absence of gravity simplifies the study of controlling the basic phenomenon of spray combustion and verification of theoretical models of spray combustion.

The first experiment of single droplet combustion in microgravity was conducted by Kumagai and Isoda over half century ago (1957) using drop-tower facilities. Since Kumagi and Isoda, 1957 find techniques to overcome buoyancy effect, the experiments on microgravity of droplet combustion widespread. The experiment of microgravity droplet combustion is not only on the single droplet combustion but also the multiple-droplet combustion, such as two droplets, droplet array and droplet cloud. Experiments of flame-spread of fuel droplet combustion have been performed in microgravity actively. This is making efforts to link knowledge from droplet combustion to elucidation of spray combustion mechanisms. However, the experiment has a limitation in the number of droplets due to relatively short microgravity durations in the ground-based facilities. Therefore, it is difficult to conduct flame spread experiments of large-scale droplet clouds in microgravity.

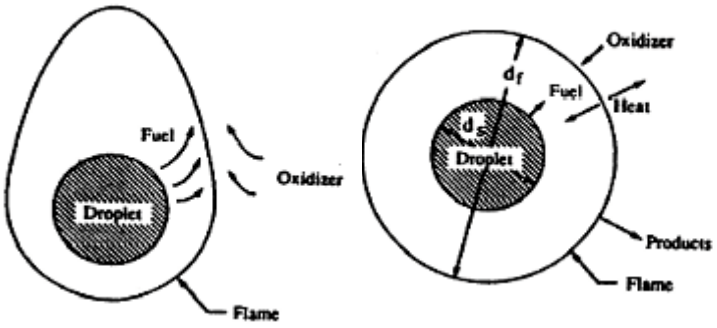

a. Normal gravity b. microgravity

Figure 1.2 Schematic of droplet envelope flame at normal gravity and microgravity (Law and Faeth, 1994)

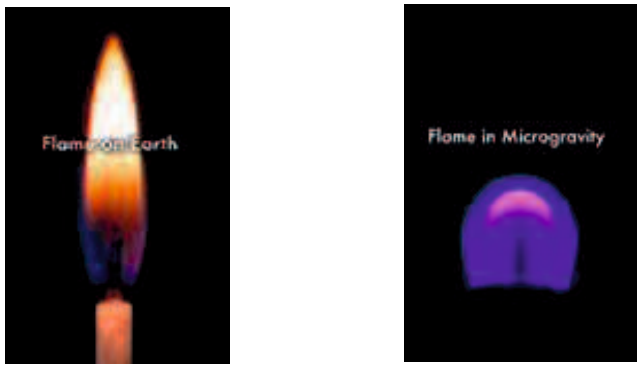

a. Normal gravity b. microgravity

Figure 1.3 The comparison between combustion in normal gravity and microgravity environment (NASA Digital libraries)

In order to make a theoretical link the gap between droplet combustion and spray combustion, some researchers have applied percolation theory to flame spread in the randomly distributed droplet cloud such as Umemura and Takamori, 2005; and Oyagi et al., 2009. Percolation theory possibly gives knowledge to the limit of the equivalence ratio over which group combustion of fuel can appear, which is important practically. Umemura and Takamori, 2005 performed flame spread calculation using percolation theory at randomly distributed droplet cloud based on so-called “Mode 1” flame spread. On the other hand, the experimental results on the flame-spread of droplet combustion show that the flame-spread

occurs not only on Mode 1 but also on Mode 2 and Mode 3 as reported by Mikami et al., 2005 and 2006. Therefore, is needed simulation of flame-spread behavior, which is not only considered the flame spread with small droplet spacing (Mode 1 flame spread) but also considering the real condition of flame-spread droplet combustion.

Flame-spread modes of linear droplet array could be described as follows (Fig. 1.4) (Mikami et al., 2006): the "Mode 1" flame spread, the vaporization of the next droplet is activated after the leading edge of an expanding group diffusion flame passes the next droplet and pushes the leading edge forward. "Mode 2" flame spread, the leading edge of the diffusion flame reaches the flammable mixture layer formed around the next droplet and the premixed flame propagates in the mixture layer to form the diffusion flame around the next droplet. "Mode 3" flame spread, the next droplet auto ignites through heating by the diffusion flame, whose leading edge does not reach the flammable-mixture layer around the next droplet. "Premixed flame propagation mode", the flame propagates in a continuous flammable-mixture layer formed around the droplet array. "Vaporization mode", the flame spread does not occur.

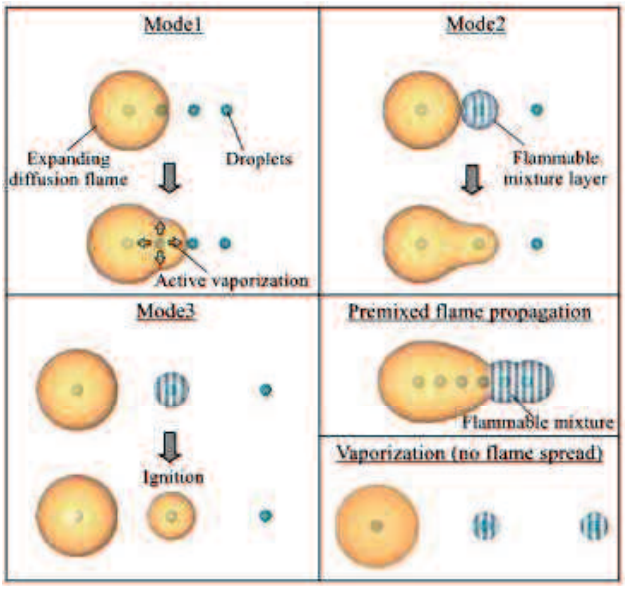

Figure 1.4 Flame-spread modes of linear droplet arrays (Mikami et al., 2006).

Oyagi et.al (2009) performed one-dimensional flame spread calculation based on “Mode 3” flame spread of droplet array and considering flame-spread-limit distance $(S/d_0)_{\text{limit}}$. This finding is relevant to flame spread with large droplet spacing (S/d_0), but limited on one-dimensional of flame spread behavior.

In this simulation, the flame-spread behavior and group combustion excitation at randomly distributed droplet clouds was studied by using a percolation approach. This study extends the percolation model by Oyagi et al. (2009). This study simulate the flame-spread based on “Mode 3” flame spread by (2009) and paying attention to $(S/d_0)_{limit}$ obtained in microgravity experiments of flame spread droplet array (Mikami et al., 2005, Mikami et al., 2006 and Mikami et al., 2014) and flame-spread droplet-cloud elements (Mikami et al., 2013). This simulation applies a simple flame-spread rule that the flame can spread to droplets existing within the flame-spread distance $(S/d_0)_{limit}$. The droplets were arranged randomly at lattice points in two-dimensional (2D) lattice or three-dimensional (3D) lattice.

1.2 Related Works

Many researchers have conducted an experiment on single droplet and multiple droplet combustion in microgravity and small-scale condition. Researchers produced many inventions in experiment of microgravity droplet combustion that provide a fundamental basis for understanding spray combustion behavior. Their inventions are reviewed here.

In 1957, Kumagi and Isoda recognized that the removal of buoyant transport through free fall in a droplet tower facility. These experiment demonstrated that the quantitative prediction of early theories of the burning rate, flame standoff ratio and flame temperature were in error. Isoda and Kumagi, 1958 and Kumagi et al., 1971 performed the isolated droplet combustion experiment of n-heptane fuel in microgravity shows that in microgravity the flame was spherically symmetric and the droplet diameter squared (d^2) measurement displayed a linear profile but the burning rate was lower than the theoretical prediction of d^2-law. Therefore, d^2-law or the droplet diameter squared decreases linearly with increasing time is

established but the burning rate and standoff ratio are not valid. The flame standoff is defined as the flame diameter divided by the droplet diameter. Therefore, by the Kumagi's research series, the needs for improved theoretical description of spherically symmetric droplet combustion was described clearly.

The research in individual droplet behavior, such as droplet ignition, droplet evaporation and combustion has long been recognized as an important component of developing a better understanding of spray combustion processes. The researchers that have performed in individual droplet combustion such as: Feath, 1977; Williams, 1981; Law 1982; Sato et al., 1990; and Hara and Kumagai, 1994. The continuation research on the individual droplet is multiple-droplet combustion, which study the interactions of arrays or clouds of burning droplets in different spacing to link isolated droplet results to the combustion of spray. The experiment on the multiple-droplet combustion such as: 1) Study on two droplet combustion (Mikami et al., 1994; Mikami et al, 1998 and Imamura et al., 2006); 2) study on droplet array combustion (Miyasaka and Law, 1981; Kato et al., 1998; Kobayashi et al., 2002; Mikami et al., 2005; Mikami has et al., 2006; Oyagi et al., 2015; Mikami, at al., 2014 and Sirignano, W.A, 2014).

Mikami et al., 2005 demonstrated the flame spread along a linear array using a new technique for generating droplets. These linear array experiments have addressed the unsteady ignition and flame spread problem, where as existing theory has addressed the quasi steady burning (Chiu et al., 1982). Therefore, comparisons between the results of these studies cannot be done. However, a clear dependence on droplet spacing is found; there is a maximum distance at certain droplet spacing or flame-spread limit distance $(S/d_0)_{limit}$ over which the flame cannot spread to the next droplet. The flame-spread limit distance $(S/d_0)_{limit}$ of evenly spaced droplet array at normal pressure (101kPa) and room temperature (300^oK) is 14.

Mikami et al., 2006 also investigated the unsteady ignition and flame-spread of the droplet array at normal pressure and high temperature (600^oK). This study reported that the flame-spread limit droplet spacing was affected by the ambient temperature. The flame-spread limit distance at high temperatures is higher than at

room temperature. The flame-spread limit distance $(S/d_0)_{limit}$ at normal pressure and high temperature is 17. This study is not only studied on flame-spread limit distance between droplets but also study the flame-spread mode, flame-spread rate and group combustion of droplet array depending on the droplet spacing and temperature, as shown in Fig. 1.5. The burning mode with a merged flame is identified as group combustion. In fuel spray combustion engine, group combustion is necessary in order to obtain a stable flame in combustor chamber. These experimental results shows that the transition from the individual flame (individual combustion) to the merged flame (group combustion) or reverse case within the range of inter droplet spacing, as shown in Fig. 1.5. The group combustion on Mikami et al., 2006 is different from existing theory by Chiu et al., 1982 (Fig. 1.6), because the existing theory used quasi steady condition and Mikami et al., used unsteady condition.

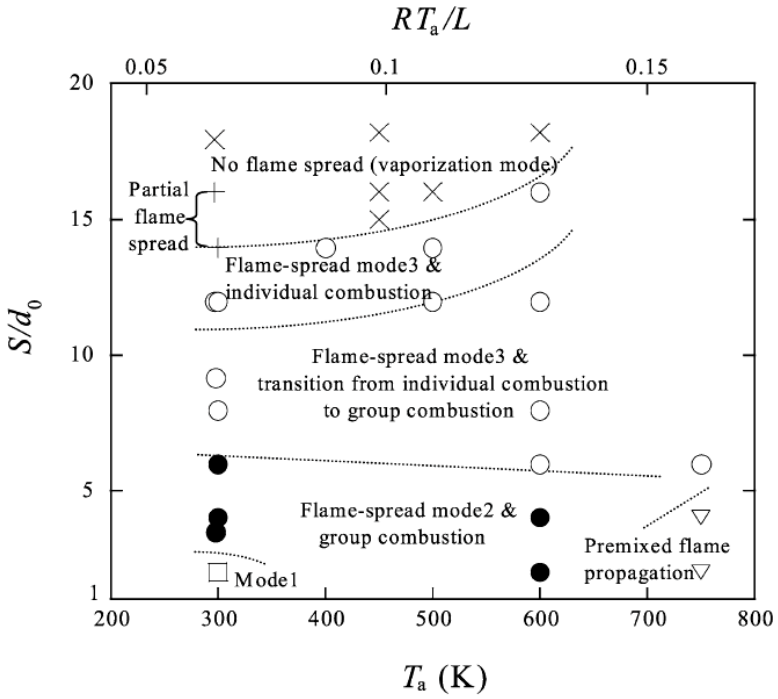

Figure 1.5 Mode map for flame-spread and burning of n-decane droplet array (Mikami et al., 2006)

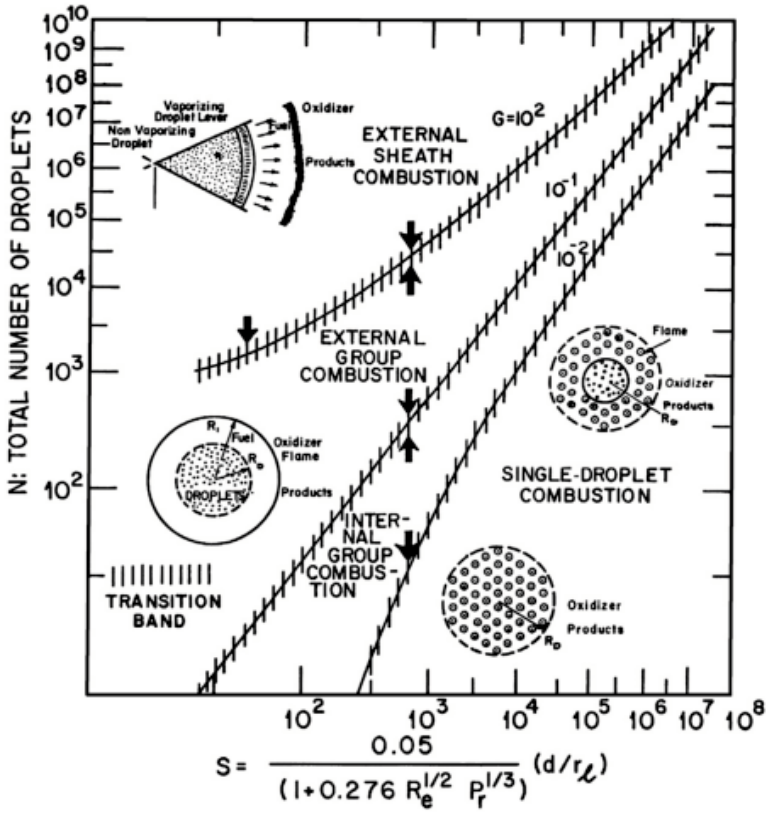

Figure 1.6 Four group combustion modes of a droplet cloud (Chiu et al., 1982)

In order to improve the understanding of flame-spread in fuel spray engine at high attitude (low pressure), Mikami et al, 2014 performed microgravity experiment of flame-spread over n-decane fuel droplet array at low pressure (25kPa) and room temperature (300^{o}K). The result shows that the flame-spread limit distance was affected by the pressure condition. The flame-spread limit distance $(S/d_0)_{limit}$ at low pressure and room temperature is 20.

Oyagi et al., 2009 conducted microgravity experiment of droplet combustion to investigate the flame-spread limit distance of an unevenly spaced n-decane droplet array at normal pressure and room temperature. They reported that if the droplet spacing is small enough, the droplet interaction becomes significant and increases the flame spread-limit distance $(S/d_0)_{limit}$. They also studied the comparison between the flame-spread limit distance by two-droplet

interaction and three-droplet interaction. The result shows that the three-droplet interaction has a minor effect on the flame spread probability.

Mikami et al., 2013 continued the Oyagi's experiment with performed microgravity experiments of an unevenly spaced droplet-cloud element. Their results show that the flame-spread limit distance $(S/d_0)_{limit}$ increases with two-droplet interaction. The flame-spread limit distance is approximated as $2^{1/3}$ times the flame-spread limit distance $(S/d_0)_{limit}$ without droplet interaction measured from midpoint of two adjacent burned droplet. Therefore, by the experimental results of Mikami et al., 2013 could be understood the correlation between the experimental results of flame-spread droplet array (without considering droplet interaction) and flame-spread of droplet-cloud element (considering droplet interaction).

By a series of Mikami's research, the flame-spread behavior of fuel droplet combustion and excitation of group combustion becomes clearly to understand. However, these experiments cannot elucidate the flame-spread and group combustion in large scale of combustion, because droplet combustion experiments have a limitation in the number of droplets due to relatively short microgravity duration in the ground-based facilities.

In this study, the experimental results of microgravity droplet combustion will be used as basic assumption to generate microgravity combustion in large scale of randomly distributed droplet clouds. The numerical simulation of flame-spread behavior and group combustion excitation in large scale of microgravity droplet combustion was created by using percolation theory approach. This research will make it possible to bridge theoretically between the droplet combustion and the spray combustion, giving a high impact on the academic field combustion science.

1.3 Motivation

The phenomenon of liquid fuel spray combustion has not been completely clarified due to the complicated phenomenon in which many processes such as liquid atomization, droplet dispersion in the gas phase, vaporization and chemical reaction, which simultaneously proceed with interaction. Therefore, the combustion of liquid fuel spray is one of the most important issues in combustion science. In the spray combustion engine, the group combustion is necessary to attain a stable flame in combustors. The group combustion will be formed because the flame spread among fuel droplets.

In order to understanding the spray combustion behavior, it is importance to clarify flame spread and group combustion excitation mechanism of fuel droplets. Although the droplet combustion research provides a fundamental basis for understanding spray combustion behavior, the flame spread and group combustion excitation mechanism have not yet well elucidated. This research attempts to make a connection between droplet combustion and spray combustion research by using “percolation approach”. This study is very important because this study will improve understanding of flame-spread modeling for better prediction of spray combustion in efficient engines and help us to deal better with the problems of pollutants, atmospheric change and global warming. It is very important to conserve energy and reduces pollution.

1.4 Problem Statement and Target

Problem statement:

Experiments of flame-spread mechanism of fuel droplet combustion have been performed actively. However, the experiment of microgravity droplet combustion has a limitation in the number of droplets due to relatively short microgravity durations in the ground-based facilities. It is difficult to conduct flame spread experiments of large scale droplet clouds in microgravity. Therefore, the results of microgravity droplet combustion experiment have not elucidated the flame-spread behavior in large scale.

Target of research:

The target of this research is “How to elucidate the flame spread and group combustion excitation mechanism in randomly-distributed droplet clouds by numerical simulation using percolation approach, based on Mode 3 flame-spread in 2D and 3D droplet arrangements with a low-volatility fuel and equal size droplets”.

1.5 Outline

In this dissertation, the contents of the research about “Study of Group Combustion Excitation in Randomly Distributed Droplet Clouds Using Percolation Approach Based on Flame-spread Characteristics in Microgravity” in this doctoral course are organized into five chapters summarized as follows:

This Chapter 1 is the introduction of research. In this chapter, the background of research, related works, the motivation, the problem statement and target are introduced.

In Chapter 2, Percolation approach for simulation of flame-spread behavior and group combustion excitation in randomly distributed droplet clouds are provided. The basic theory of percolation, percolation theory for flame-spread in fuel spray, Flame-spread limit distance distribution, and the calculation procedure are explained to give the understanding of the research.

In Chapter 3, Simulating flame-spread behavior of randomly distributed droplet clouds without considering droplet interaction are explained. Simulation based on the flame-spread characteristic of droplet array in normal pressure (101kPa) and room temperature (300^{o}K), Simulation based on the flame-spread characteristic of droplet array in normal pressure (101kPa) and high temperature (600^{o}K), and Simulation based on the flame-spread characteristic of droplet array in low pressure (25kPa) and room temperature (300^{o}K) are discussed in detail.

In Chapter 4, Simulating flame-spread behavior of randomly distributed droplet clouds with considering two-droplet interaction are explained. Simulation based on the flame-spread characteristic of droplet-clouds element in normal pressure (101kPa) and room temperature (300^{o}K) is discussed in detail.

Finally, in Chapter 5, The conclusions about simulation of flame-spread behavior and group combustion excitation in randomly distributed droplet clouds provided and also the further scope for future work is discussed.

Chapter 2

Percolation approach for Simulation of Flame-spread behavior and Group Combustion Excitation in Randomly Distributed Droplet Clouds

2.1 Basic theory of percolation

Percolation is a branch of probability theory and part of a general framework of statistical theory that deal with structural and transport properties of random media. Percolation theory was developed by Broadbent and Hammersley in 1957. Percolation is a very general phenomenon applicable in almost every area of science as the simplest model for spatial disorder.

Many properties of a macroscopic system are essentially determined by the connectivity of the system element. The properties of a system which emerge at the onset of macroscopic connectivity within it are known as percolation properties (Berkowitz and Ewing, 1998).

The percolation theory describes particle connection characteristic in randomly distributed particles. In site percolation, if particles are in adjacent distance, the particle will be connected as a cluster. When the cluster connects from the bottom side to the other sides of the lattice, it forms a large cluster or percolation cluster, as shown in Fig. 2.1.

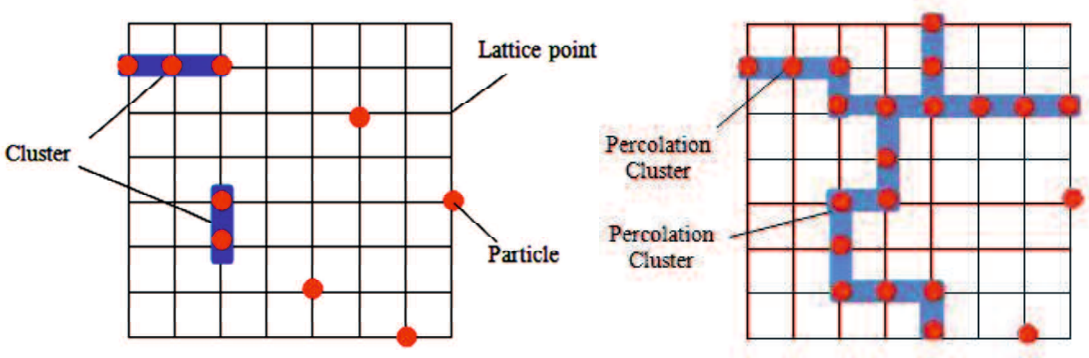

Figure 2.1 Particle and cluster in site percolation

While performing simulation with percolation model one observes a percolation threshold, because it has hope that the universal behavior near the percolation threshold could be used to guide understanding of real physical system, (for example: Berkowitz and Balberg, 1993; Sahimi, 1994; and Hunt, 2005). As the particles are randomly arranged at lattice point (N) and the ratio of the particles number to the lattice point is defined as the occupation fraction (p). In order to observe a percolation threshold, could be used increasing the occupation fraction (p) and the lattice size. Since it is a small lattice size, the graph of occurrence probability of large cluster (percolation cluster) versus occupation fraction (p) is not completely sharp. When the lattice size is increased to infinite the graph of occurrence probability of large cluster (percolation cluster) versus occupation fraction (p) becomes sharper and finds a step function behavior, as shown in Fig. 2.2. From the series of simulations with increasing lattice size, it is also possible to determine the exact position of the percolation threshold, namely (p_c).

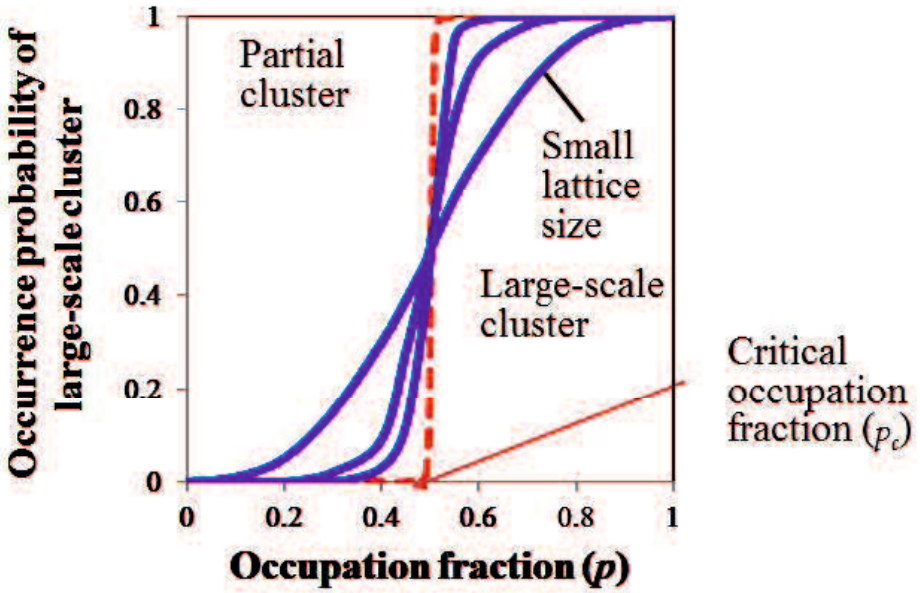

Figure 2.2 The occurrence probability of large scale cluster as function of the occupation fraction (p) for different lattice size.

The percolation threshold is a characteristic value for given type of lattice. For different lattices different percolation threshold are found. Table 2.1 shows values for some lattice type.

Table 2.1 Percolation threshold for different lattices (Torquato, 2013)

lattice	**Dimention**	p_c **(site percolation)**	p_c **(bond percolation)**
	1	1	1
square	2	0.592746	0.50000*
honeycomb	2	0.6962	0.65271*
triangular	2	0.50000*	0.34729*
cubic (simple)	3	0.3116	0.2488
cubic (body-centered)	3	0.246	0.1803
cubic (face-centered)	3	0.198	0.119
diamond	3	0.43	0.388
4-hypercubic	3	0.197	0.1601
5-hypercubic	3	0.141	0.1182
6-hypercubic	3	0.107	0.0942
7-hypercubic	3	0.089	0.0787

2.2 Percolation theory for flame-spread in fuel spray

As shown in Fig 2.3, the flame-spread on the spray combustion show the percolation properties, which is flame-spread from burned droplets to next droplets shows a macroscopic connectivity. Percolation theory as defined the rule of particle connection that describes the characteristic of macroscopic connection in a randomly distributed particle cloud. Thus, when the percolation theory is applied in the flame-spread of fuel spray combustion, the definition of percolation theory turned into the rule of flame-spread that describes the behavior of macroscopic group combustion in a randomly distributed droplet cloud.

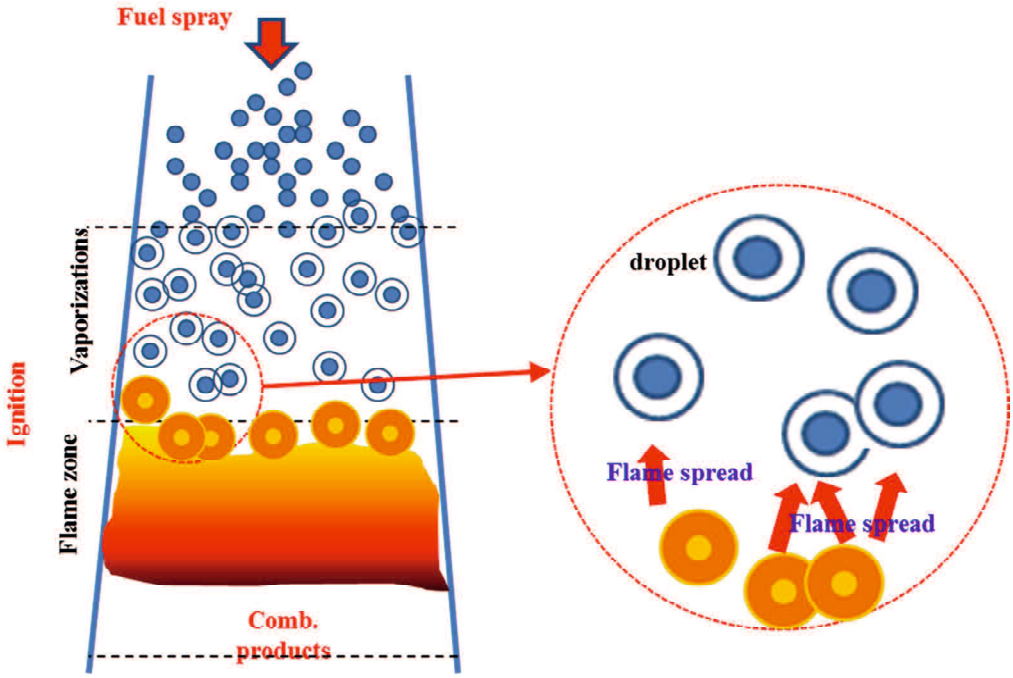

Figure 2.3 Flame-spread of fuel spray combustion

Droplet is characterized as the particle, when the percolation theory is applied to fuel spray combustion. The flame-spread between droplets is characterized as the connection. Hence, the inter particle distance or droplet spacing (S/d_0) has an important role in the flame-spread. Mikami et al., 2006 reported that there is a maximum distance or certain droplet spacing or flame-spread limit $(S/d_0)_{\text{limit}}$ over which the flame cannot spread to the next droplets, as explained in the chapter 1.

This study created percolation modeling based on "Mode 3" flame-spread with paying attention to the flame-spread limit distance $(S/d_0)_{\text{limit}}$ which was obtained in microgravity experiment of flame-spread droplet array and droplet cloud element with n-decane as a fuel. Therefore, flame will spread to next droplets which is the droplets spacing under $(S/d_0)_{\text{limit}}$, but flame cannot spread to the next droplets over the $(S/d_0)_{limit}$.

In this study, in order to study the group combustion excitation in large scale of randomly distributed droplet clouds could be classified as follows:

a. Simulating flame-spread behavior of randomly distributed droplet clouds without considering droplet interaction. These simulation was created based on microgravity experimental results of evenly spaced droplet array at this following condition:
   1) Normal pressure (101kPa) and room temperature (300^{o}K) (Mikami et al., 2005).
   2) Normal pressure (101kPa) and high temperature (600^{o}K) (Mikami et al., 2006).
   3) Low pressure (25kPa) and room temperature (300^{o}K) (Mikami et al., 2014).
b. Simulating flame-spread behavior of randomly distributed droplet clouds with considering two-droplet interaction. This simulation was created based on microgravity experiments of droplet clouds element (Mikami et al., 2013).

2.3 Flame-spread limit distance distribution

The flame-spread limit distance $(S/d_0)_{\text{limit}}$ plays an important role on the flame-spread connection between burned droplet to next droplets on the lattice. This following will be explained the flame-spread limit distance distribution for each simulation condition.

2.3.1 The simulation of flame-spread behavior without considering droplet interaction at normal pressure (101kPa) and room temperature (300^{o}K)

As explained in the chapter 1.2 that the flame-spread limit distance $(S/d_0)_{\text{limit}}$ for droplet array experimental results in normal pressure (101kPa) and room temperature (300^{o}K) is 14, as shown in Fig. 2.4. The simulation parameters are taken from microgravity experimental results such as: flame-spread limit distance $(S/d_0)_{limit}$ =14 and flame-spread time (t_f/d_0^2) or flame-spread rate $(V_f d_0)$. Therefore, by using Fig. 2.4 could be derived into flame-spread limit distribution for

simulation of flame-spread behavior in normal pressure (101kPa) and room temperature (300°K), as shown in Fig.2.5.

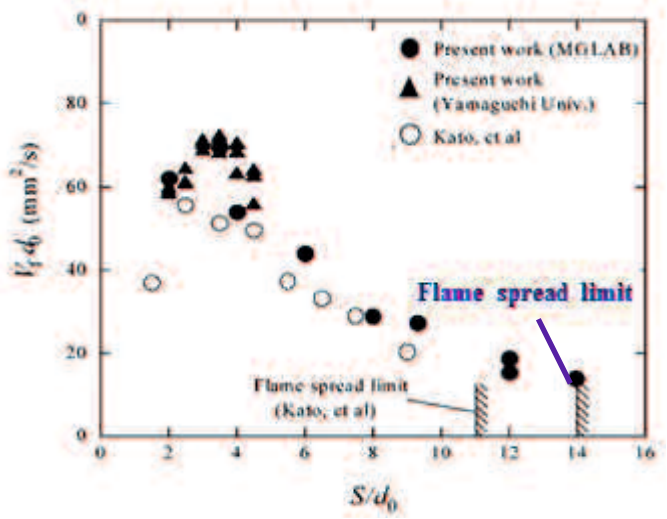

Figure 2.4 Flame-spread limit distance $(S/d_0)_{\text{limit}}$ and flame-spread rate $(V_f d_0)$ obtained from microgravity experiment at normal pressure (101kPa) and room temperature (300°K) (Mikami et al., 2005)

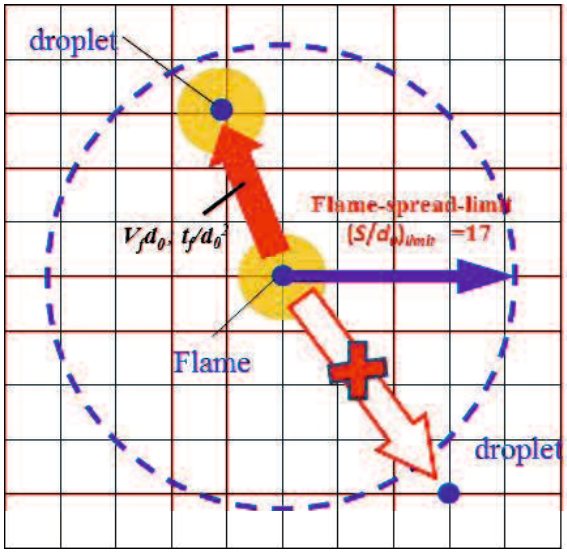

Figure 2.5 Fame spread rule considering the flame-spread-limit distance $(S/d_0)_{limit}$ based on microgravity experiments by Mikami et al., (2005) for simulation of flame-spread behavior in normal pressure (101kPa) and room temperature (300°K)

2.3.2 The simulation of flame-spread behavior without considering droplet interaction at normal pressure (101kPa) and high temperature (600°K)

As explained in the chapter 1.2 that the flame-spread limit distance $(S/d_0)_{limit}$ for droplet array experimental results in normal pressure (101kPa) and high temperature (600°K) is 17, as shown in Fig. 2.6. The simulation parameters are taken from microgravity experimental results such as: flame-spread limit distance $(S/d_0)_{limit}$ =17 and flame-spread time (t_f/d_0^2) or flame-spread rate $(V_f d_0)$. Therefore, by using Fig. 2.6 could be derived into flame-spread limit distribution for simulation of flame-spread behavior in normal pressure (101kPa) and room temperature (300°K), as shown in Fig.2.7.

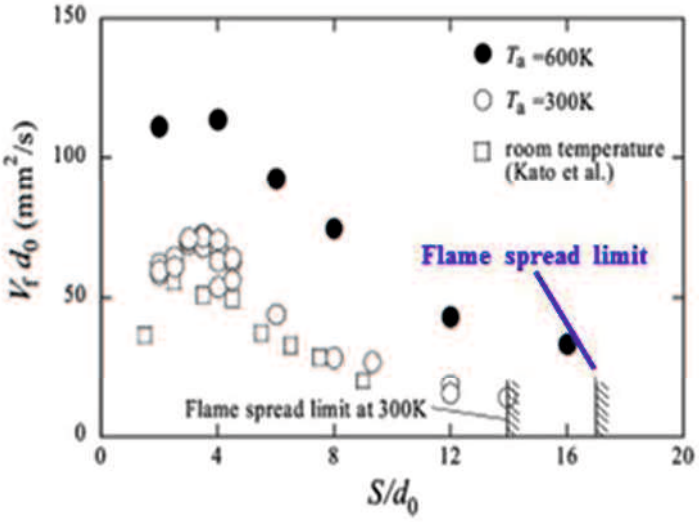

Figure 2.6 Flame-spread limit distance $(S/d_0)_{limit}$ and flame-spread rate $(V_f d_0)$ obtained from microgravity experiment at normal pressure (101kPa) and high temperature (600°K) (Mikami et al., 2006)

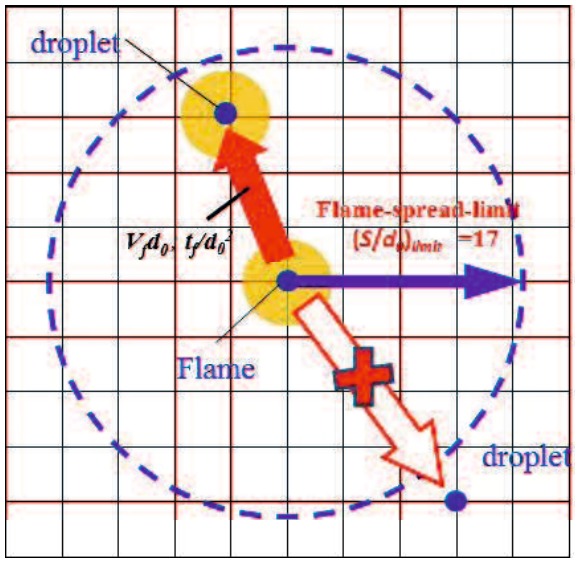

Figure 2.7 Fame spread rule considering the flame-spread-limit distance $(S/d_0)_{limit}$ based on microgravity experiments by Mikami et al., (2006) for simulation of flame-spread behavior in normal pressure (101kPa) and high temperature (600^{o}K)

2.3.3 The simulation of flame-spread behavior without considering droplet interaction at low pressure (25kPa) and room temperature (300^{o}K)

As explained in the chapter 1.2 that the flame-spread limit distance $(S/d_0)_{limit}$ for droplet array experimental results in low pressure (25kPa) and room temperature (300^{o}K) is 20, as shown in Fig. 2.8. The simulation parameters are taken from microgravity experimental results such as: flame-spread limit distance $(S/d_0)_{limit}$ =20 and flame-spread time (t_f/d_0^2) or flame-spread rate $(V_f d_0)$. Therefore, by using Fig. 2.8 could be derived into flame-spread limit distribution for simulation of flame-spread behavior in normal pressure (101kPa) and room temperature (300^{o}K), as shown in Fig.2.9.

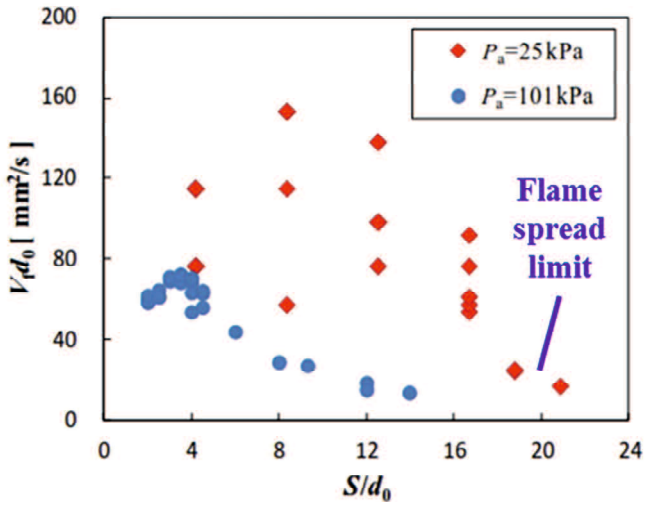

Figure 2.8 Flame-spread limit distance $(S/d_0)_{limit}$ and flame-spread rate $(V_f d_0)$ obtained from microgravity experiment at low pressure (25kPa) and room temperature (300°K) (Mikami et al., 2014)

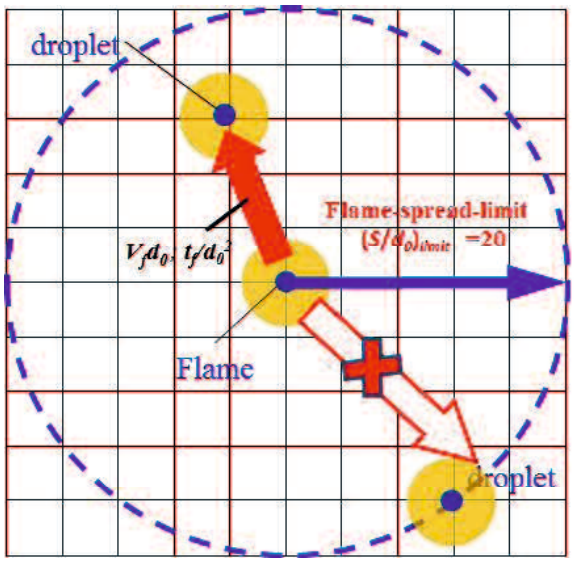

Figure 2.9 Fame spread rule considering the flame-spread-limit distance $(S/d_0)_{limit}$ based on microgravity experiments by Mikami et al., (2014) for simulation of flame-spread behavior in low pressure (25kPa) and room temperature (300°K)

2.3.4 The simulation of flame-spread behavior with considering tow-droplet interaction at normal pressure (101kPa) and room temperature (300^{o}K)

The effect of two-droplet interaction to the flame-spread limit distance was studied by Oyagi et al., 2009. They reported that as the droplet spacing is small enough, the droplet interaction becomes significantly and increases the flame-spread limit distance (Fig. 2.10b). Mikami et al., 2013 have extended Oyagi's experiment on flame-spread over two-dimensional droplet-cloud elements with uneven droplet spacing using n-decane as fuel in microgravity condition. They reported that flame-spread limit distance around interactive burning two droplet is approximated as $2^{1/3}$ times the flame-spread limit distance $(S/d_0)_{limit}$ without droplet interaction measured from midpoint of two adjacent burned droplet) as shown in Fig. 2.10c. Therefore, by the experimental results of Mikami et al., 2013 could be understood the correlation between the droplet array experiment and droplet cloud elements.

In the context of flame-spread-limit distance $(S/d_0)_{limit}$ for simulation of flame-spread behavior with considering two-droplet interaction at normal pressure (101kPa) and room temperature (300^{o}K) could be derived from the experimental results of flame-spread droplet array (Mikami et al., 2005 and Oyagi et al., 2009) and from flame-spread droplet-cloud elements (Mikami et al., 2013) as shown in Fig. 2.10. Finally by using Fig. 2.10, the flame-spread limit distribution for simulation of flame-spread behavior with considering two-droplet interaction at normal pressure (101kPa) and room temperature (300^{o}K) could be generated as shown in Fig. 2.11.

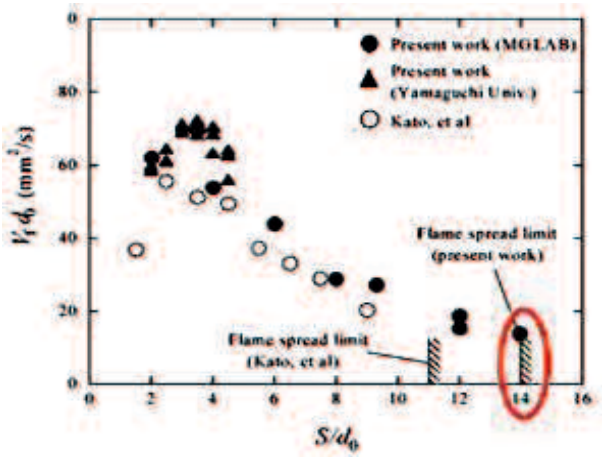

a. Mikami et al., 2005

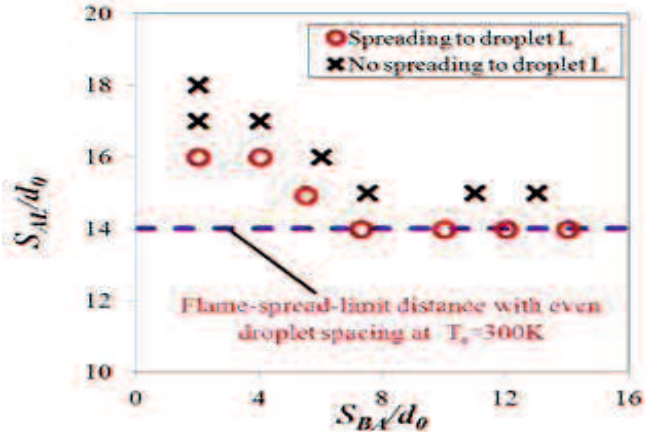

b. Oyagi et al., 2009

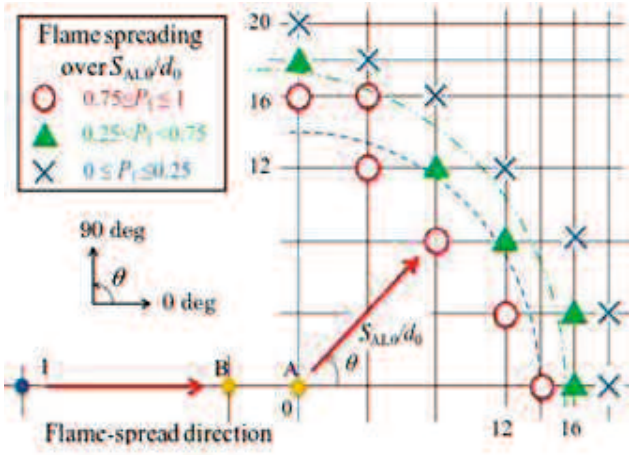

c. Mikami et al., 2013

Figure 2.10 Flame-spread limit distances was obtained from microgravity experimental results of droplet array and droplet cloud element at normal pressure (101kPa) and room temperature (300^{o}K)

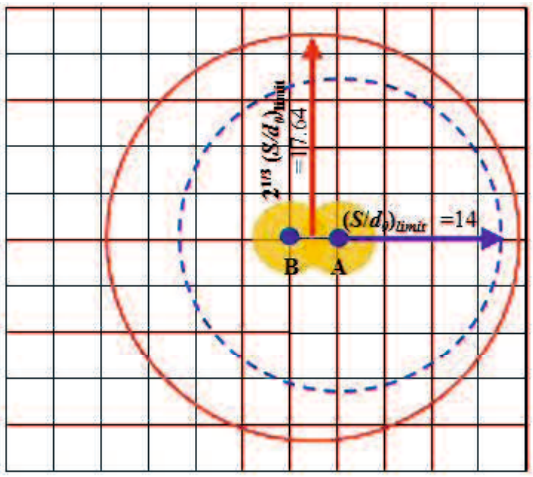

a. $S_{BA}/d_0 < 7.26$

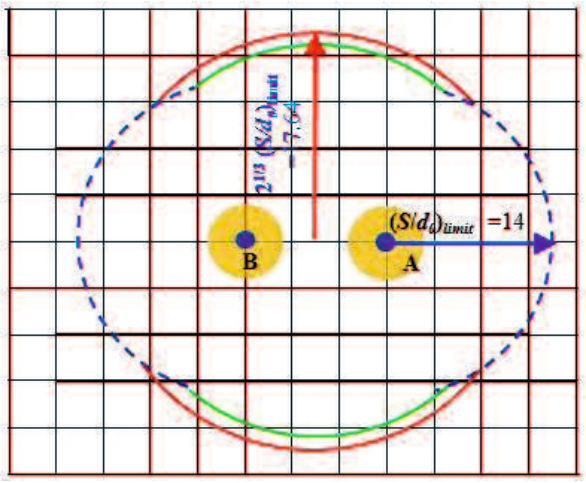

b. $7.26 \leq S_{BA}/d_0 < 12$

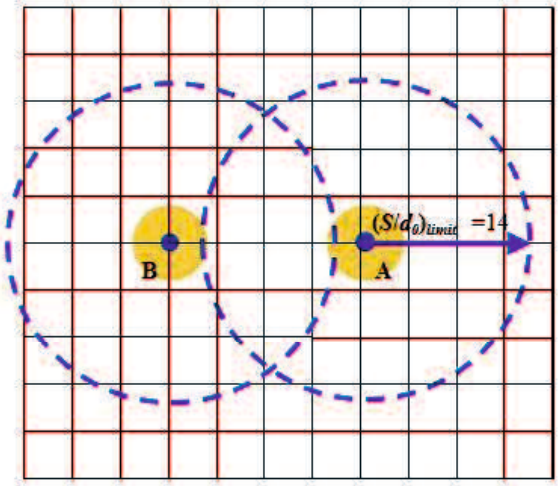

c. $S_{BA}/d_0 \geq 12$

Figure 2.11 Distribution of the flame-spread limit distance $(S/d_0)_{limit}$ considering two-droplet interaction at normal pressure and room temperature

Figure 2.11 explains that the flame-spread limit distance distribution is separated into three type based on the distance of two adjacent burning droplet as follows.

a. If the distance of two adjacent burning droplets is $S_{BA}/d_0 < 7.26$, the local-flame-spread-limit distance is $2^{1/3}(S/d_0)_{limit}$ or 17.64 measured from the midway of two adjacent burning droplets (Fig. 2.11a)
b. If the distance of two adjacent burning droplets is $7.26 \leq S_{BA}/d_0 < 12$, the local-flame-spread-limit distance is the large one in 17.64 to 17.09 measured from the midway of two adjacent burning droplets and $(S/d_0)_{limit}$ measured from a burning droplet (Fig. 2.11b)
c. If the distance of two adjacent burning droplets is $S_{BA}/d_0 \geq 12$, the interaction effect doesn't occur and the local-flame-spread-limit distance is $(S/d_0)_{limit}$ measured from a burning droplet (Fig. 2.11c)

2.4 Calculation procedure

In this simulation, the parameters to calculate the flame-spread behavior using percolation could be separated as follows.

a. The parameters was obtained from microgravity experimental results, such as: flame-spread limit distance $(S/d_0)_{limit}$ and flame-spread time (t_f/d_0^2) or flame-spread rate $(V_f d_0)$.
b. The variable parameters, such as: lattice point interval (L/d_0), lattice size (NL/d_0) and droplet number (M).

While the percolation approach is used for simulation of flame-spread behavior, the droplets number (M) are randomly arranged at lattice point (N) and the ratio between the droplets number (M) and lattice point (N) is defined as occupation fraction (p). In this simulation, the calculation was conducted for 1000 different droplet patterns (n) for each occupation fraction (p) or mean droplet spacing $(S/d_0)_m$. This is because in this calculation is used mean error as the uncertainty of Occurrence probability of group combustion (OPGC) due to the droplet arrangements number (n), which is written as Eq. 2.1. The mean error for

i.e. OPGC = 0.5 are: 33.3 % for n=10, 10.1 % for n=100, 10.1 % for n=100 and 3.2 % for n=1000. Therefore 1000 droplet arrangements are sufficient to predict the probability of flame-spread.

$$\text{Uncertainty of OPGC} = \left\{\frac{OPGC(1-OPGC)}{(n-1)}\right\}^{1/2} \quad (2.1)$$

2.4.1 The calculation procedure for simulation of flame-spread behavior without considering droplet interaction

The numerical calculation procedure of 2D and 3D droplet arrangement of flame-spread behavior without considering droplet interaction using percolation approach is conducted as follows (Fig. 2.12 and 2.13).

a. Step 1, the droplets on the bottom side of the lattice in 2D case and on the bottom surface of the lattice in 3D case are first ignited (Fig. 2.12a and 2.13a).
b. Step 2, the flame spreads to the next droplet within the local-flame-spread-limit distance $(S/d_0)_{limit}$ =14 without considering droplets interaction (Fig. 2.12b and 2.13b).
c. Step 3, the calculations procedure is repeated until the flame cannot spread to the next droplets or the flame reaches all the sides of the lattice (Fig. 2.12c and 2.13c). Even after the flame reaches the top side, the flame might spread back toward the bottom side by the end of droplet burning

The group combustion of droplet cloud appears if the flame starting from a side in 2D droplet arrangements and a face in 3D droplet arrangements reaches the all sides in 2D droplet arrangements and all faces in 3D droplet arrangements. This type of the flame-spread is defined as the occurrence of group combustion of the droplet cloud.

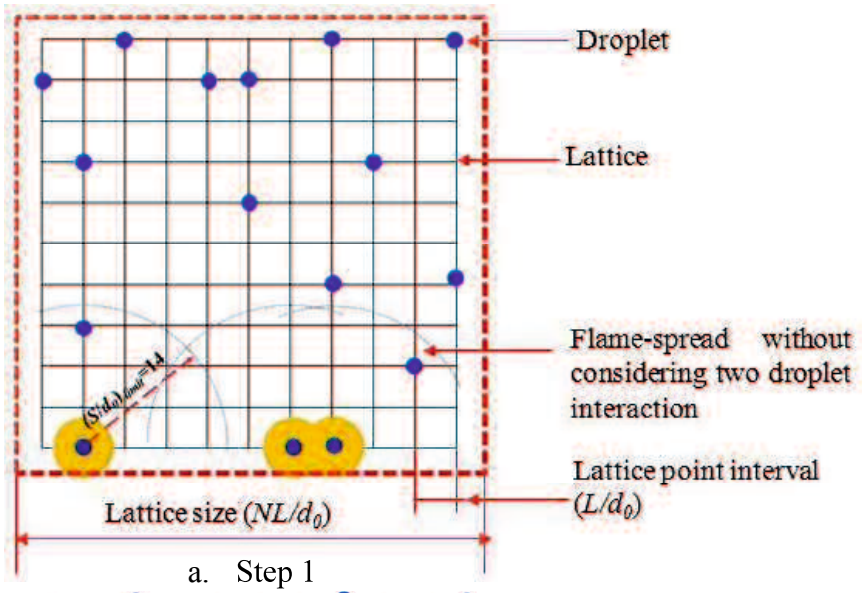

a. Step 1

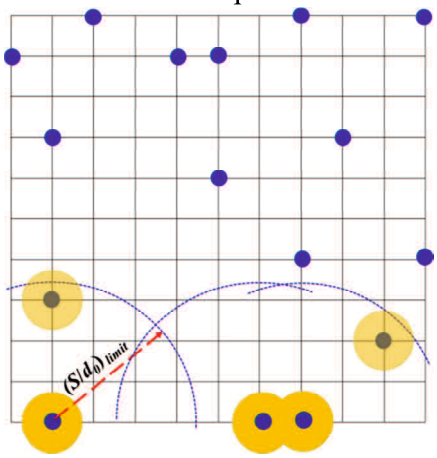

b. Step 2

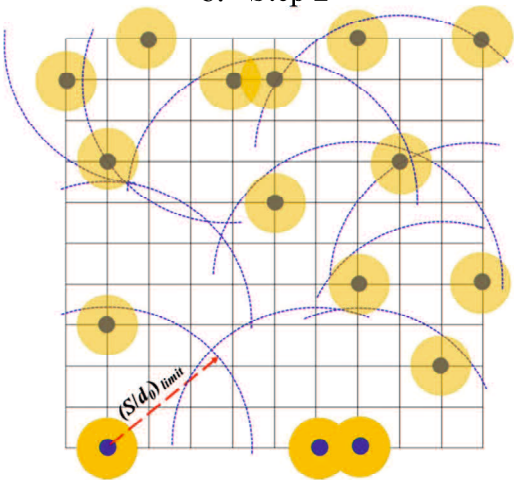

c. Step 3

Figure 2.12 Calculation procedure of flame-spread in randomly distributed droplet cloud without considering droplet interaction for 2D droplet arrangement

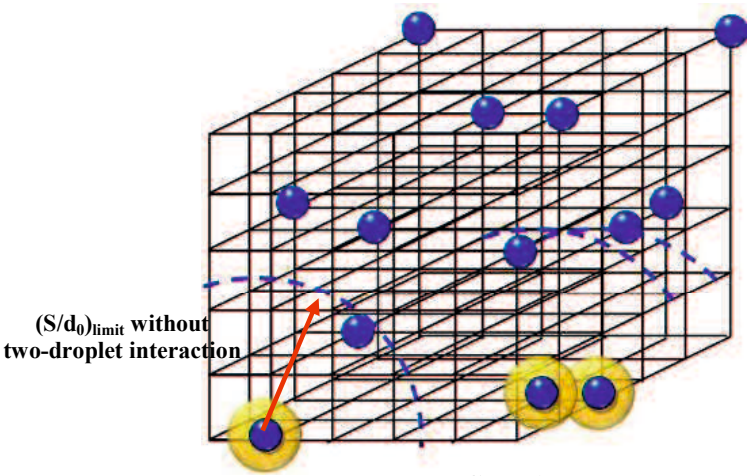

a. Step 1

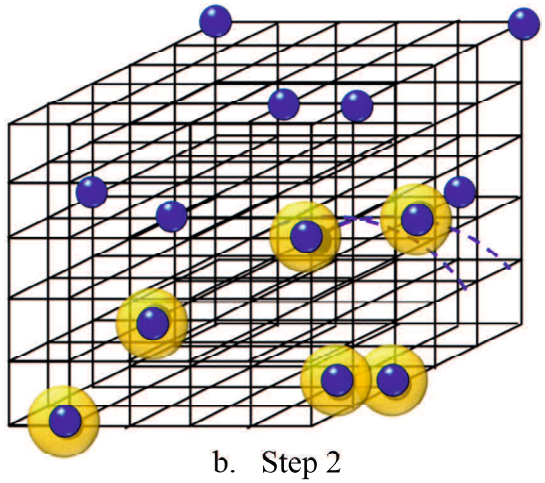

b. Step 2

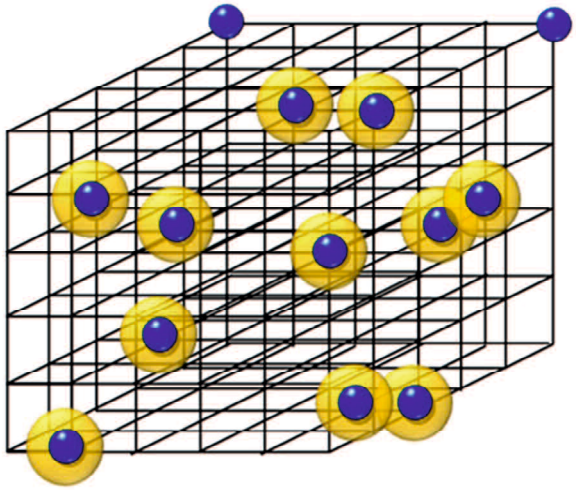

c. Step3

Figure 2.13 Calculation procedure of flame-spread in randomly distributed droplet cloud without considering droplet interaction for 3D droplet arrangement

2.4.2 The calculation procedure for simulation of flame-spread behavior with considering two-droplet interaction

As shown in Figure 2.14 and 2.15, the calculation procedure of flame-spread with considering two-droplet interaction was conducted as follows:

a. Step 1, the droplets on the bottom side of the lattice in 2-D case and on the bottom surface of the lattice in 3-D case are first ignited (Fig. 2.14a and 2.15a).
b. Step 2, the flame spreads to the next droplet within the local-flame-spread-limit distance considering two droplets interaction (Fig. 2.14b and 2.15b).
c. Step 3, the calculations procedure is repeated until the flame cannot spread to the next droplets or the flame reaches all the sides of the lattice. Even after the flame reaches the top side, the flame might spread back toward the bottom side by the end of droplet burning (Fig. 2.14c and 2.15c).

Only when the flame spreads to droplets on the top side, the left side and the right side of the lattice, this type of the flame-spread is defined as the occurrence of group combustion of the droplet cloud.

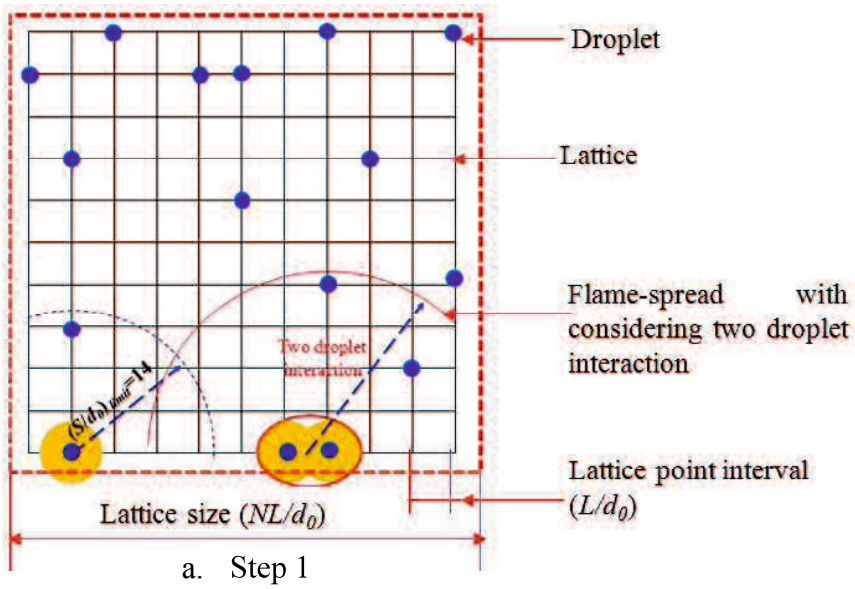

a. Step 1

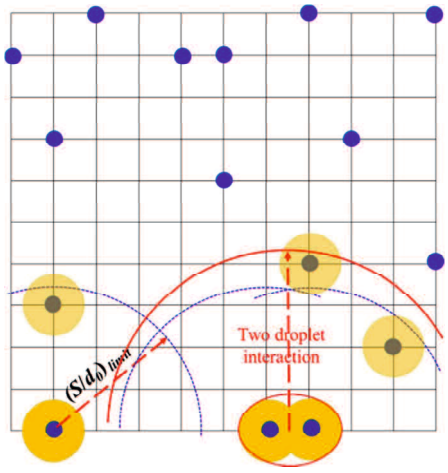

b. Step 2

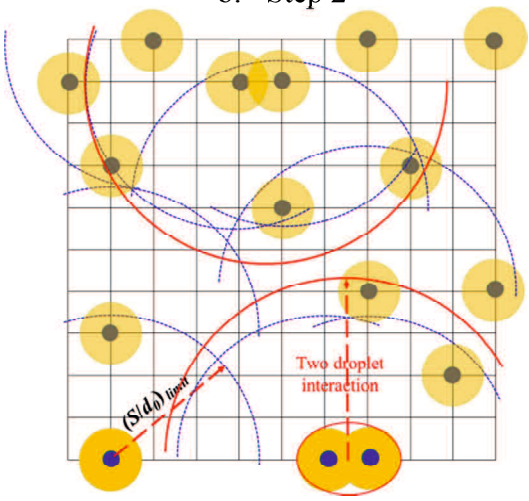

c. Step 3

Figure 2.14 Calculation procedure of flame-spread in randomly distributed droplet cloud with considering two-droplet interaction for 2D droplet arrangement

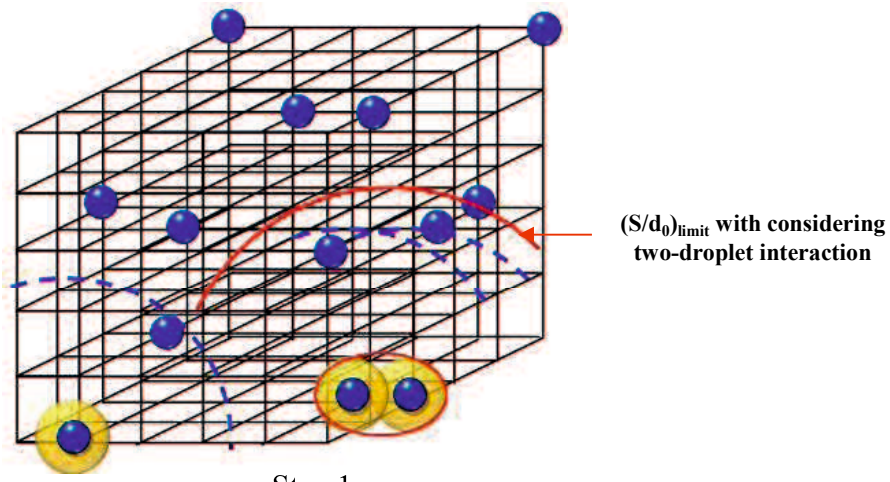

a. Step 1

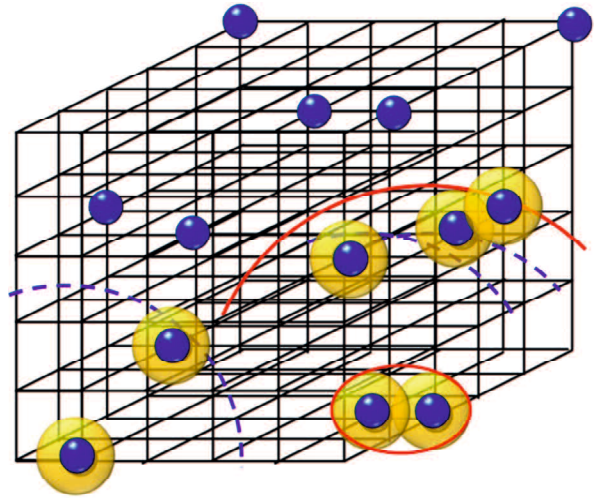

b. Step 2

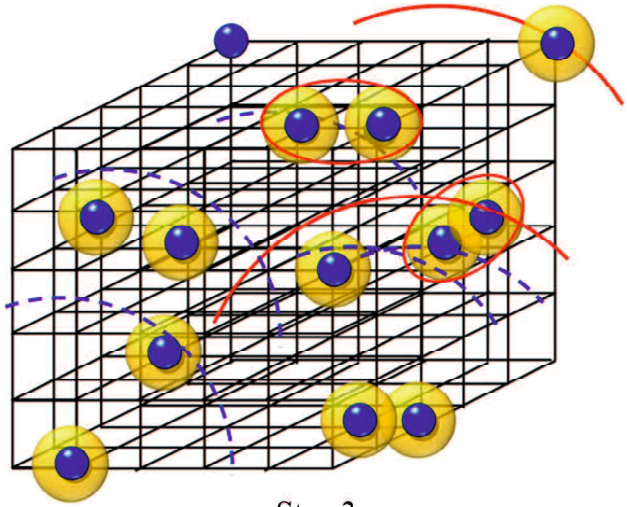

c. Step 3

Figure 2.15 Calculation procedure of flame-spread in randomly distributed droplet clod with considering two-droplet interaction for 2D droplet arrangement

Chapter 3

Simulating Flame-spread Behavior of Randomly Distributed Droplet Clouds without Considering Droplet Interaction

In this Chapter the simulation of flame-spread behavior of randomly distributed droplet clouds without considering droplet interaction is explained. Simulation based on flame-spread characteristic of droplet array at normal pressure (101kPa) and room temperature (300^{o}K), Simulation based on flame-spread characteristic of droplet array at normal pressure (101kPa) and high temperature (600^{o}K), and Simulation based on flame-spread characteristic of droplet array at low pressure (25kPa) and room temperature (300^{o}K) are discussed in detail.

3.1 Simulation based on flame-spread characteristics of droplet array in normal pressure and room temperature

Experimental results on the droplet array of n-decane fuel at normal pressure (101kPa) and room temperature (300^{o}K) has shown that the flame-spread have a maximum limit distance $(S/d_0)_{limit}$ =14, thus flame cannot spread to the next unburned droplet if the position is over the flame-spread limit distance $(S/d_0)_{limit}$.

3.1.1 Occurrence Probability of Group Combustion (OPGC)

3.1.1.1 Effects of occupation fraction (*p*) on the OPGC

Figure 3.1 shows dependences of the occurrence probability of group combustion (OPGC) on the occupation fraction (p) for L/d_0=2 and different lattice sizes (NL/d_0) at 2D and 3D droplet arrangements without considering droplet interactions. As the occupation fraction (p) increases, the *OPGC* rapidly increases around a specific value of (p) for each case of (NL/d_0). This is because the flames

have high probability spread to next unburned droplets and reaches all sides or faces of lattice when the occupation fraction (p) is increased.

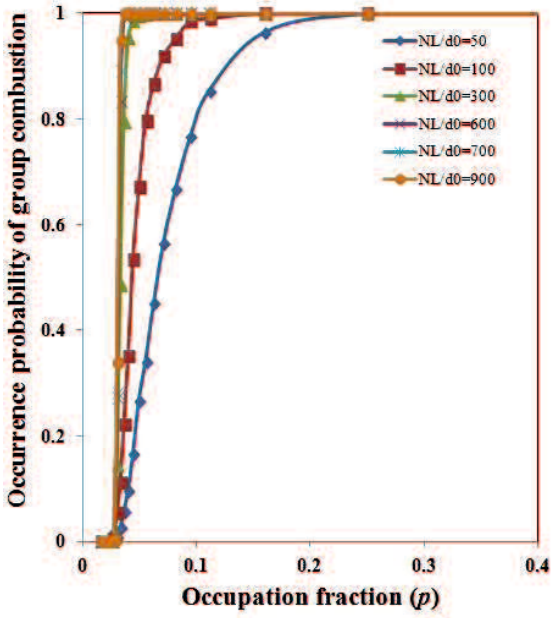

a. 2D droplet arrangement

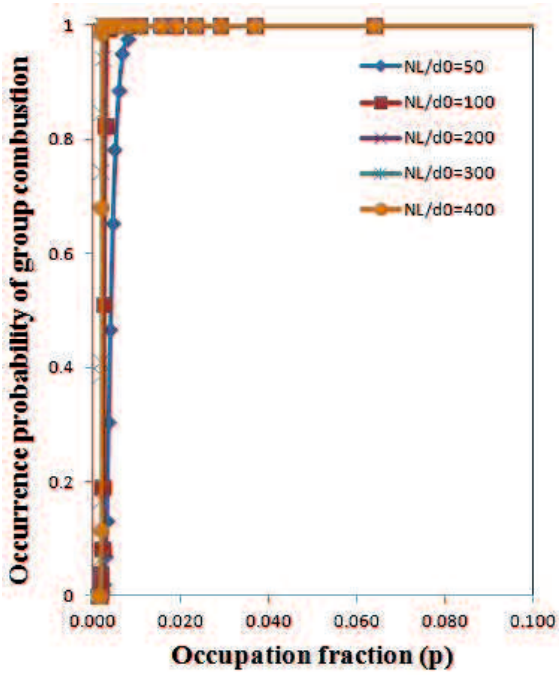

b. 3D droplet arrangement

Figure 3.1 Dependence of occurrence probability of group combustion (OPGC) on occupation fraction (p) for L/d_0=2 and different lattice sizes (NL/d_0)

The effect of increasing occupation fraction (p) is also shows in Fig. 3.2, wherein the occupation fraction (p) is small enough, the flame-spread terminates on its way to the lattice and leading to incomplete combustion or partial combustion (Fig. 3.2a). When the occupation fraction is increased (Fig. 3.2b and 3.2c), the flame area increases and flame reach all sides or faces of the lattice and finally the group combustion occur.

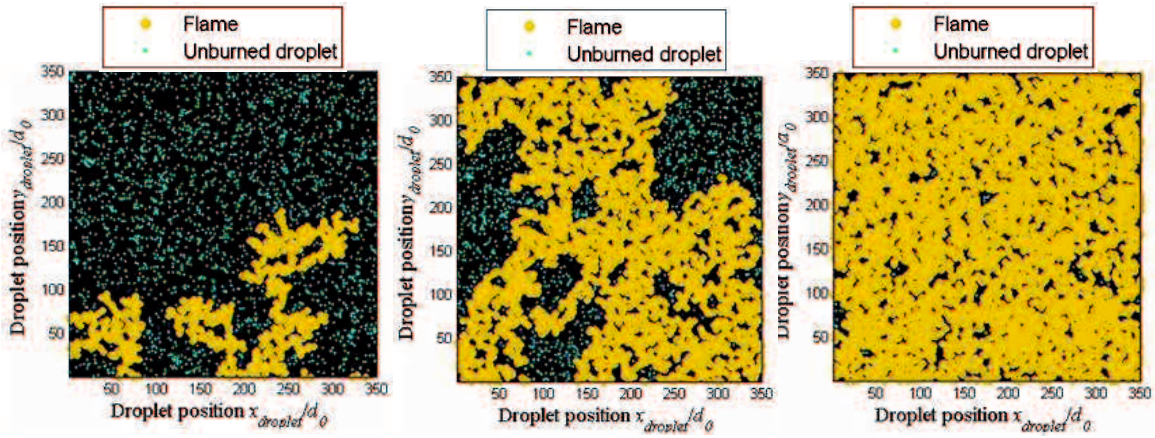

a. p=0.0237 b. p=0.0312 p=0.0400

Figure 3.2 Flame patterns of randomly distributed droplet cloud in 2D droplets arrangement, L/d_0= 2 and NL/d_0= 700 for three different of occupation fraction (p). a) partial combustion (p= 0.0237), b) critical condition (p= 0.0312) and c) group combustion (p= 0.0400)

3.1.1.2 Effects of lattice size (NL/d_0) on the OPGC

The effect of lattice size (NL/d_0) on the OPGC is shown in Fig. 3.1. As the lattice size (NL/d_0) increases, the slope of OPGC graph is become sharper. This means that at same value of occupation fraction (p), the OPGC for large NL/d_0 is higher than that small NL/d_0. According to the percolation theory, when the NL/d_0 is increased to infinity, the graph of percolation probability approach step function and the percolation threshold appears. As shown in Fig. 3.1 the OPGC graph approach a step function with increasing NL/d_0.

The OPGC become step function means that OPGC is zero for occupation fraction less than threshold value and unity for occupation fraction (p) greater than threshold value. This means that the flame-spread behavior less than threshold value is close to partial combustion of droplet clouds and the flame-spread behavior greater than threshold value is close to group combustion of droplet clouds (Fig. 3.3).

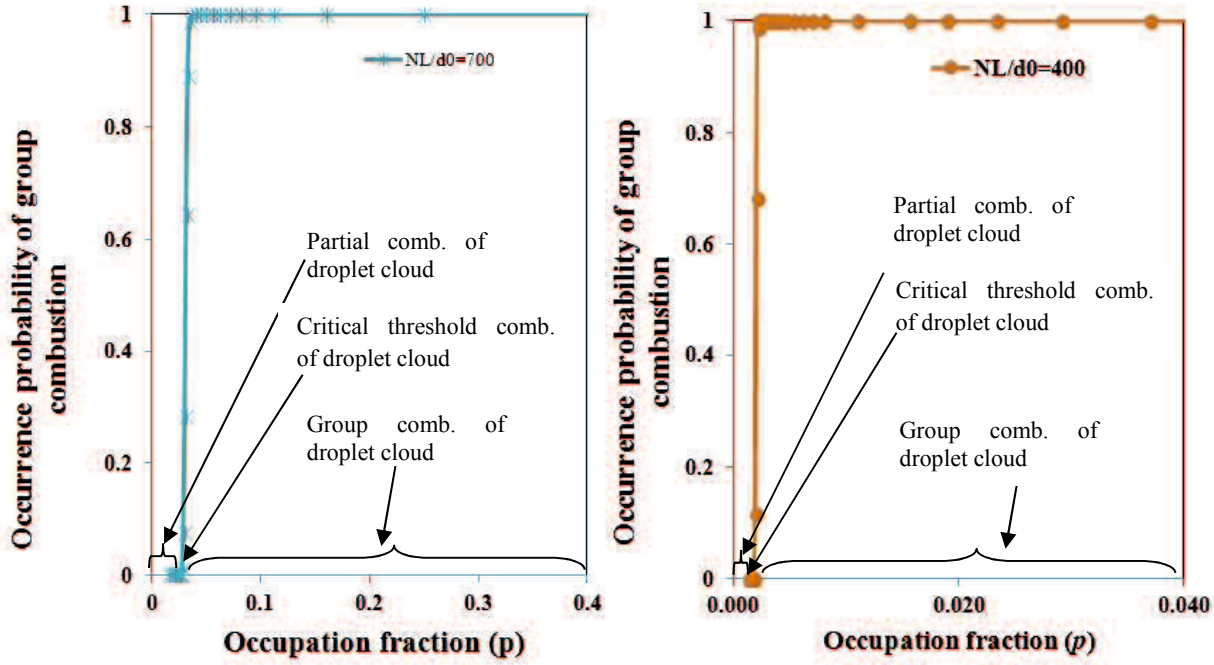

a. 2D droplet arrangement b. 3D droplet arrangement

Figure 3.3 The OPGC graph approach a step function on occupation fraction (p) for 2D and 3D droplet arrangements

The occupation fraction largely depends on the lattice point interval, but there is no lattice in real spray. Although the OPGC could be determined by using the occupation fraction (p), it is difficult get the general characteristics of flame-spread through the occupation fraction. Therefore, in order to study the flame-spread behavior and group combustion excitation, the occupation fraction (p) should be transformed to the parameter that can describe the real condition in the practical fuel spray combustion. The parameter that can describe the real condition in the practical fuel spray combustion is mean droplet spacing $(S/d_0)_m$.

When the mean droplet spacing $(S/d_0)_m$ is introduced, the critical value (critical mean droplet spacing) is nearly independent of lattice characteristics, if the lattice point interval (L/d_0) is small and lattice size (NL/d_0) is large enough.

Figure 3.4 and 3.5 shows how to transform the occupation fraction (p) to the mean droplet spacing $(S/d_0)_m$. In order to transform the occupation fraction (p) to the mean droplet spacing $(S/d_0)_m$, the droplets on the lattice should be rearranged into a two-dimensional droplet matrix or three-dimensional droplet matrix with an equal inter droplet distance in the same area or volume. The equal distance between the droplets on the matrix is identified as mean droplet spacing.

The numerical approach to transform the occupation fraction (p) to the mean droplet spacing $(S/d_0)_m$ can be used the Eq. 3.1 for 2D droplet arrangement and Eq. 3.2 for 3D droplet arrangement.

$$(S/d_0)_m = L/d_0 p^{-1/2} \tag{3.1}$$

$$(S/d_0)_m = L/d_0 p^{-1/3} \tag{3.2}$$

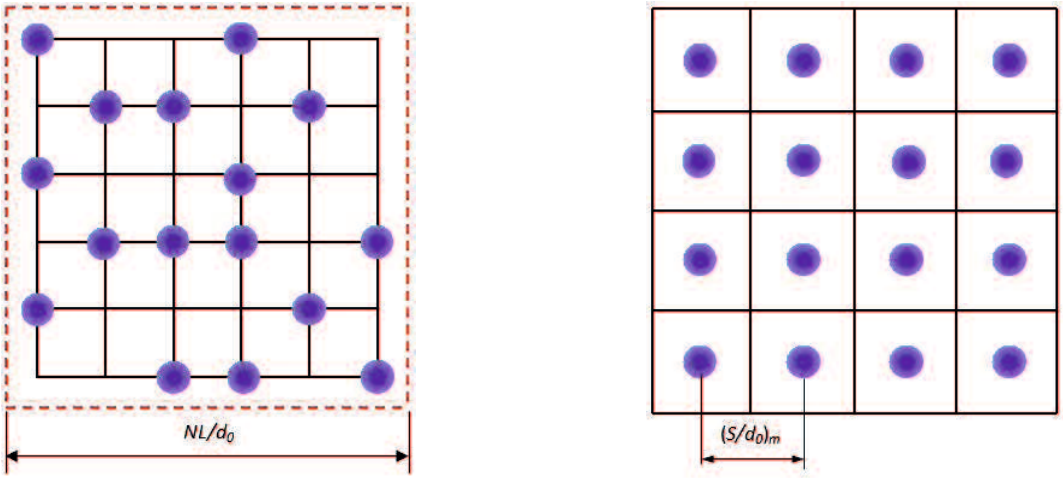

a. Before rearrangement b. After rearrangement

Figure 3.4 The transformation of occupation fraction (p) into mean droplet spacing $(S/d_0)_m$ by rearranged two dimensional droplet matrix with an equal inter droplet distance in the same area

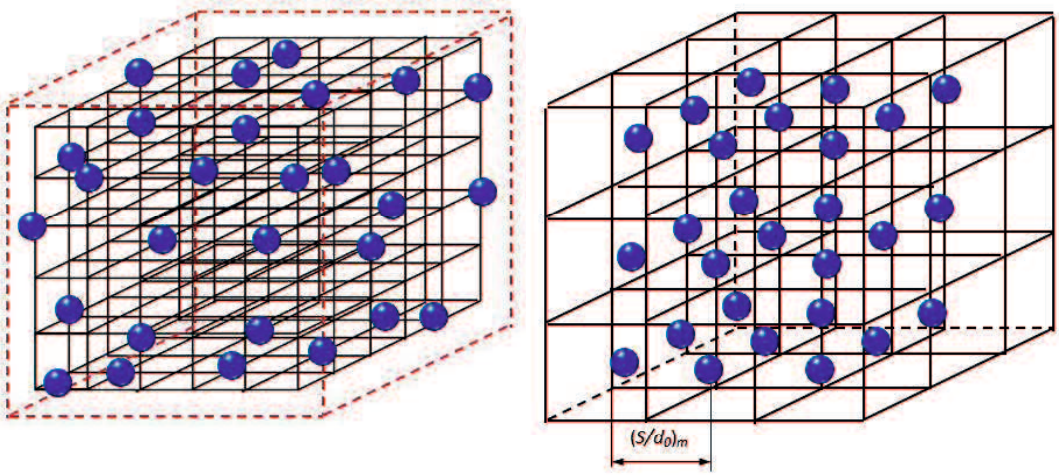

b. Before rearrangement b. After rearrangement

Figure 3.5 The transformation of occupation fraction (p) into mean droplet spacing $(S/d_0)_m$ by rearranged three dimensional droplet matrix with an equal inter droplet distance in the same volume

Figure 3.6 shows dependence of the OPGC on the mean droplet spacing $(S/d_0)_m$ for $L/d_0 = 2$ and different NL/d_0 at 2D droplet arrangement and 3D droplet arrangement after occupation fraction (p) was transformed into $(S/d_0)_m$. As the mean droplet spacing $(S/d_0)_m$ is increased, the OPGC rapidly decreases around a specific value of $(S/d_0)_m$ for each case. This is look like opposite with the graph of OPGC versus occupation fraction (p), because if the $(S/d_0)_m$ is small the occupation fraction is large enough.

In order to predict the threshold value of $(S/d_0)_m$, we pay attention $(S/d_0)_m$ for 0.5 OPGC. The mean droplet spacing that shown the 0.5 OPGC was identified as the critical mean droplet spacing $(S/d_0)_{critical}$. From Fig. 3.6 we can see that $(S/d_0)_{critical}$ increases with the increasing lattice size (NL/d_0). In case of increasing NL/d_0 are obtained the constant tendency of $(S/d_0)_{critical}$ and the OPGC graph become step function, the percolation threshold is appears.

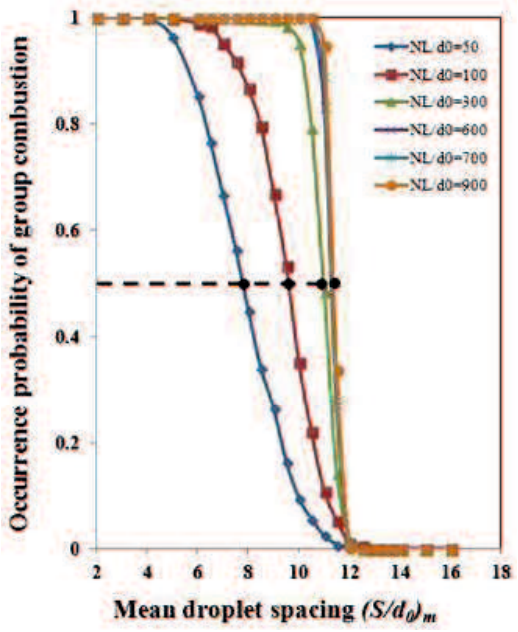

a. 2D droplet arrangement

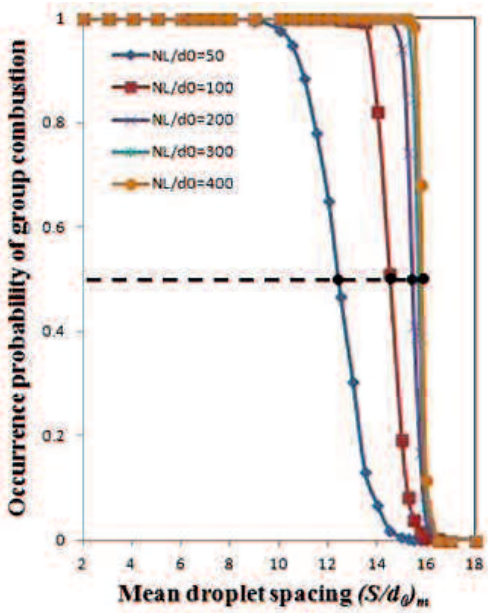

b. 3D droplet arrangement

Figure 3.6 Dependence of occurrence probability of group combustion (OPGC) on mean droplet spacing $(S/d_0)_m$ for $L/d_0 = 2$ and different lattice size (NL/d_0)

On the simulation of flame-spread behavior without considering droplet interaction, the mean droplet spacing $(S/d_0)_m = 11.3$ with $NL/d_0 = 700$ and $L/d_0 = 2$ is close to the critical mean droplet spacing $(S/d_0)_{critical}$ 2D droplet arrangement. While, the 3D droplet arrangement show that the mean droplet spacing $(S/d_0)_m = 15.8$ with $NL/d_0 = 400$ and $L/d_0 = 2$ is close to the critical mean droplet spacing $(S/d_0)_{critical}$. This results show that critical mean droplet spacing at 3D droplet arrangement is larger than that at 2D droplet arrangement. This is because at the 3D lattice, the droplet connection source comes from three directions while at the 2D lattice the particle connection source comes from two directions. Hence, in order to achieve the critical threshold, the 3D droplet arrangement can be achieved by using larger mean droplet spacing $(S/d_0)_m$ than that 2D droplet arrangement.

The critical threshold mean droplet spacing separates the droplet cloud into two groups; relatively dense droplet clouds in which the group combustion is exited through flame spread and dilute droplet clouds in which the group combustion is never excited.

3.1.1.3 Effects of lattice point interval (L/d_0) on the OPGC

The previous section has been discussed the flame-spread behavior without considering droplet interaction for lattice point interval $(L/d_0) = 2$. This section will be discussed flame-spread behavior for various lattice point intervals (L/d_0). Figure 3.7 shows the OPGC on occupation fraction (p) for different L/d_0. As the L/d_0 is decreases, the OPGC shifted to the left side. When the lattice point interval (L/d_0) is equal to the flame-spread limit distance $(S/d_0)_{limit}$ the occupation fraction is large and closed to the theoretical of percolation threshold ($p_c = 0.593$ for 2D lattice and $p_c = 0.347$ for 3D lattice).

Figure 3.8 shows the dependences of $(S/d_0)_{critical}$ on NL/d_0 for different L/d_0. As the L/d_0 is decreased, the critical mean droplet spacing $(S/d_0)_{critical}$ decreases. The $(S/d_0)_{critical}$ will attain a specific value, if the L/d_0 is decreasing. Therefore, the L/d_0 is representing the minimum droplet spacing on the lattice. As lattice point interval (L/d_0) is small, the flame distribution is more heterogeneous and as the lattice point interval (L/d_0) is large, the flame distribution is more homogeneous

(Fig. 3.9 and 3.10). Therefore, in order to apply percolation model to real fuel spray combustion, the small lattice point interval (L/d_0) with small limit value of $(S/d_0)_{critical}$ and heterogeneous flame distribution is important.

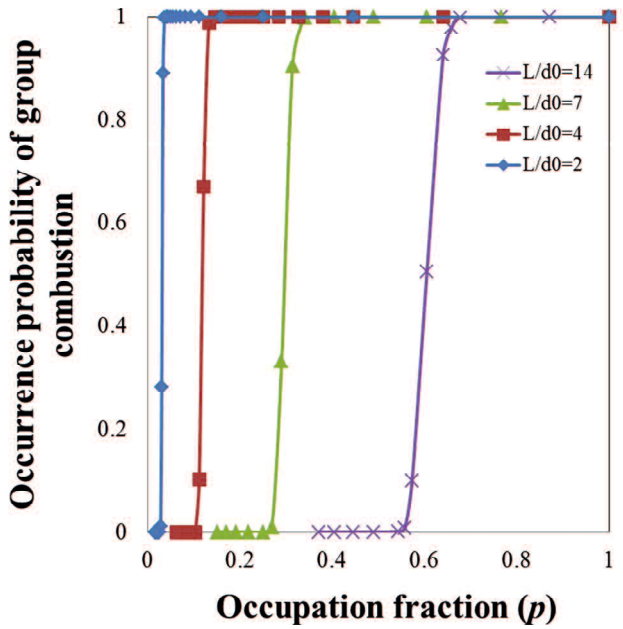

Figure 3.7 Dependence of occurrence probability of group combustion (OPGC) on occupation fraction (p) for different lattice point interval (L/d_0) at NL/d_0 = 700 and 2D droplet arrangement

The effect of increasing L/d_0 on OPGC and critical mean droplet spacing $(S/d_0)_m$ is higher at 3D droplet arrangement than 2D droplet arrangement as shown in Fig. 3.8. Figure 3.8 also shows the effect of lattice size (NL/d_0) on critical mean droplet spacing $(S/d_0)_{\mathrm{m}}$. As the lattice size (NL/d_0) is increased, the $(S/d_0)_{critical}$ increases, but at the specific value of NL/d_0 the increasing of NL/d_0 obtained the constant tendency of increasing $(S/d_0)_{critical}$. On this position we identify as critical threshold mean droplet spacing, it has been explained on the previous section. The critical threshold mean droplet spacing for various L/d_0 are almost similar, appears at NL/d_0 = 700 for 2D droplet arrangement and NL/d_0 = 400 for 3D droplet arrengement.

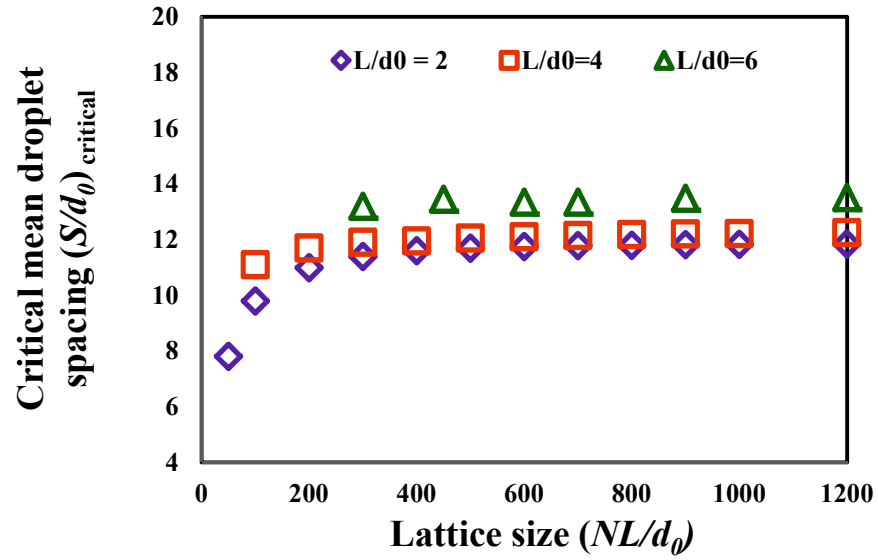

a. 2D droplet arrangement

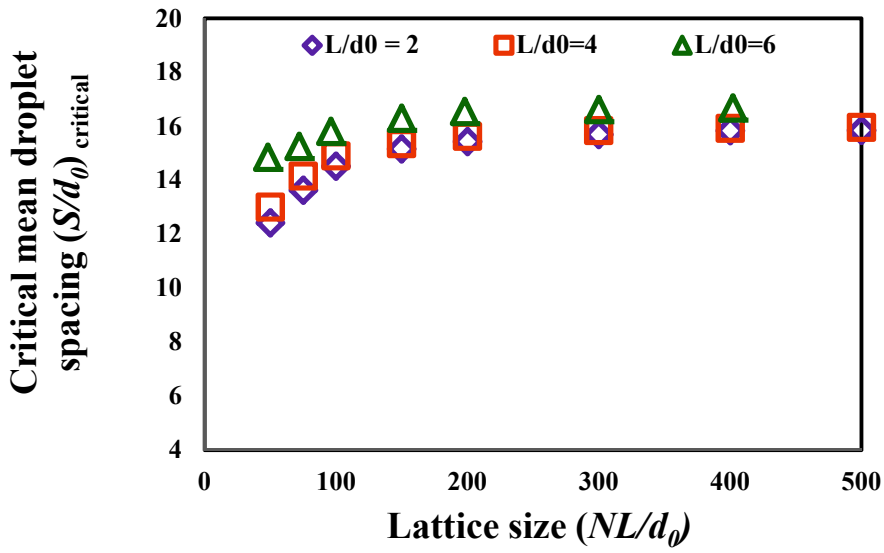

b. 3D droplet arrangement

Figure 3.8 Dependences of critical mean droplet spacing $(S/d_0)_{critical}$ on lattice size NL/d_0 without considering droplet interaction in 2D and 3D droplet arrangements

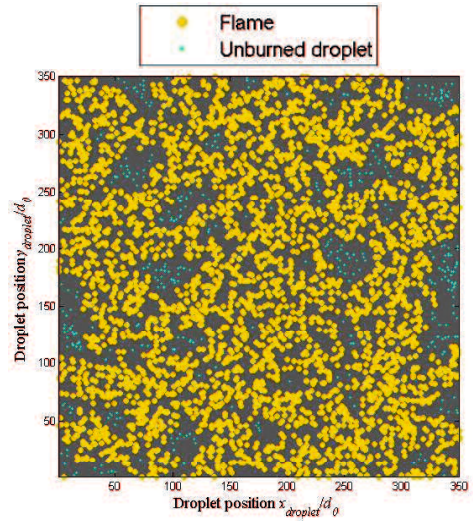

a. $L/d_0 = 2$ and $(S/d_0)_m = 11.32$

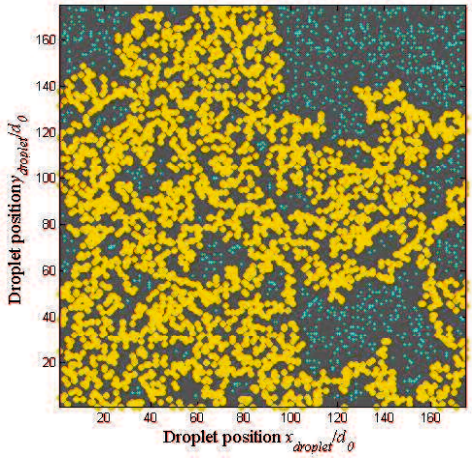

b. $L/d_0 = 4$ and $(S/d_0)_m = 11.65$

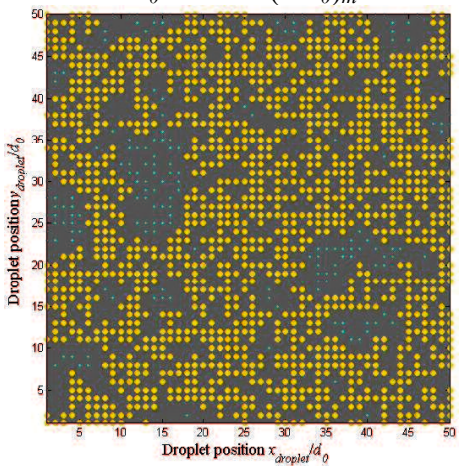

c. $L/d_0 = 14$ and $(S/d_0)_m = 18.01$

Figure 3.9 Typical distribution of flame 2D droplet arrangement in critical threshold mean droplet spacing for NL/d_0=700 and different lattice point interval (L/d_0= 2, 4, and 14), simulation without considering droplet interaction

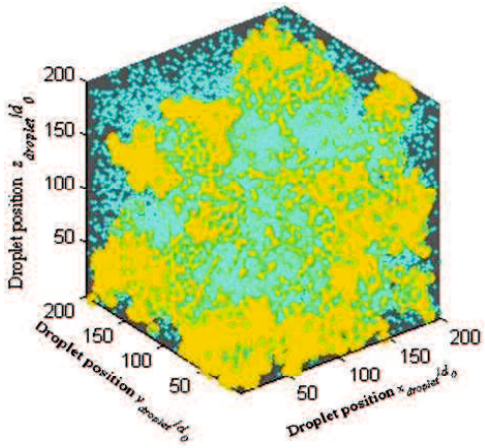

a. $L/d_0 = 2$ and $(S/d_0)_m = 15.83$

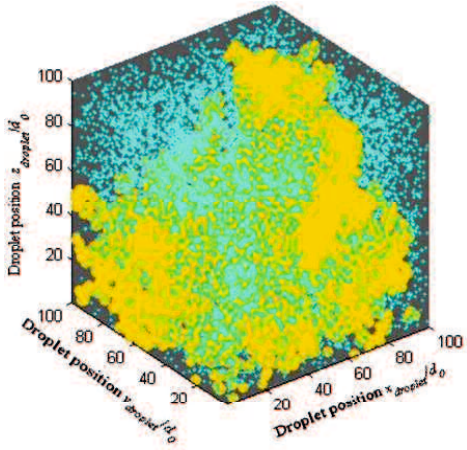

b. $L/d_0 = 4$ and $(S/d_0)_m = 15.912$

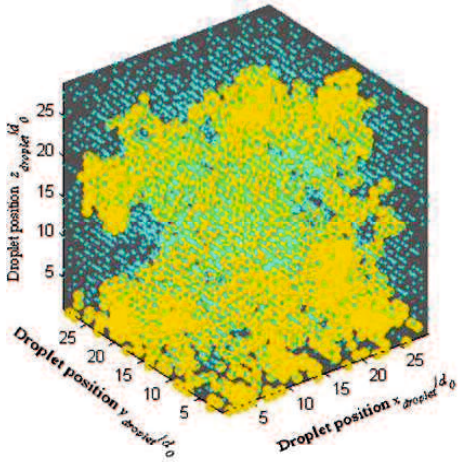

c. $L/d_0 = 14$ and $(S/d_0)_m = 20.35$

Figure 3.10 Typical distribution of flame 3D droplet arrangement in critical threshold mean droplet spacing for $NL/d_0 = 400$ and different lattice point interval ($L/d_0 = 2$, 4, and 14), simulation without considering two-droplet interaction

3.1.2 Flame-spread behavior near the critical threshold mean droplet spacing

As discussed on the previous section that the critical threshold mean droplet spacing separates the flame-spread behavior into group combustion is exited through flame spread and group combustion is never excited. Thus, this is an interesting point to observe the detail flame-spread behavior near critical threshold mean droplet spacing. Figure 3.11 and 3.12 shows example of flame-spread distribution near the critical threshold mean droplet spacing, wherein the flame spread reaches all the sides of lattice in 2D droplet arrangement and all faces of lattice in 3D droplet arrangement. Even when the group combustion occurs, a portion of the droplets remains unburned.

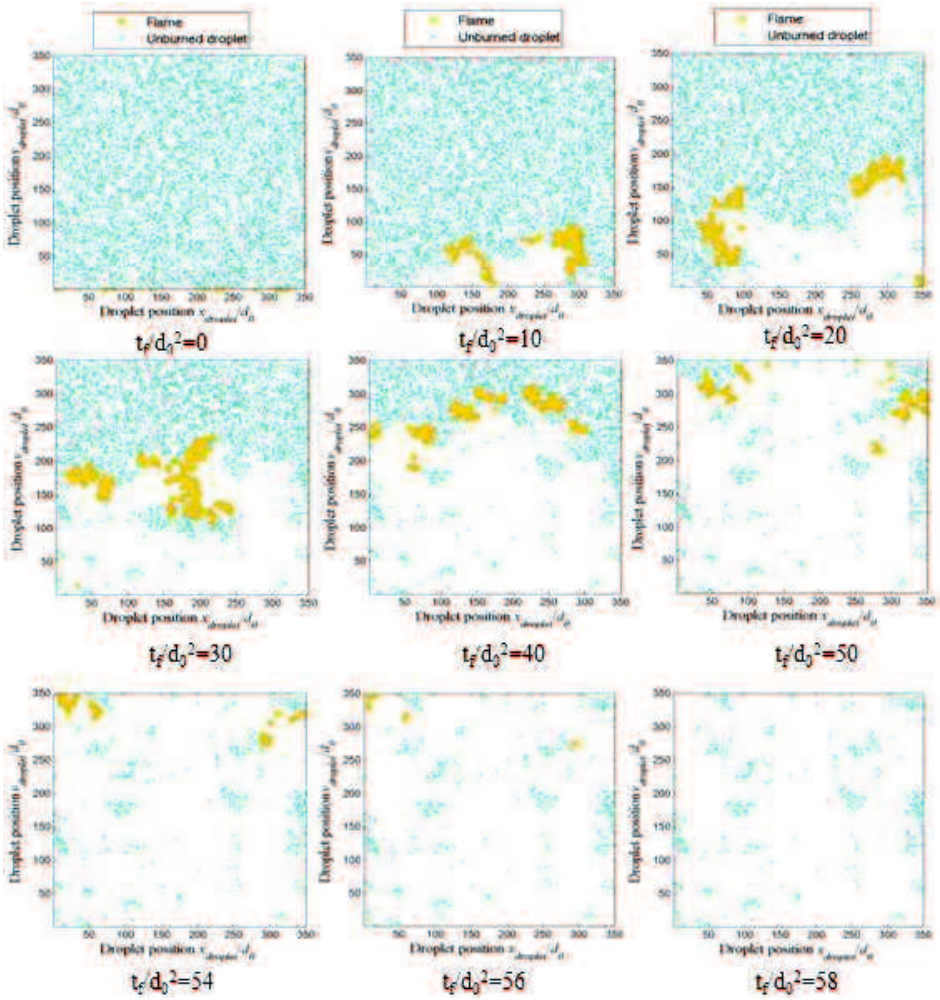

Figure 3.11 Flame-spread behavior for 2D droplet arrangement near the critical mean droplet spacing for $(S/d_0)_{critical}$ = 11.32, NL/d_0 = 700 and L/d_0 = 2

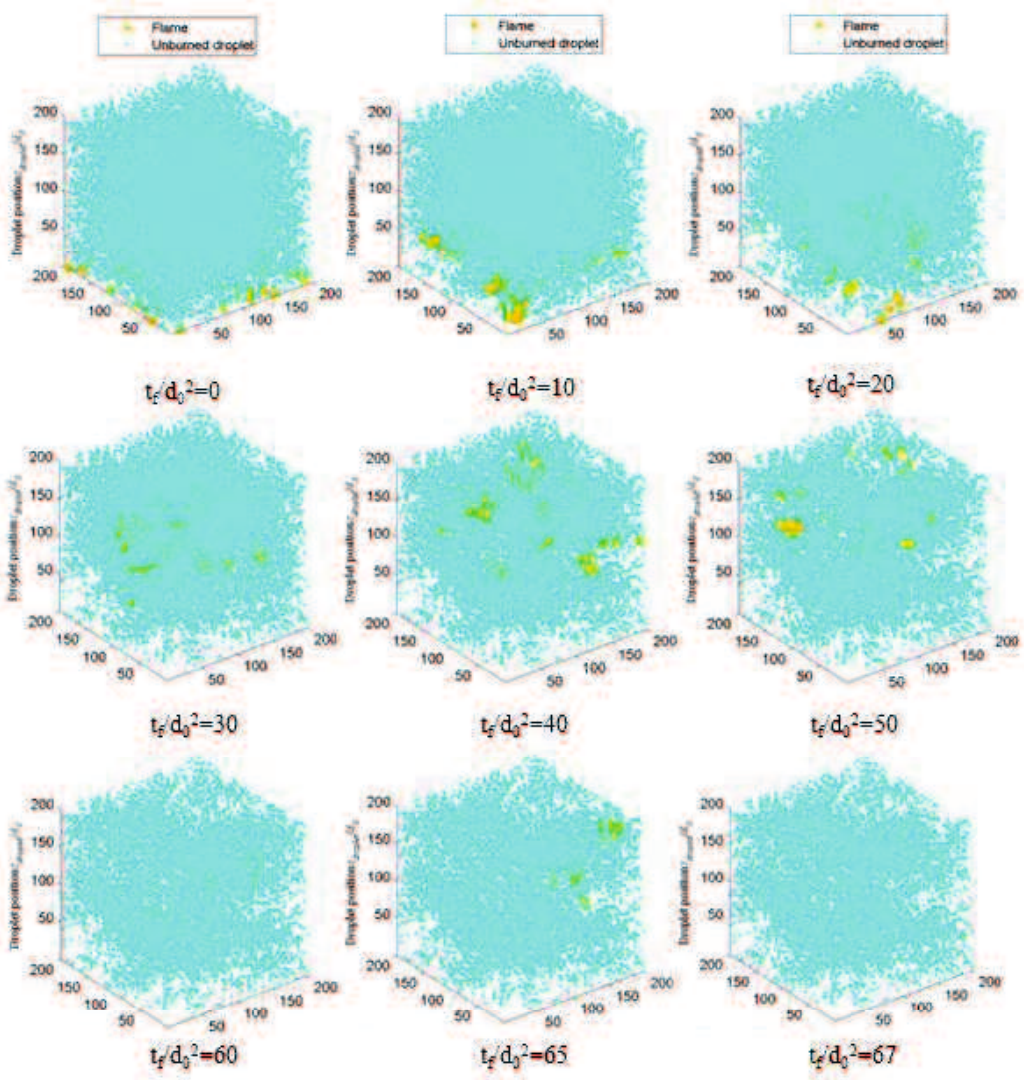

Figure 3.12 Flame-spread behavior for 3D droplet arrangement near the critical mean droplet spacing for $(S/d_0)_{\text{critical}} = 15.83$, $NL/d_0 = 400$ and $L/d_0 = 2$

In order to understand the portion of unburned droplet, we have observed the ratio between the number of unburned droplet (M_{ub}) and lattice area $(NL)^2$ for 2D droplet arrangement and the ratio between the number of unburned droplet (M_{ub}) with lattice volume $(NL)^3$ for 3D droplet arrangement. Therefore, we have the behavior of unburned droplet for each droplet arrangement per mm^2 or mm^3.

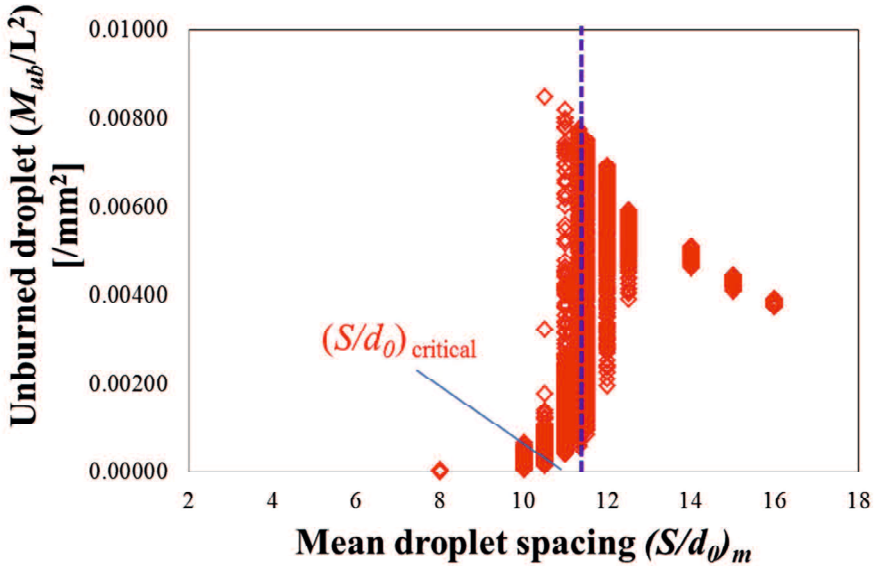

Figure 3.13 Unburned droplet on mean droplet spacing $(S/d_0)_m$ 2D droplet arrangement for $L/d_0 = 2$ and $NL/d_0 = 400$

Figure 3.13 shows the number of unburned droplet (M_{ub}/L^2) on the mean droplet spacing $(S/d_0)_m$ 2D droplet arrangement for $L/d_0 = 2$ and $NL/d_0 = 700$. From this figure, we know that for $(S/d_0)_m < 8$ flame spread to all the droplets on the lattice or group combustion always occurs, so there is no unburned droplet on the lattice. The unburned droplets (M_{ub}/L^2) appears start from $(S/d_0)_m = 8$ and increases with increasing mean droplet spacing. For $8 \leq (S/d_0)_m \leq 11.32$ the number of unburned droplet (M_{ub}/L^2) has a wide range of value and attains the maximum value near the critical mean droplet spacing. This is because for $8 \leq (S/d_0)_m \leq 11.32$ have two type of flame-spread i.e. flame can spread to all the side of lattice (group combustion occurs) and flame cannot spread to all the side of lattice (group combustion doesn't occurs). If the mean droplet spacing is increased after reach the critical mean droplet spacing $(S/d_0)_{critical}$, the number of unburned droplet (M_{ub}/L^2) shows the decreasing function. This is due to decreasing of the occurrences of group combustion on the lattice which has the large value of mean droplet spacing. Therefore, the number of unburned droplets attains maximum for the mean droplet spacing slightly greater than the critical mean droplet spacing.

3.1.3 Flame spread rate

In this simulation, the flame-spread time (t_f/d_0) or flame-spread rate ($V_f d_0$) was taken from microgravity experiment by Mikami et al., 2005. They reported that flame-spread was classified as follows. Case 1 where the droplet spacing (S/d_0) is relatively small, the thermal conduction time (t_c) is small and flame-spread time (t_f) was accounted from droplet heating time (t_h). Case 2 where the droplet spacing (S/d_0) is relatively large, the flame-spread time was accounted from thermal conduction time (t_c).

Figure 3.14 and 3.15 shows example of flame-spread behavior of ignition time at critical threshold mean droplet spacing for L/d_0 = 2, 2D droplet arrangement and 3D droplet arrangement. We can see that on the critical mean droplet spacing, the droplets randomly distributed on the lattice in various droplet spacing. Therefore flame-spread time from bottom side or bottom face to all sides or faces of lattice doesn't spread straightly but spread in complicated path.

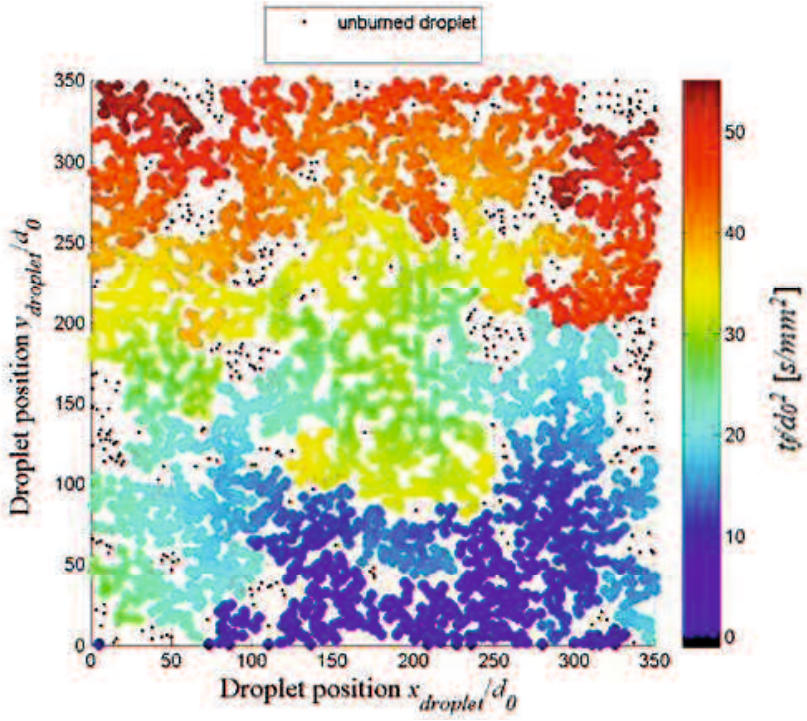

Figure 3.14 Flame-spread behaviors of ignition time at critical threshold mean droplet spacing 2D droplet arrangement $(S/d_0)_{critical}$=11.32 (M = 3825), NL/d_0=700 and L/d_0 = 2

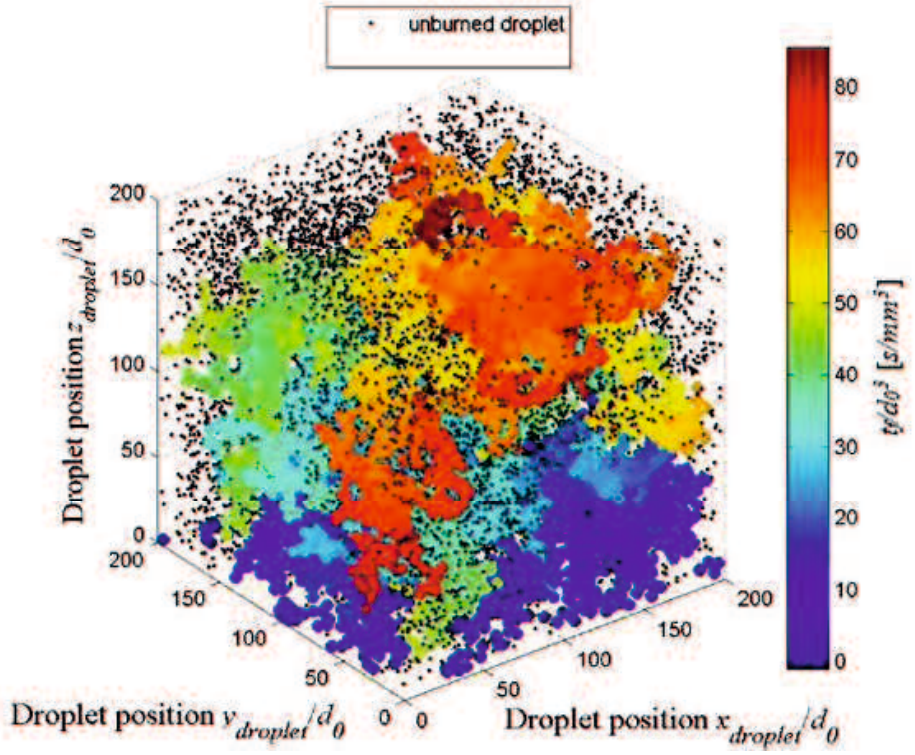

Figure 3.15 Flame-spread behaviors of ignition time at critical threshold mean droplet spacing 3D droplet arrangement $(S/d_0)_{critical}$=15.83 (M = 16134), NL/d_0=400 and L/d_0 = 2

In order to investigate the characteristic of ignition time of flame-spread, we observe the ignition time of last burned droplet. Figure 3.16 shows the ignition time of last burned droplet on mean droplet spacing $(S/d_0)_m$. When the mean droplet spacing $(S/d_0)_m$ is small, the ignition time of last burned droplet is almost constant. However, as the $(S/d_0)_m$ increases, the ignition time of last burned droplet is increases and for $(S/d_0)_m$ near the critical threshold mean droplet spacing, the ignition time of last burned droplet has wide range of values.

Same as flame-spread time (t_f/d_0), the flame-spread rate ($V_f d_0$) is controlled by the droplet heating for relatively small droplet spacing (S/d_0) and by thermal conduction for large droplet spacing $(S/d_0)_m$ (Mikami et al., 2005). The simulation results (Fig. 3.17) shows that flame-spread rate at small $(S/d_0)_{\mathrm{m}}$ is almost constant and flame-spread rate ($V_f d_0$) is decreases, when the $(S/d_0)_m$ increases. Same as

time ignition of last burned droplet, the flame spread rate near the critical threshold mean droplet spacing has a wide range of value.

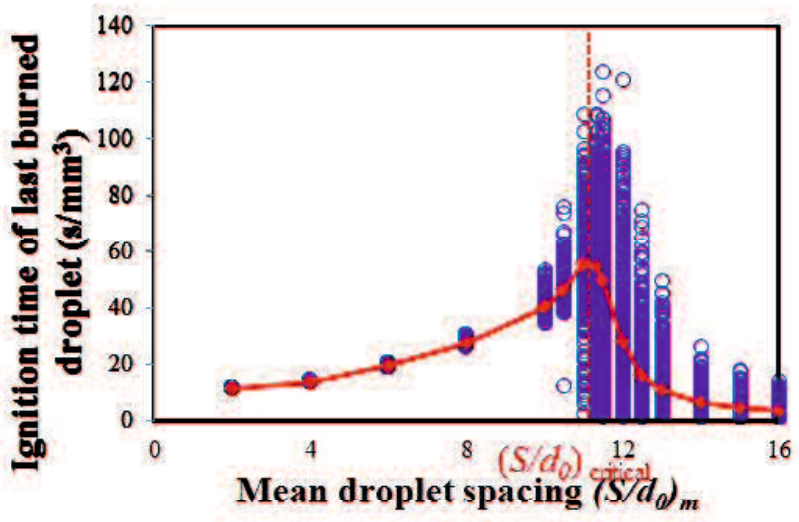

a. 2D droplet arrangement for $NL/d_0 = 700$ and $L/d_0 = 2$

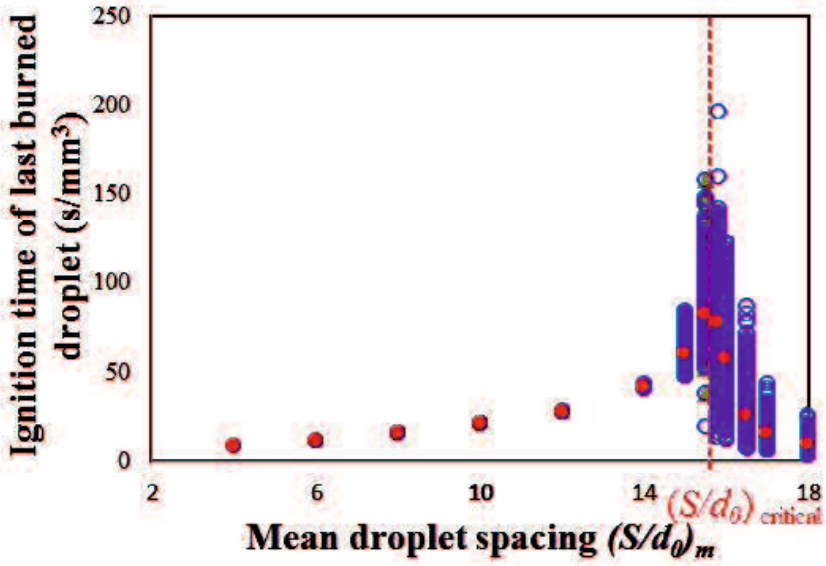

b. 3D droplet arrangement for $NL/d_0 = 400$ and $L/d_0 = 2$

Figure 3.16 Ignition time of last burned droplet on mean droplet spacing $(S/d_0)_m$

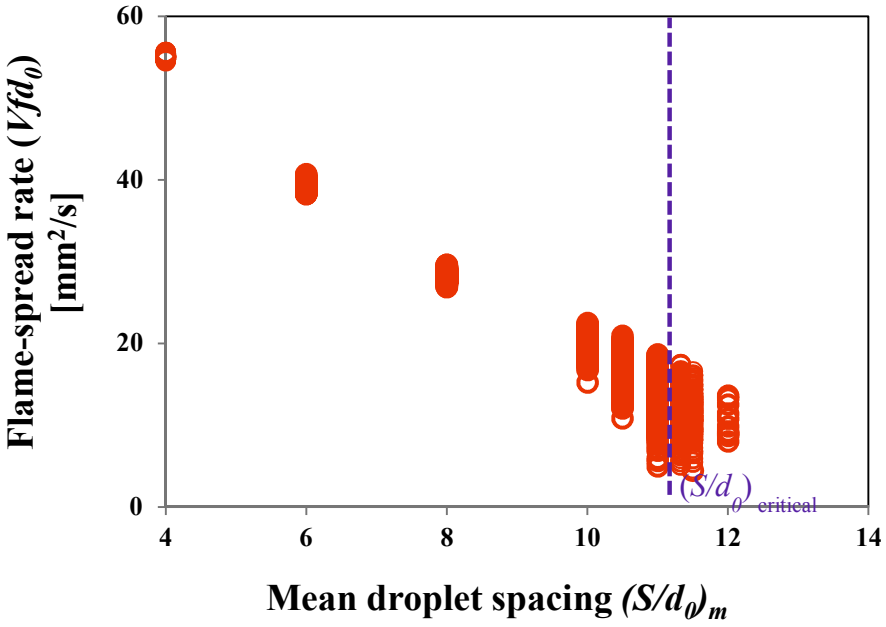

a. 2D droplet arrangement for $NL/d_0 = 700$ and $L/d_0 = 2$

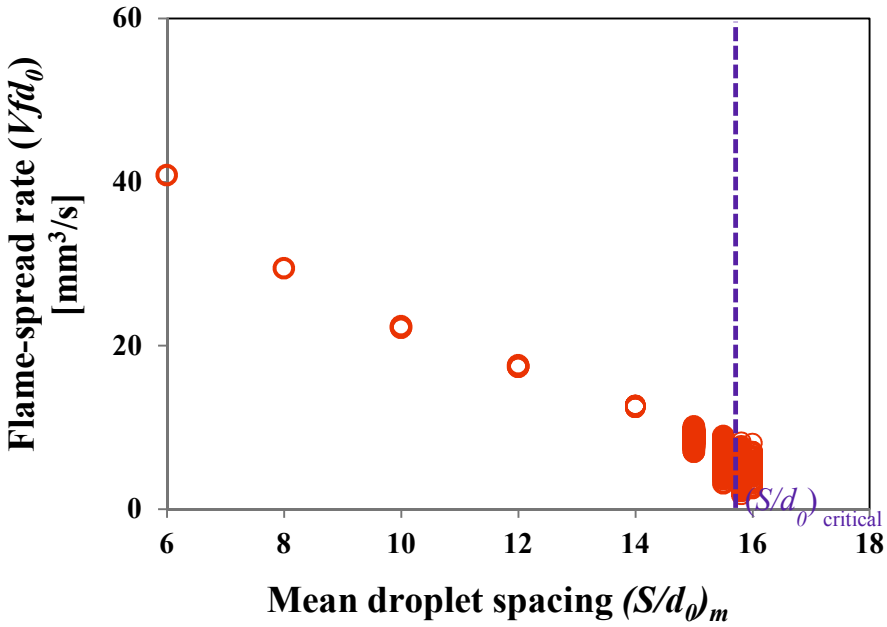

b. 3D droplet arrangement for $NL/d_0 = 400$ and $L/d_0 = 2$

Figure 3.17 Flame-spread rate on mean droplet spacing $(S/d_0)_m$

3.1.4 Summary

This research conducted the numerical study on flame spread behavior based on the microgravity experimental results, in order make a theoretical link between droplet combustion and spray combustion. The simulations of flame-spread behavior in randomly distributed droplet clouds without considering droplet interaction is performed in 2D and 3D droplet arrangements. Mean droplet spacing $(S/d_0)_m$, lattice size (NL/d_0) and lattice point interval (L/d_0) were varied in order to calculate the occurrence probability of group combustion (OPGC) and investigate the flame behavior in large-scale droplet clouds. The result shows that;

1. The occurrence probability of group combustion OPGC rapidly decreases around the critical mean droplet spacing $(S/d_0)_{critical}$ as the mean droplet spacing $(S/d_0)_m$ is increased.
2. When the lattice size, NL/d_0 is increased, the OPGC graph approaches a step function in which OPGC is unity for $(S/d_0)_m$ less than the threshold value and zero for $(S/d_0)_m$ greater than the threshold value, and the critical mean droplet spacing $(S/d_0)_{critical}$ approaches the threshold value.
3. The $(S/d_0)_{critical}$ in 3D droplet arrangement is greater than that in 2D droplet arrangement.
4. Even when the group combustion occurs, a portion of the droplets remains unburned. The number of unburned droplets attains maximum for the mean droplet spacing slightly greater than the critical mean droplet spacing.
5. The ignition time of the last burned droplet has a wide range of values, and the averaged ignition time attains maximum around the critical mean droplet spacing, showing the characteristic time of flame spread in randomly distributed droplet cloud attains maximum. Thus, the flame spread rate over the droplet cloud also has a wide range of values around the critical mean droplet spacing.

3.2 Simulation based on flame-spread characteristics of droplet array at normal pressure and high temperature

On the Chapter 3.1, the simulation of flame-spread behavior and group combustion excitation has been discussed at normal pressure and room temperature, but most of the real fuel spray combustion has been occurred at high-temperature condition. Mikami et al., 2006 reported that the flame spread-limit droplet spacing was affected by the ambient temperature and the flame-spread rate at high temperature (600^{o}K) is approximately twice as high as that at room temperature (300^{o}K). Thus, the investigation of flame-spread behavior and group combustion excitation of large-scale droplet cloud at high-temperature condition is also important.

Experimental study on the droplet array of n-decane fuel at in normal pressure (101kPa) and high temperature (600^{o}K) has shown that the flame-spread have a maximum limit distance $(S/d_0)_{limit} = 17$, flame cannot spread to the next droplet if the position is over the flame-spread limit distance. In order to simulate the flame-spread behavior and group combustion excitation at high-temperature condition, we used percolation approach same as the previous simulation. The simulation results of flame-spread behavior and group combustion excitation at normal pressure and high temperature are discussed in detail.

3.2.1 Occurrence Probability of Group Combustion (OPGC)

The effect of increasing mean droplet spacing on the simulation at room temperature and high temperature shows the similar tendency (Fig. 3.18). When the mean droplet spacing $(S/d_0)_m$ is increased, the OPGC rapidly decreases around a specific value of $(S/d_0)_m$ for each case. However, at the same value of mean droplet spacing $(S/d_0)_m$ the OPGC value of flame-spread simulation at high temperature is higher than that flame-spread simulation at room temperature. So, the graph of OPGC versus mean droplet spacing $(S/d_0)_m$ for flame-spread simulation at high temperature shift to the right side from graph of OPGC versus mean droplet spacing $(S/d_0)_m$ flame-spread simulation at room temperature.

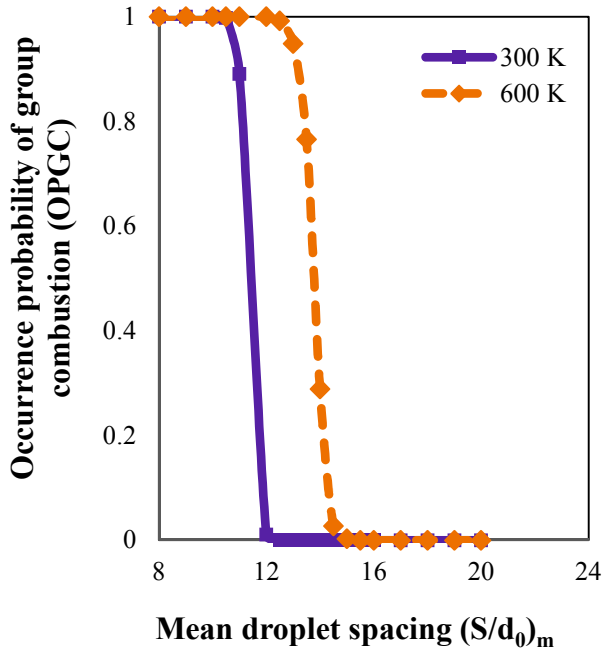

a. 2D droplet arrangement

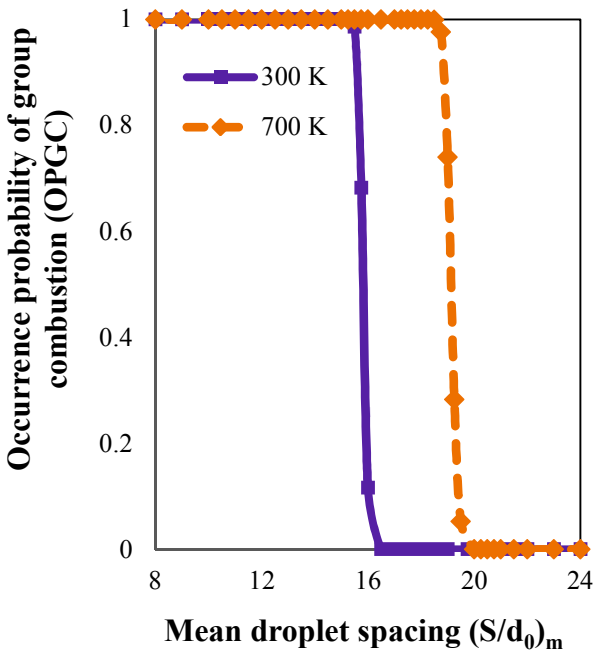

b. 3D droplet arrangement

Figure 3.18 The comparison of OPGC on mean droplet spacing $(S/d_0)_m$ for L/d_0= 2 between simulation of flame-spread behavior at room temperature (300°K) and high temperature (600°K)

This phenomenon certainly affects to the critical mean droplet spacing $(S/d_0)_{critical}$. As shown in Fig. 3.19 when the lattice size (NL/d_0) is increased, the critical mean droplet spacing increases at the specific value of NL/d_0 and the increasing of $(S/d_0)_{critical}$ shown the constant tendency when the lattice size approach the threshold value.

However, in order to observe the relation and comparison between the flame-spread phenomena at room temperature and high temperature is needed the normalization analysis of data from both simulations. By using data in Fig. 3.19 the normalization data was calculated, wherein vertical axis is ratio between critical mean droplet spacing $(S/d_0)_{critical}$ and flame-spread limit distance $(S/d_0)_{limit}$ and the horizontal axis is ratio between lattice size (NL/d_0) and flame-spread limit distance $(S/d_0)_{limit}$. Figure 3.20 shows the normalization analysis of data from the flame-spread simulation at room temperature (300^oK) and high temperature (600^oK). The results show that the both condition has similar tendency in normalization graph. Therefore, the comparison between flame-spread simulation at room temperature (300^oK) and high temperature (600^oK) can be done.

From the Fig. 3.18 we can see that the threshold value of $(S/d_0)_m$ appears at lattice size (NL/d_0) = 700 for 2D droplet arrangement and NL/d_0 = 400 for 3D droplet arrangement. This is because at that position the graph of OPGC versus mean droplet spacing $(S/d_0)_m$ approach the step function. The lattice size (NL/d_0) location of appearance of threshold value is similar as flame-spread simulation at room temperature, but the threshold value of $(S/d_0)_m$ simulation at high temperature is higher than that simulation at room temperature. Figure 3.19 shows that the critical mean droplet spacing $(S/d_0)_{critical}$ of flame-spread simulation at high temperature (600^oK) is higher than that flame-spread simulation at room temperature (300^oK). The critical mean droplet spacing of flame-spread simulation at high temperature is 13.8 for 2D droplet arrangement and 19.1 for 3D droplet arrangement. This means, when the flame spread occurs at high temperature, the excitation of group combustion could be occurred in large of mean droplet spacing $(S/d_0)_m$ comparing with room temperature.

Thus, by this simulation is obtained information that the excitation of group combustion is affected by the ambient temperature. If comparing with flame-spread simulation at room temperature, the excitation of group combustion at high temperature is higher than that at room temperature. Therefore, this is in line with the microgravity experimental results of droplet array at high temperature by Mikami et al., 2006, wherein the flame spread-limit droplet spacing was affected by the ambient temperature.

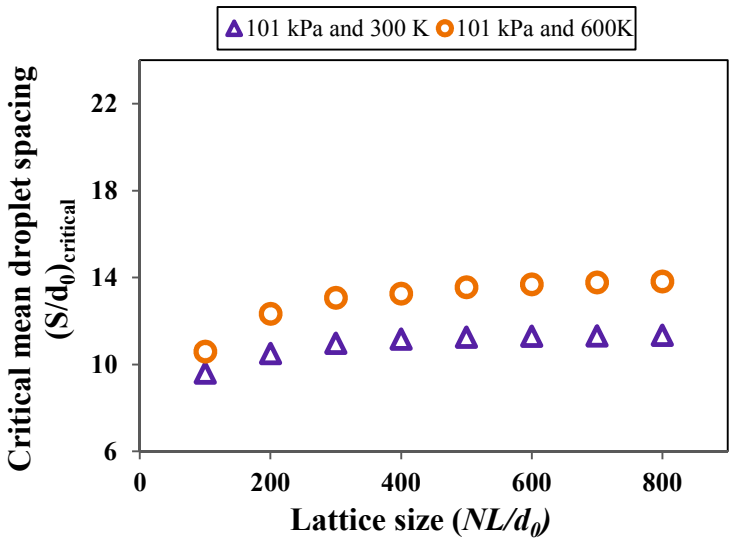

a. 2D droplet arrangement

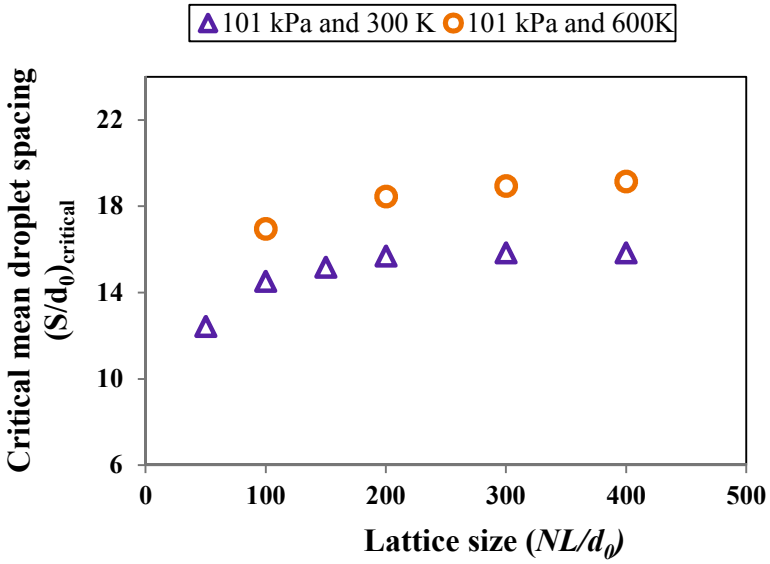

b. 3D droplet arrangement

Figure 3.19 Dependences of critical mean droplet spacing $(S/d_0)_{critical}$ on lattice size NL/d_0 flame-spread at room temperature (300°K) and high temperature (600°K) for 2D and 3D droplet arrangements

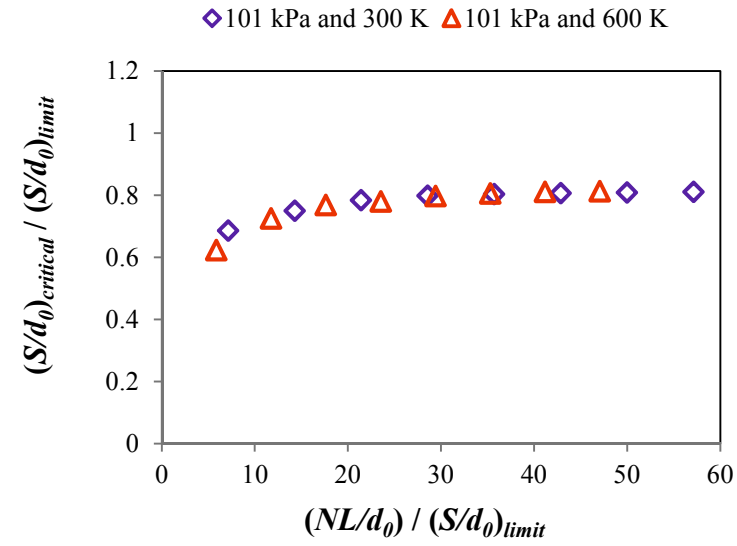

a. 2D droplet arrangement

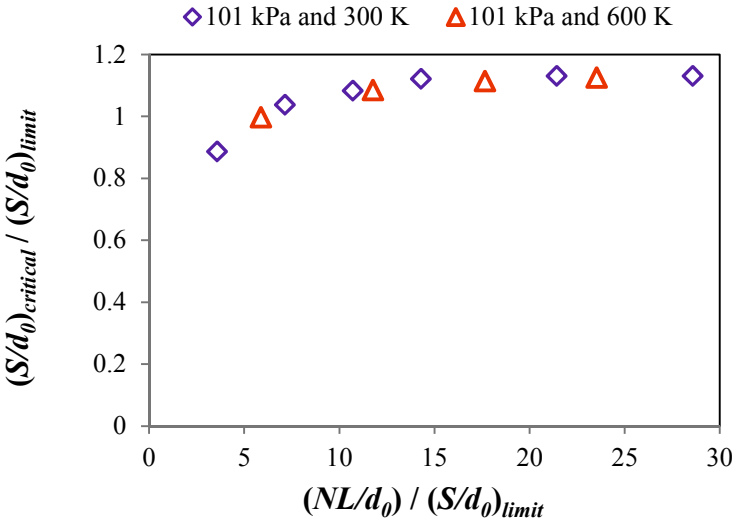

b. 3D droplet arrangement

Figure 3.20 the normalization analysis of data from the flame-spread simulation at room temperature (300^{o}K) and high temperature (600^{o}K) for 2D and 3D droplet arrangements

3.2.2 Flame-spread behavior near the critical threshold mean droplet spacing

The critical threshold mean droplet spacing separates the droplet cloud into two group; relatively dense droplet clouds in which the group combustion is exited through flame spread and dilute droplet clouds in which the group combustion is never excited. Therefore, in this simulation critical threshold mean droplet spacing is interesting to be explored because the condition near the percolation threshold could be to guide understanding of real physical of flame-spread in large scale.

Figure 3.21 and 3.22 show examples of distribution of flame-spread on the lattice, including the flame-spread ignition time for 2D droplet arrangement and 3D droplet arrangement near the critical mean droplet spacing $(S/d_0)_{critical}$. This figure shows that the flame spread reaches all the sides of lattice in 2D droplet arrangement and all the surfaces of the lattice in 3D droplet arrangement and the group combustion excited. Even when the group combustion excited, a portion of the droplet remains unburned. This behavior is relevant with the real condition of the spray combustion engine which is almost impossible to achieve the complete combustion or the incomplete combustion is much more common.

By the flame-spread time history in Fig. 3.21 and 3.22, we can see that the flame doesn't spread straightly from bottom side or surface of lattice to the upper side or surface of lattice, but flame spreads in complicated paths. This behavior shows similarities with the real condition of flame-spread in fuel spray combustion engine.

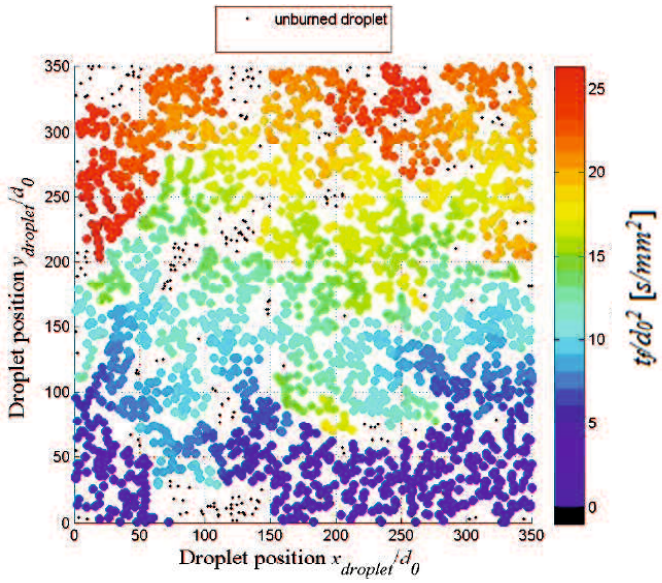

Figure 3.21 Flame-spread behaviors of ignition time at near critical threshold mean droplet spacing 2D droplet arrangement $(S/d_0)_{critical}$ =13.8, NL/d_0 = 700 and L/d_0=2

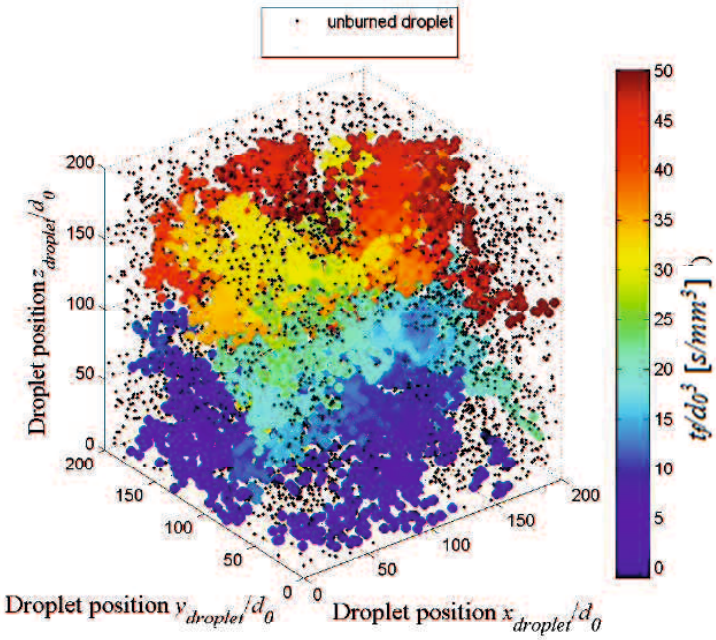

Figure 3.22 Flame-spread behaviors of ignition time at near critical threshold mean droplet spacing 3D droplet arrangement $(S/d_0)_{critical}$ =19.1, NL/d_0 = 400 and L/d_0 = 2

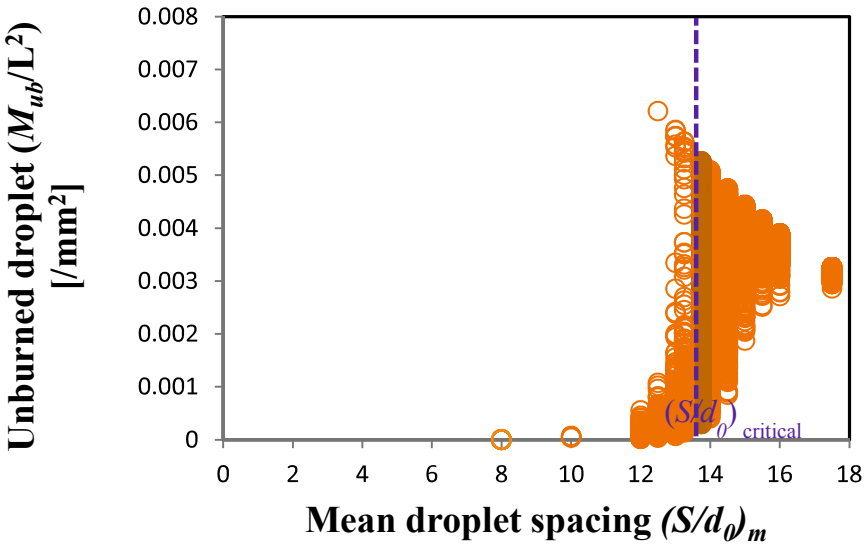

Figure 3.23 The unburned droplet on mean droplet spacing $(S/d_0)_m$ 2D droplet arrangement for $L/d_0 = 2$ and $NL/d_0 = 700$ flame-spread simulation at high temperature

In order to understand the portion of unburned droplet, we have observed the ratio between the number of unburned droplet (M_{ub}) with lattice area $(NL)^2$ for 2D droplet arrangement or the ratio between the number of unburned droplet (M_{ub}) with lattice volume $(NL)^3$ for 3D droplet arrangement. Therefore, we have the behavior of unburned droplet for each droplet arrangement per mm^2 or mm^3.

Figure 3.23 shows the unburned droplet (M_{ub}/L^2) on mean droplet spacing $(S/d_0)_m$ 2D droplet arrangement for $L/d_0 = 2$ and $NL/d_0 = 700$. From this figure, we can see that for $(S/d_0)_m < 8$ flame spread to all the droplets on the lattice or group combustion always occurs, there is no unburned droplet on the lattice. The number of unburned droplet (M_{ub}/L^2) appears start from $(S/d_0)_m = 8$ and increases with increasing mean droplet spacing. For $8 \leq (S/d_0)_m \leq 13.8$ the unburned droplet (M_{ub}) has a wide range of value. This is because for $8 \leq (S/d_0)_m \leq 13.8$ has two type of flame-spread i.e. flame can spread to all the side of lattice (group combustion occurs) and flam cannot spread to all the side of lattice (group combustion doesn't occurs). As the mean droplet spacing is increased after reach the critical mean droplet spacing $(S/d_0)_{critical}$, the number of unburned droplet

(M_{ub}/L^2) shows the decreasing function. This is due to decreasing of the occurrences of group combustion on the lattice which has the large value of mean droplet spacing. Therefore, the number of unburned droplets attains maximum for the mean droplet spacing slightly greater than the critical mean droplet spacing.

In order to observes the effect of ambient temperature in flame-spread behavior, Fig. 3.24 and 3.25 shows the flame spread behavior for $(S/d_0)_m$ which is between $(S/d_0)_{critical}$ flame-spread at room temperature and high temperature. This figure is comparison between flame-spread at room temperatur and high temperature, wherein the simillar of droplet arrangement was simulated in role of flame-spread at room temperature and high temperature. In order to get the detail discription of comparison of both condition, we taken $(S/d_0)_m = 14$ for 2D droplet arrangement and $(S/d_0)_m = 17.5$ for 3D droplet arrangement.

When the mean droplet spacing $(S/d_0)_m$ greater than that $(S/d_0)_{critical}$, the flame-spread simulation at room temperature shown that flame spread in complicated path but flame-spread terminates on its way to the sides or surface of lattice (Fig. 3.24a and 3.25a). However, the flame-spread can reach all the sides or surface of lattice and the group combustion exited when the simulation conducted at high temperature (600^oK) (Fig. 3.24b and 3.25b). When the droplet arrangement was simulated at high temperature the unburned droplet region decreases. This is because the flame-spread limit distance $(S/d_0)_{limit}$ increases when the flame spread at high temperature, as explained on the previous Chapter.

From the comparison between flame-spread simulation at room temperature and high temperature, we know that ambient temperature has the effect on the flame-spread behavior and group combustion excitation. This is due to the effect of local-flame spread limit distance, wherein the $(S/d_0)_{limit}$ at high temperature is higher than that at room temperature.

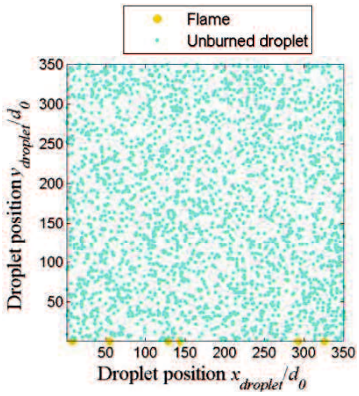

(a1). Elapsed time= 0 s/mm^2

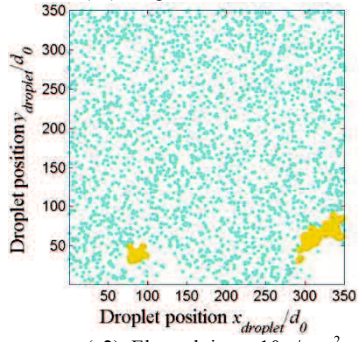

(a2). Elapsed time= 10 s/mm^2

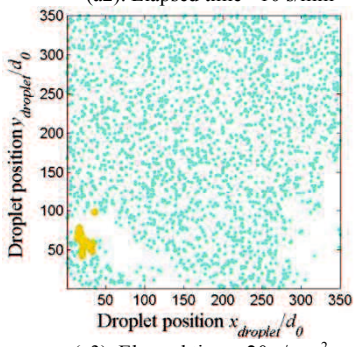

(a3). Elapsed time= 20 s/mm^2

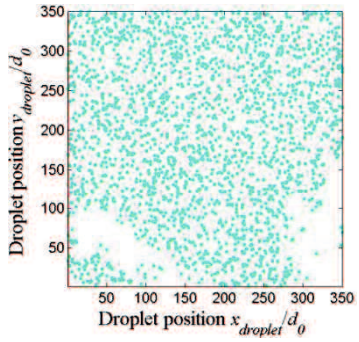

(a4). Elapsed time= 25 s/mm^2

a. Flame-spread simulation at normal pressure and room tempt. (300^{o}K)

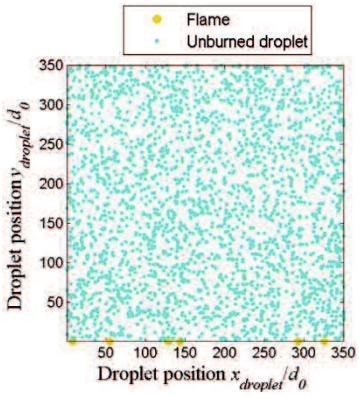

(b1). Elapsed time= 0 s/mm^2

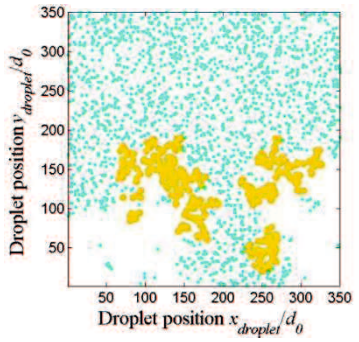

(b2). Elapsed time= 10 s/mm^2

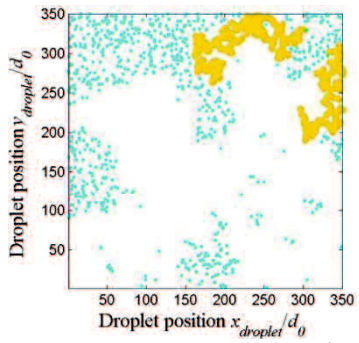

(b3). Elapsed time= 25 s/mm^2

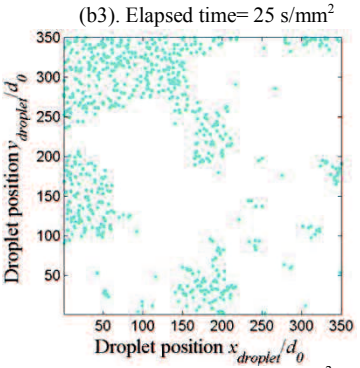

(b4). Elapsed time=32 s/mm^2

b. Flame-spread simulation at normal pressure and high tempt. (600^{o}K)

Figure 3.24 Flame-spread behavior in a 2-D droplet arrangement for $(S/d_0)_m$=14, which is between $(S/d_0)_{critical}$ flame-spread at room temperature and $(S/d_0)_{critical}$ flame-spread at high temperature

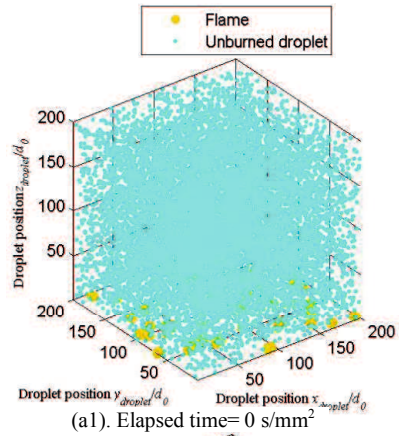

(a1). Elapsed time= 0 s/mm^2

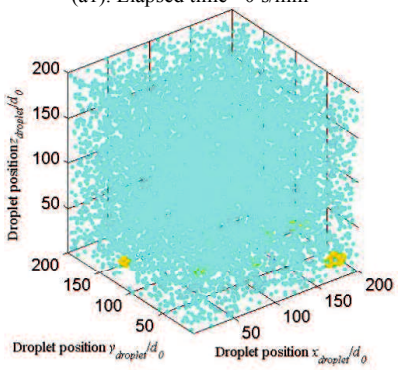

(a2). Elapsed time= 5 s/mm^2

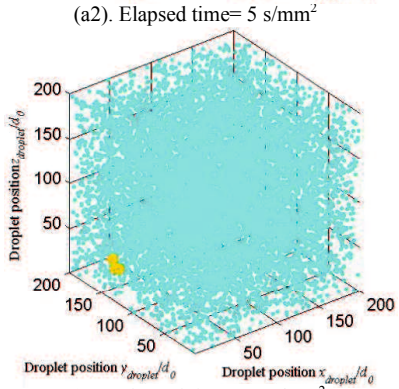

(a3). Elapsed time= 10 s/mm^2

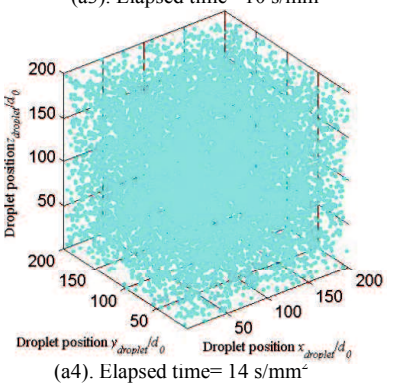

(a4). Elapsed time= 14 s/mm^2

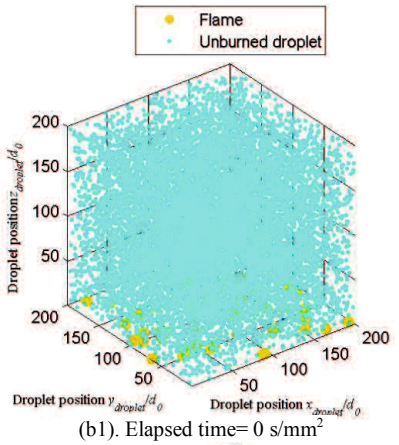

(b1). Elapsed time= 0 s/mm^2

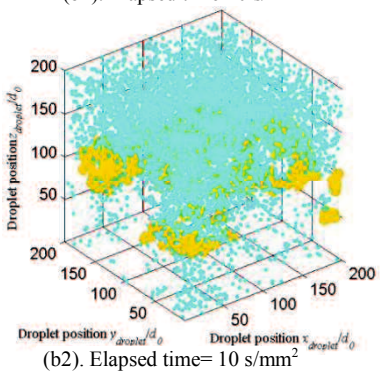

(b2). Elapsed time= 10 s/mm^2

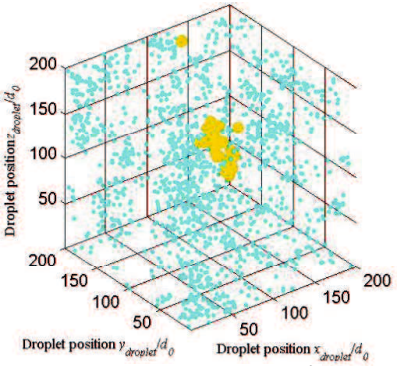

(b3). Elapsed time= 20 s/mm^2

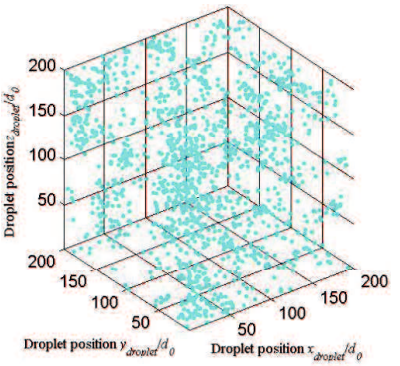

(b4). Elapsed time= 14 s/mm^2

a. Flame-spread simulation at normal pressure and room tempt. (300^{o}K)

b. Flame-spread simulation at normal pressure and high tempt. (600^{o}K)

Figure 3.25 Flame-spread behavior in a 3D droplet arrangement for $(S/d_0)_m$=17.5, which is between $(S/d_0)_{critical}$ flame-spread at room temperature and $(S/d_0)_{critical}$ flame-spread at high temperature

3.2.3 Flame-spread rate

Figure 3.21 and 3.22 shows examples of flame-spread behavior ignition time at critical threshold mean droplet spacing for L/d_0 = 2, 2D droplet arrangement and 3D droplet arrangement. The flame-spread time from bottom side or bottom face to all sides or faces of lattice doesn't spread straightly but spread in complicated path. This section compares the ignition time of last burned droplet [s/mm^2] and flame-spread rate [mm^2/s] between flame-spread simulation at room temperature and high temperature as shown in Fig. 3.26 and 3.27.

When the mean droplet spacing $(S/d_0)_m$ is small enough, the ignition time of last burned and flame-spread rate are almost constant. However, as the $(S/d_0)_m$ increases, the ignition time of last burned droplet is increases and the flame-spread rate is decreases. The ignition time of the last burned droplet has a wide range of values, and the averaged of ignition time attains maximum around the critical mean droplet spacing. Therefore, this is showing the characteristic time of flame spread in randomly distributed droplet cloud. Thus, the flame spread rate over the droplet cloud also has a wide range of values around the critical mean droplet spacing and the flame-spread rate reaches minimum around the critical mean droplet spacing.

The comparison shows that the ignition time of last burned droplet at high temperature is smaller than at room temperature. Therefore, the flame-spread rate at high temperature is faster than at room temperature Fig. 3.26 and 3.27. This result is in line with the experimental results of Mikami et al., 2006 wherein the ambient temperature was increased from 300 to 600 K, the flame-spread rate increases to approximately twice as large as that for 300 K.

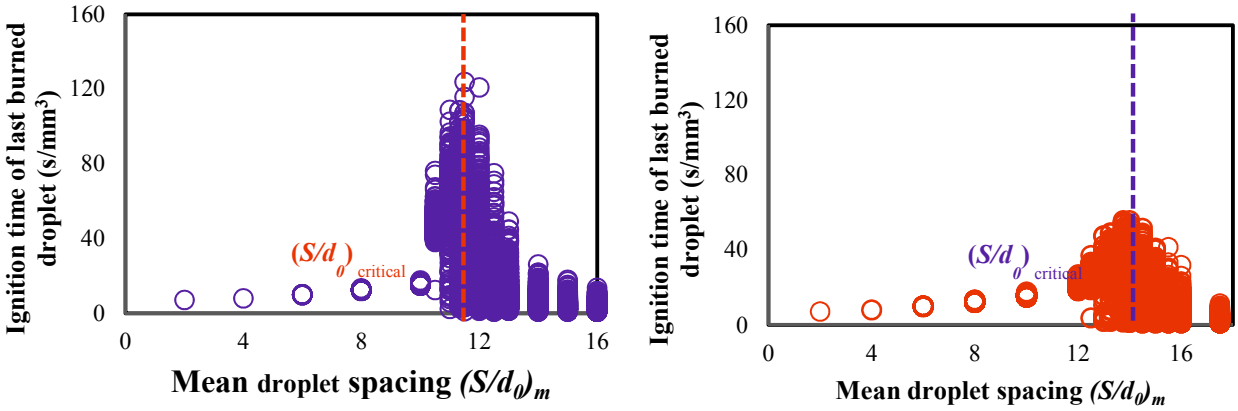

a. The ignition time of last burned droplet at normal pressure and room tempt. (300°K)

b. The ignition time of last burned droplet at normal pressure and high tempt. (600°K)

Figure 3.26 The ignition time of last burned droplet on mean droplet spacing $(S/d_0)_m$ for flame-spread at room temperature and high temperature 2D droplet arrangement

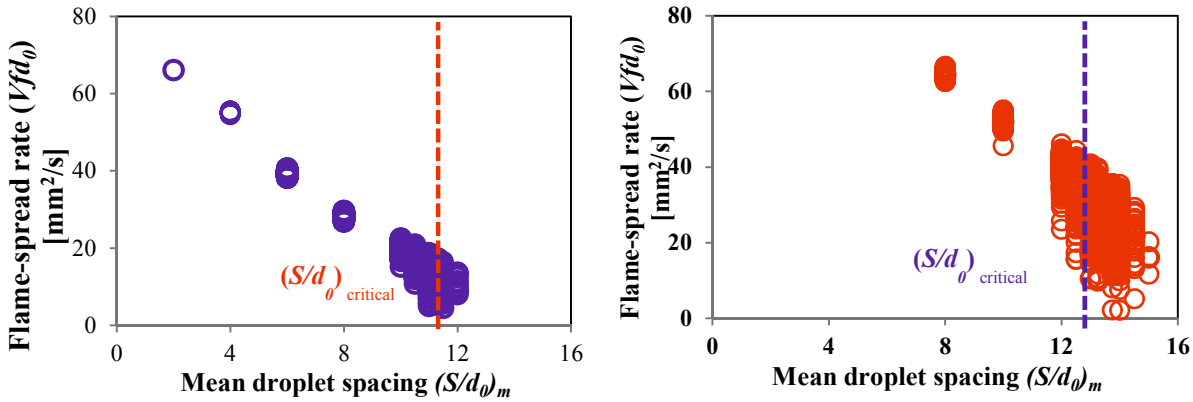

b. Flame-spread rate at normal pressure and room tempt. (300°K)

a. Flame-spread rate at normal pressure and high tempt. (600°K)

Figure 3.27 The flame-spread rate on mean droplet spacing $(S/d_0)_m$ for flame-spread at room temperature and high temperature 2D droplet arrangement

3.2.4 Summary

In this section we have discussed the comparison of flame-spread behavior at normal pressure but different ambient temperature i.e. room temperature (300^oK) and high temperature (600^oK). We conclude that:

a. The ambient temperature affects the flame-spread behavior and group combustion excitation. Wherein the excitation of group combustion at high temperature is higher than that at normal temperature. This is due to the effect of local-flame spread limit distance, wherein the $(S/d_0)_{limit}$ at high temperature is higher than that at room temperature
b. The unburned droplet region for flame-spread simulation at high temperature is lower than that flame-spread simulation at room temperature.
c. The ignition time of last burned droplet at high temperature is smaller than at room temperature and the flame-spread rate at high temperature is faster than at room temperature.

3.3 Simulation based on flame-spread characteristics of droplet array at low pressure and normal temperature

On the Chapter 3.1 and 3.2 have been discussed the simulation of flame-spread behavior and group combustion excitation at normal pressure and room temperature, and normal pressure and high temperature. In this Chapter the flame-spread behavior at low pressure and room temperature is discussed. The objective of this study is to understanding of the flame spread of fuel sprays under the high-altitude, i.e. relight conditions of jet engines. Mikami et al., 2014 reported that the flame-spread rate and flame-spread limit distance at the low pressure are greater than those at atmospheric pressure. Experimental study on the droplet array of n-decane fuel at low pressure (25kPa) and room temperature (300^{o}K) shown that the flame-spread have a maximum limit distance $(S/d_0)_{limit}$ = 20. Therefore, investigation of flame-spread behavior and group combustion excitation at low pressure condition is also important to be explored. In order to simulate the flame-spread behavior and group combustion excitation, we used percolation approach same as the previous simulation. The simulation results of flame-spread behavior and group combustion excitation at low pressure and room temperature are explained as follows.

3.3.1 Occurrence Probability of Group Combustion (OPGC)

As shown on Fig. 3.28 the effect of increasing mean droplet spacing between the simulation at normal pressure and low pressure has similar tendency, i.e. when the mean droplet spacing $(S/d_0)_m$ is increased, the OPGC rapidly decreases around a specific value of $(S/d_0)_m$ for each case. However, at the same value of mean droplet spacing $(S/d_0)_m$ the OPGC value of flame-spread simulation at low pressure is higher than that flame-spread simulation at normal pressure. Thus, the graph of OPGC versus mean droplet spacing $(S/d_0)_m$ for the flame-spread simulation at high temperature shift to the right side from the simulation at normal pressure.

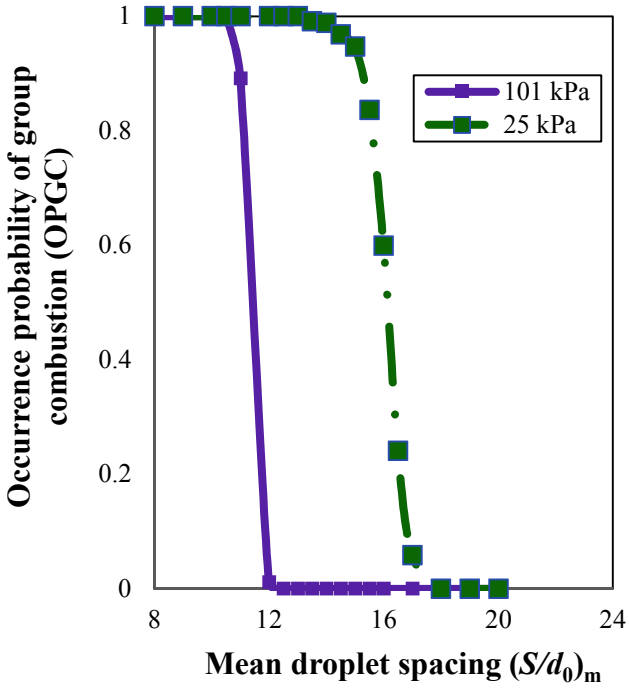

a. 2D droplet arrangement

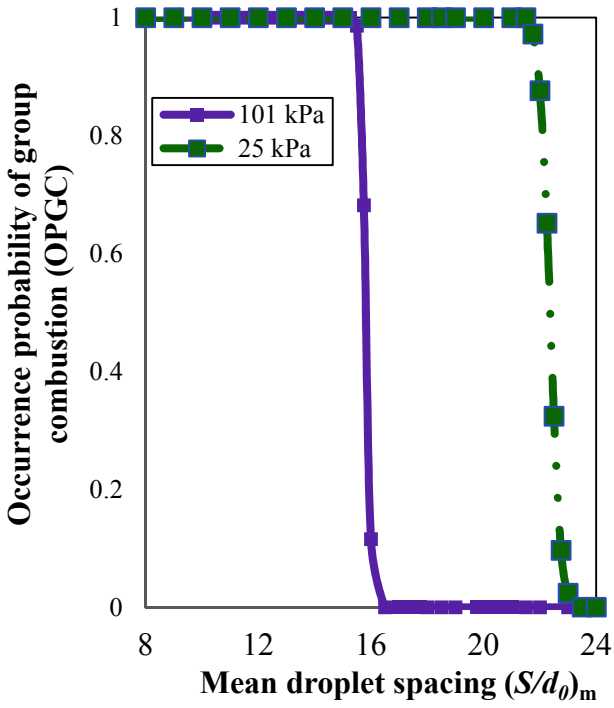

b. 3D droplet arrangement

Figure 3.28 The comparison of OPGC on mean droplet spacing $(S/d0)_m$ for L/d_0=2 between simulation of flame-spread behavior at normal pressure (101kPa) and low pressure (25kPa)

This phenomenon certainly affects to the critical mean droplet spacing $(S/d_0)_{critical}$. As shown in Fig. 3.29 when the lattice size (NL/d_0) is increased, the critical mean droplet spacing increases at the specific value of NL/d_0 and the increasing of $(S/d_0)_{critical}$ shown the constant tendency when the lattice size approach the threshold value.

However, in order to observe the relation and comparison between the flame-spread phenomena at normal pressure and low pressure is needed the normalization analysis of data from both simulation results. By using data in Fig. 3.29 the normalization data was calculated, wherein vertical axis is ratio between critical mean droplet spacing $(S/d_0)_{critical}$ and flame-spread limit distance $(S/d_0)_{limit}$ and the horizontal axis is ratio between the lattice size (NL/d_0) and flame-spread limit distance $(S/d_0)_{limit}$. Figure 3.30 shows the normalization analysis of data from the flame-spread simulation at normal pressure (101kPa) and low pressure (25kPa). The results show that the both condition has similar tendency in normalization graph. Therefore, the comparison between flame-spread simulation at normal pressure (101kPa) and low pressure (25kPa) could be done.

Figure 3.28 shows that the threshold value of $(S/d_0)_m$ appears at lattice size (NL/d_0) = 700 for 2D droplet arrangement and NL/d_0 = 400 for 3D droplet arrangement. This is because at that position the graph of OPGC versus mean droplet spacing $(S/d_0)_m$ approach the step function. The lattice size (NL/d_0) location of appearance of threshold value is similar as flame-spread simulation at normal pressure, but the threshold value of $(S/d_0)_m$ simulation at low pressure is higher than that simulation at normal pressure. Figure 3.29 show that the critical mean droplet spacing $(S/d_0)_{critical}$ of flame-spread simulation at low pressure (25kPa) is higher than flame-spread simulation at normal pressure (101kPa). The critical thresholds mean droplet spacing of flame-spread simulation at low pressure is 16.1 for 2D droplet arrangement and 22.3 for 3D droplet arrangement. This means, when the flame spread occurs at low pressure, the excitation of group combustion could be occurred in large of mean droplet spacing $(S/d_0)_m$ comparing with normal pressure.

Therefore, from this simulation we know that the excitation of group combustion is affected by the pressure condition. When it is compared with flame-spread simulation at normal pressure (101kPa), the excitation of group combustion at low pressure is higher than that at normal pressure. Therefore, this is in line with the microgravity experimental results of droplet array at low pressure by Mikami et al., 2014, wherein the flame-spread limit distance at the low pressure is greater than those at atmospheric pressure.

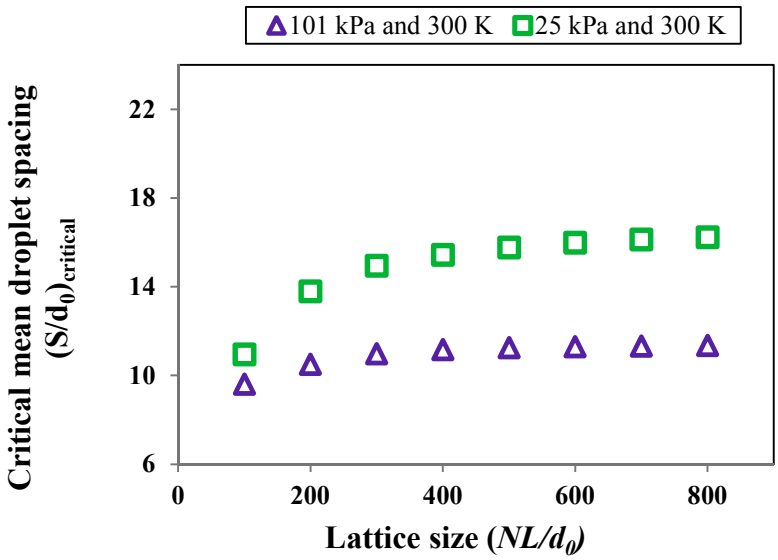

a. 2D droplet arrangement

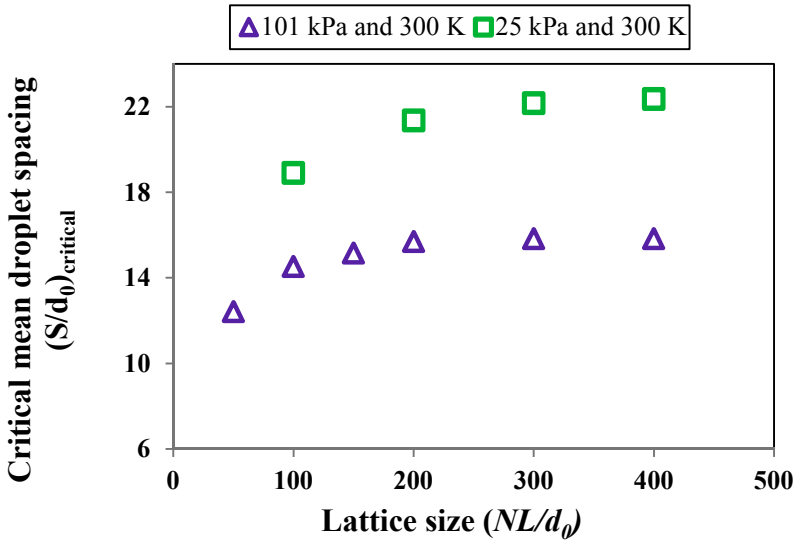

b. 3D droplet arrangement

Figure 3.29 Dependences of critical mean droplet spacing $(S/d_0)_{critical}$ on lattice size NL/d_0 flame-spread at normal pressure (101kPa) and low pressure (25kPa) for 2D and 3D droplet arrangements

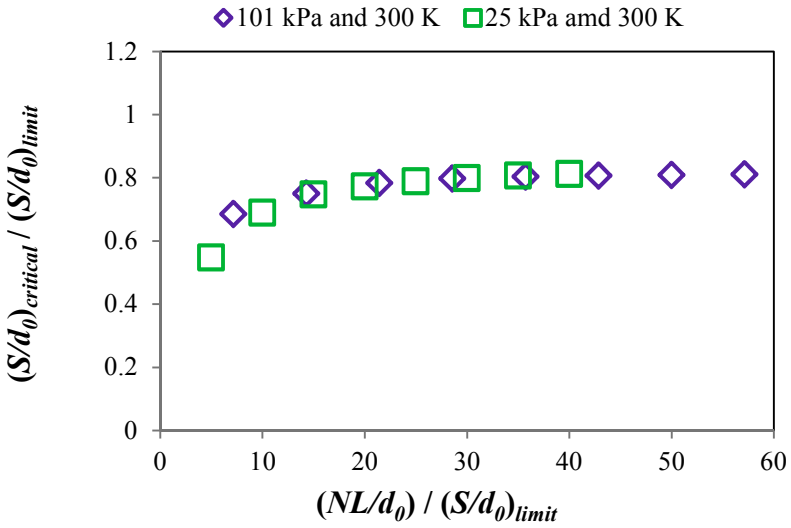

a. 2D droplet arrangement

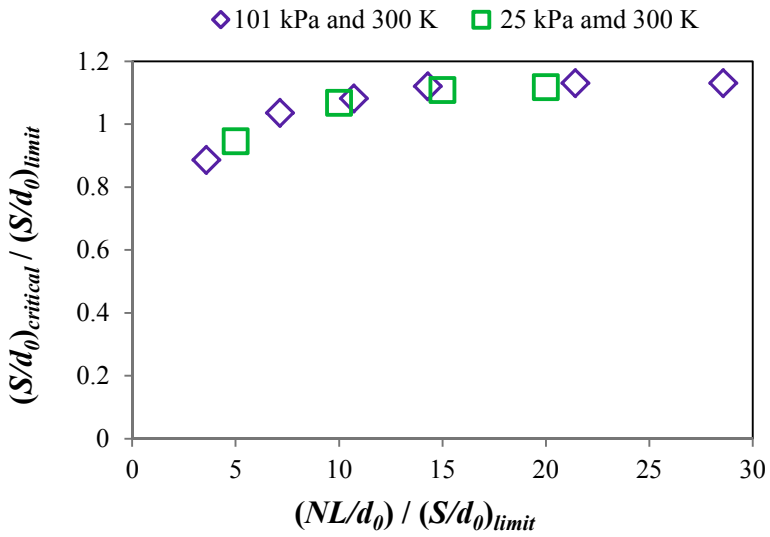

b. 3D droplet arrangement

Figure 3.30 The normalization analysis of data from the flame-spread simulation at normal pressure (101kPa) and low pressure (25kPa) for 2D and 3D droplet arrangements

3.3.2 Flame-spread behavior near the critical threshold mean droplet spacing

Figure 3.31 and 3.32 show examples of distribution of flame-spread on the lattice including the flame-spread time for 2D droplet arrangement and 3D droplet arrangement near the critical mean droplet spacing $(S/d_0)_{critical}$. This figure shows that the flame spread reaches all the sides of lattice in 2D droplet arrangement and all the surfaces of the lattice in 3D droplet arrangement and the group combustion excited. Even when the group combustion excited, a portion of the droplet remains unburned. This behavior is relevant with the real condition in spray condition engine that there is almost impossible to achieve the complete combustion or in other words that the incomplete combustion is much more common.

By the flame-spread time history in Fig. 3.31 and 3.32, we can see that the flame doesn't spread straightly from bottom side or surface of lattice to the upper side or surface of lattice, but flame spreads in complicated paths. This behavior is also shown the real condition of flame-spread in fuel spray combustion engine.

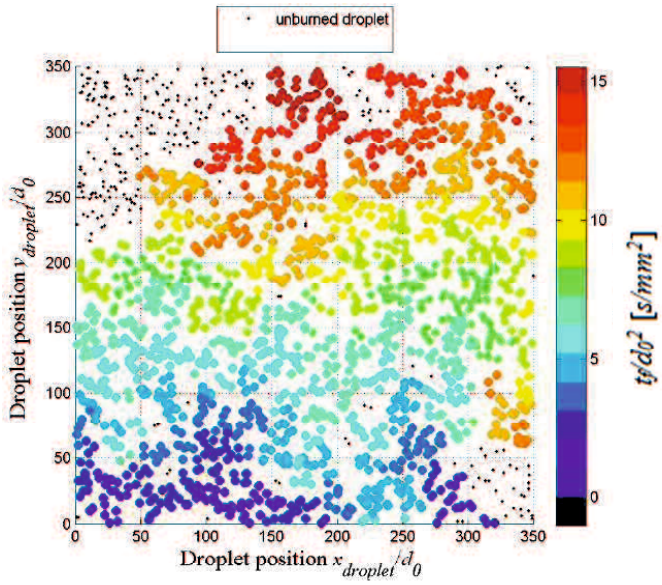

Figure 3.31 Flame-spread behaviors of ignition time at near critical threshold mean droplet spacing 2D droplet arrangement $(S/d_0)_{critical}$=16.1, NL/d_0= 700 and L/d_0=2

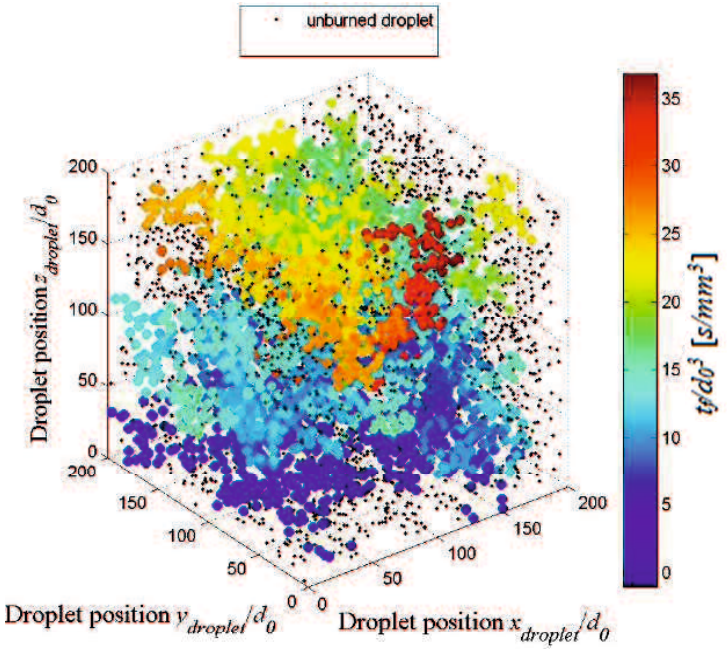

Figure 3.32 Flame-spread behaviors of ignition time at near critical threshold mean droplet spacing 3D droplet arrangement $(S/d_0)_{critical} = 22.3$, $NL/d_0 = 400$ and $L/d_0 = 2$

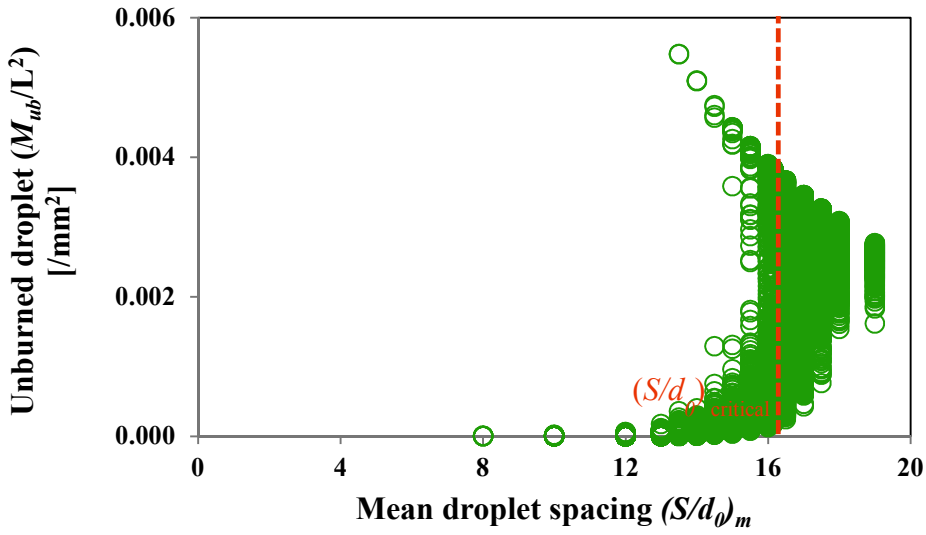

Figure 3.33 The unburned droplet on mean droplet spacing $(S/d_0)_m$ 2D droplet arrangement for $L/d_0 = 2$ and $NL/d_0 = 700$ flame-spread simulation at low pressure

In order to understand the portion of unburned droplet, we have observed the ratio between the number of unburned droplet (M_{ub}) and lattice area $(NL)^2$ for 2D droplet arrangement and the ratio between the number of unburned droplet (M_{ub}) with lattice volume $(NL)^3$ for 3D droplet arrangement. Therefore, we have the behavior of unburned droplet for each droplet arrangement per mm^2 or mm^3.

Figure 3.33 shows the unburned droplet (M_{ub}/L^2) on mean droplet spacing $(S/d_0)_m$ 2D droplet arrangement for L/d_0= 2 and NL/d_0= 700. From this figure, we know that for $(S/d_0)_m < 8$ flame spread to all the droplets on the lattice or group combustion always occurs, so there is no unburned droplet (M_{ub}/L^2) on the lattice. The unburned droplets (M_{ub}/L^2) appears start from $(S/d_0)_m$= 8 and increases with increasing mean droplet spacing. For $8 \leq (S/d_0)_m \leq 16.1$ the unburned droplet (M_{ub}) has a wide range of value and attains the maximum value near the critical mean droplet spacing. This is because for $8 \leq (S/d_0)_m \leq 16.1$ have two type of flame-spread i.e. flame can spread to all the side of lattice (group combustion occurs) and flame cannot spread to all the side of lattice (group combustion doesn't occurs). If the mean droplet spacing is increased after reach the critical mean droplet spacing $(S/d_0)_{critical}$, the number of unburned droplet (M_{ub}/L^2) shows the decreasing function. This is due to decreasing of the occurrences of group combustion on the lattice which has the large value of mean droplet spacing. Therefore, the number of unburned droplets attains maximum for the mean droplet spacing slightly greater than the critical mean droplet spacing.

In order to observes the effect of pressure condition in flame-spread behavior, Fig. 3.34 and 3.35 shows the flame spread behavior for $(S/d_0)_m$ which is between $(S/d_0)_{critical}$ flame-spread at room temperature and $(S/d_0)_{critical}$ flame-spread at high temperature. This figure is comparison between flame-spread at normal pressure and flame-spread at low pressure, wherein the simillar of droplet arrangement was simulated in role of flame-spread at normal pressure and at low pressure. In order to get the detail discription of comparison of both condition, we taken $(S/d_0)_m$ = 14 for 2D droplet arrangement and $(S/d_0)_m$ = 17.5 for 3D droplet arrangement.

While the mean droplet spacing $(S/d_0)_{\mathrm{m}}$ greater than $(S/d_0)_{critical}$, the flame-spread simulation at normal pressure shown that flame spread in complicated path but flame-spread terminates on its way to the sides or surface of lattice (Fig. 3.34a and 3.35a). However, the flame-spread can reach all the sides or surface of lattice and the group combustion exited when the simulation conducted at low pressure (Fig. 3.34b and 3.35b). When the droplet arrangement was simulated at low pressure the unburned droplet region decreases. This is because the flame-spread limit distance $(S/d_0)_{limit}$ increases when the flame spread at low pressure, as explained on the previous Chapter.

From the comparison results between flame-spread simulation at normal pressure and low pressure we know that pressure condition has affect the flame-spread behavior and group combustion excitation. This is due to the effect of local-flame spread limit distance, wherein the $(S/d_0)_{limit}$ at low pressure is higher than at normal pressure.

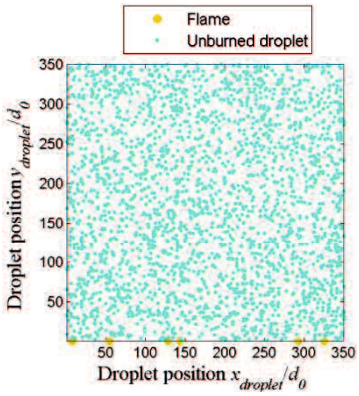

(a1). Elapsed time= 0 s/mm^2

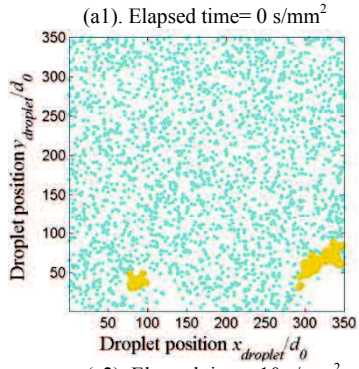

(a2). Elapsed time= 10 s/mm^2

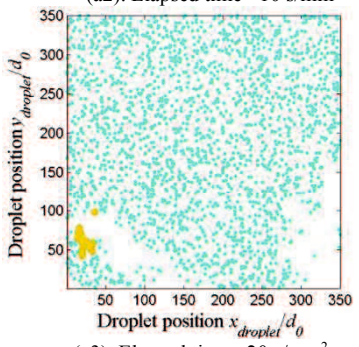

(a3). Elapsed time= 20 s/mm^2

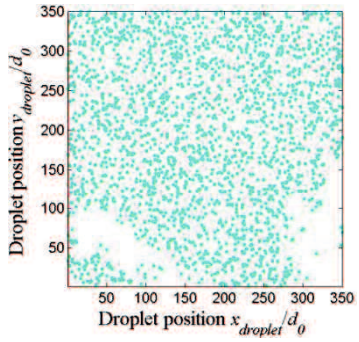

(a4). Elapsed time= 25 s/mm^2

a. Flame-spread simulation at normal pressure and room tempt. (300^{o}K)

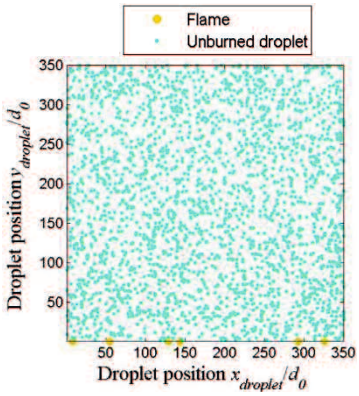

(b1). Elapsed time= 0 s/mm^2

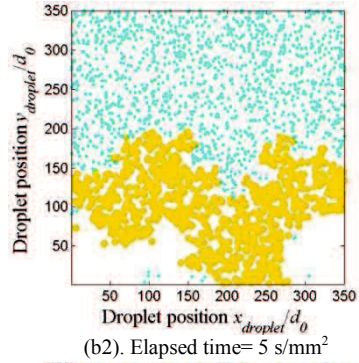

(b2). Elapsed time= 5 s/mm^2

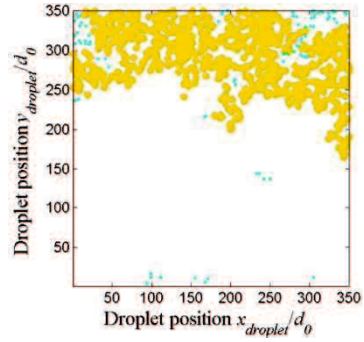

(b3). Elapsed time= 10 s/mm^2

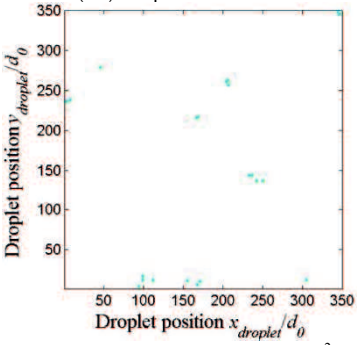

(b4). Elapsed time=16 s/mm^2

b. Flame-spread simulation at low pressure and normal tempt. (300^{o}K)

Figure 3.34 Flame-spread behavior in a 2-D droplet arrangement for $(S/d_0)_m$=14, which is between $(S/d_0)_{critical}$ flame-spread at normal pressure and $(S/d_0)_{critical}$ flame-spread at low pressure

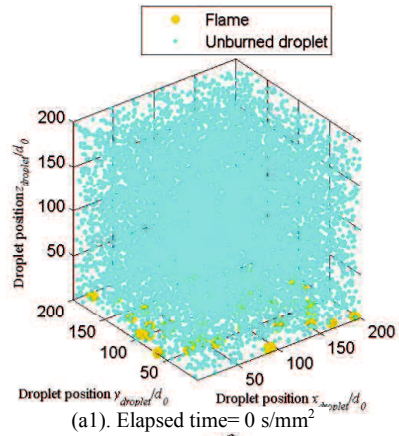

(a1). Elapsed time= 0 s/mm^2

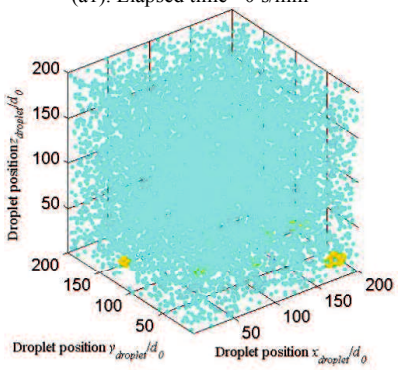

(a2). Elapsed time= 5 s/mm^2

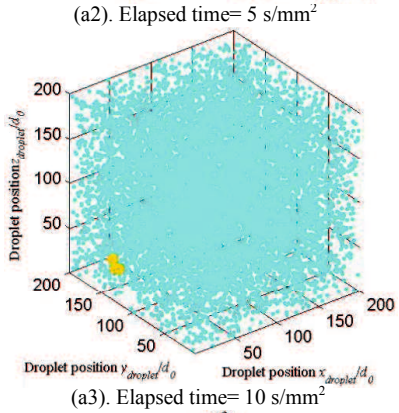

(a3). Elapsed time= 10 s/mm^2

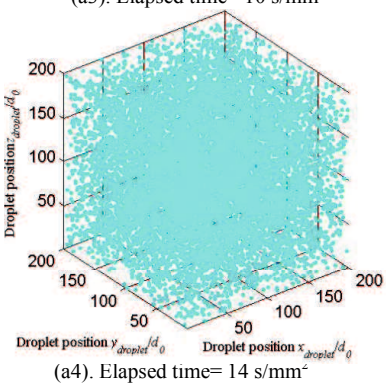

(a4). Elapsed time= 14 s/mm^2

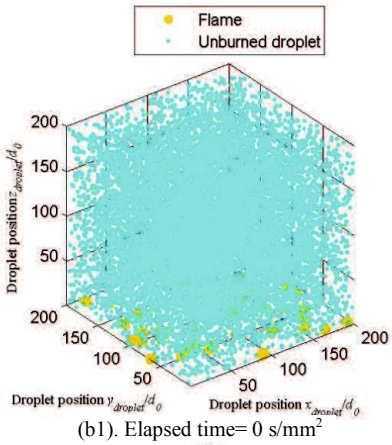

(b1). Elapsed time= 0 s/mm^2

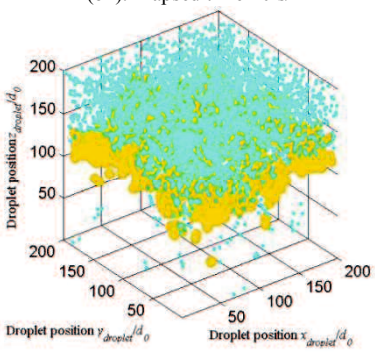

(b2). Elapsed time= 5 s/mm^2

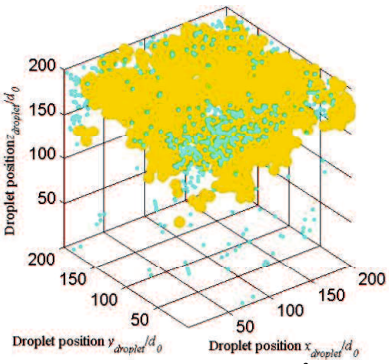

(b3). Elapsed time= 7 s/mm^2

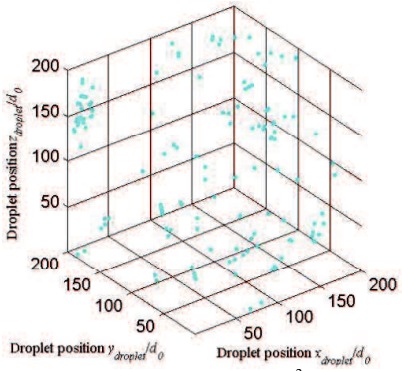

(b4). Elapsed time= 11 s/mm^2

a. Flame-spread simulation at normal pressure and room tempt. (300^{o}K)

b. Flame-spread simulation at low pressure and normal tempt. (300^{o}K)

Figure 3.35 Flame-spread behavior in a 3D droplet arrangement for $(S/d_0)_m$=17.5, which is between $(S/d_0)_{critical}$ flame-spread at normal pressure and $(S/d_0)_{critical}$ flame-spread at low pressure

3.3.3 Flame-spread rate

Figure 3.21 and 3.22 shows example of flame-spread behavior ignition time at critical threshold mean droplet spacing for L/d_0 = 2, 2D droplet arrangement and 3D droplet arrangement. The flame-spread time from bottom side or bottom face to all sides or faces of lattice doesn't spread straightly but spread in complicated path. This section compares the ignition time of last burned droplet [s/mm^2] and flame-spread rate [mm^2/s] between flame-spread simulation at room temperature and high temperature as shown in Fig. 3.36 and 3.37.

When the mean droplet spacing $(S/d_0)_m$ is small enough, the ignition time of last burned and flame-spread rate are almost constant. However, as the $(S/d_0)_m$ increases, the time ignition of last burned droplet is increases and the flame-spread rate is decreases. The ignition time of the last burned droplet has a wide range of values, and the averaged of ignition time attains maximum around the critical mean droplet spacing. Therefore, this is showing the characteristic time of flame spread in randomly distributed droplet cloud. Thus, the flame spread rate over the droplet cloud also has a wide range of values around the critical mean droplet spacing and the flame-spread rate reaches minimum around the critical mean droplet spacing.

The comparison shows that the ignition time of last burned droplet at low pressure is smaller than at normal pressure. Therefore, the flame-spread rate at low pressure is faster than at room temperature Fig. 3.36 and 3.37. This result is in line with the experimental results of Mikami et al., 2014 wherein the flame-spread rate at the low pressure are greater than those at atmospheric pressure.

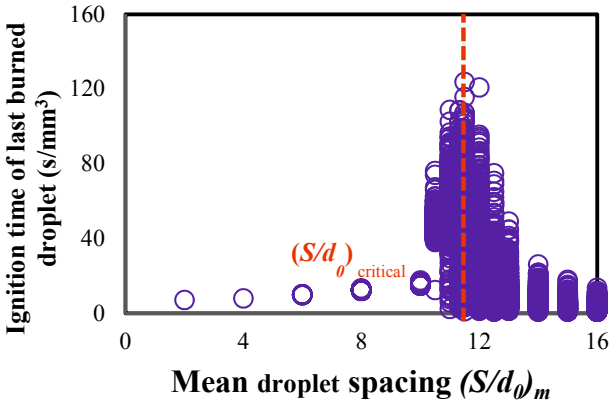

b. The ignition time of last burned droplet at normal pressure and room tempt. (300°K)

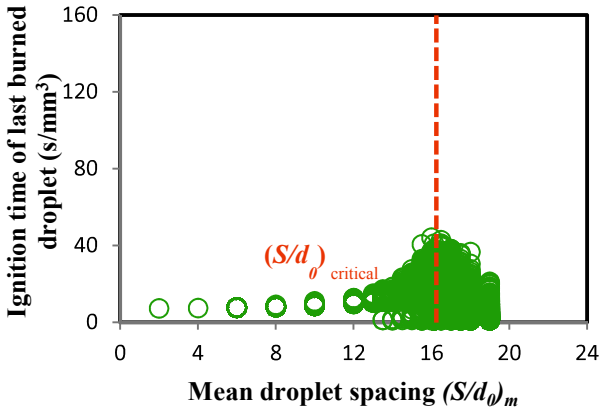

a. The ignition time of last burned droplet at low pressure and room tempt. (300°K)

Figure 3.36 The ignition time of last burned droplet on mean droplet spacing $(S/d_0)_m$ for flame-spread at normal pressure and low pressure 2D droplet arrangement

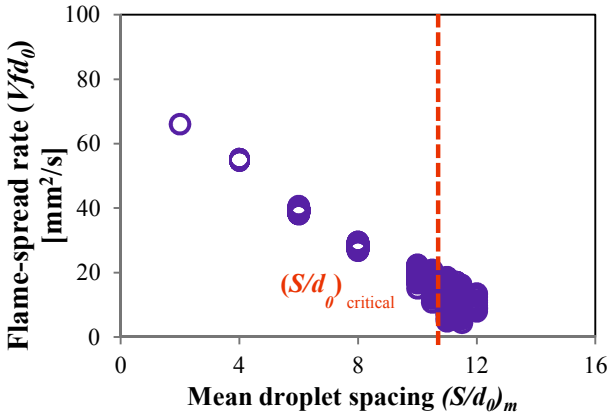

b. Flame-spread rate at normal pressure and room tempt. (300°K)

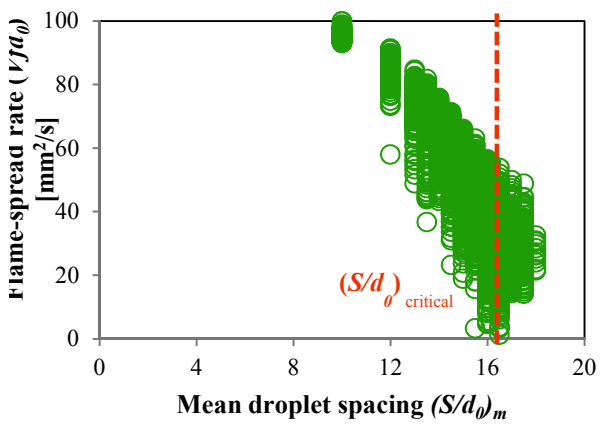

a. Flame-spread rate at low pressure and room tempt. (300°K)

Figure 3.37 The flame-spread rate on mean droplet spacing $(S/d_0)_m$ for flame-spread at normal pressure and low pressure 2D droplet arrangement

3.3.4 Summary

In this section we have discussed the comparison of flame-spread behavior at room temperature but different in pressure condition i.e. normal pressure (101kPa) and low pressure (25kPa). We conclude that the pressure condition has big effect on the flame-spread behavior and group combustion excitation, wherein the excitation of group combustion at low pressure is higher than at normal pressure. This is due to the effect of local-flame spread limit distance and flame-spread rate, wherein the $(S/d_0)_{limit}$ and flame-spread rate at low pressure is higher than at normal pressure.

Chapter 4

Simulating Flame-spread Behavior of Randomly Distributed Droplet Clouds with Considering Two-droplet Interaction

On the previous, chapter the flame-spread behavior and group combustion excitation has been discussed without considering droplet interaction. However, the latest microgravity experimental results shown that the interaction effect two adjacent droplet has significant effect to the flame-spread limit distance $(S/d_0)_{\text{limit}}$ (Oyagi et al., 2009 and Mikami et al., 2013).

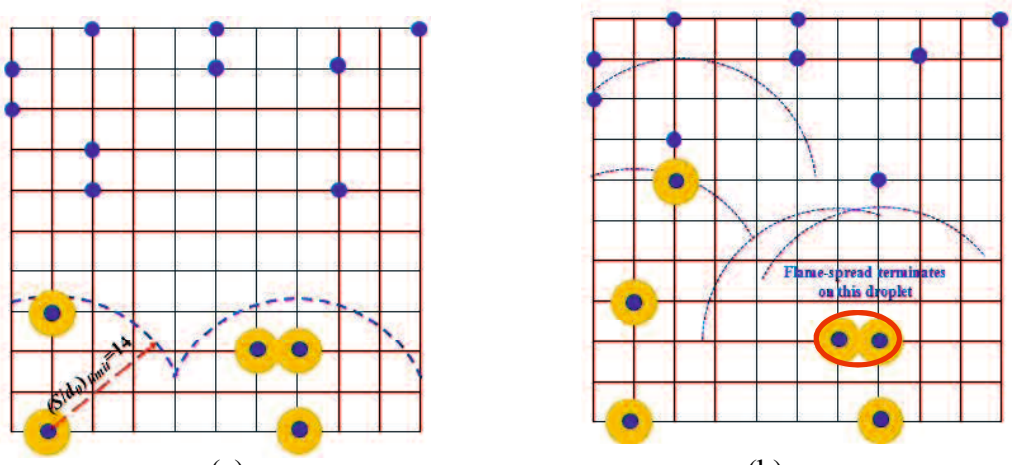

(a) (b)

Figure 4.1 Calculation procedure of flame-spread in randomly distributed droplet cloud without considering droplet interaction

As illustrated in Fig. 4.1 tell about the calculation procedure of flame-spread in randomly distributed droplet cloud without considering droplet interaction. This figure illustrates the flame spreads from a burning droplet to unburned droplets within the flame-spread limit distance. But the flame spread terminates on its way if there are not any droplets within the flame-spread limit distance. The circle in Fig. 4.1b shows the two-adjacent burning droplet. Due to the simulation without considering droplet interaction and existence of unburned

droplet within each of the flame-spread limit distance $(S/d_0)_{limit}$ =14, flame cannot spread to the next unburned droplet on the lattice. So the flame-spread terminate here. However, if the flame-spread simulations consider the droplet interaction effect, flame-spread limit distance become large or increases and the flame can continue spread to the next unburned droplet.

This study extends the previous percolation in Chapter 3 with considering the effect of two-droplet interaction on the flame-spread limit distance. In this chapter, the flame-spread behavior and group combustion excitation at normal pressure (101kPa) and room temperature (300^oK) is performed. The flame-spread limit distance and calculation procedure for simulation of flame-spread behavior with considering droplet interaction refers to the explanation on the Chapter 2.

4.1 Occurrence Probability of Group Combustion (OPGC)

Figure 4.2 shows dependence of the OPGC on the mean droplet spacing $(S/d_0)_m$ for L/d_0 = 2 and different NL/d_0 at 2D droplet arrangement and 3D droplet arrangement of flame-spread simulation with considering two-droplet interaction. If we compare Fig. 4.2 with Fig. 3.6, we can see that the effect of increasing mean droplet spacing to the OPGC between the simulation without and with considering two-droplet interaction has similar tendency, i.e. when the mean droplet spacing $(S/d_0)_m$ is increased, the OPGC rapidly decreases around a specific value of $(S/d_0)_m$ for each case. However, at the same value of mean droplet spacing $(S/d_0)_m$ the OPGC value of flame-spread simulation with considering two-droplet interaction is greater than that flame-spread simulation without considering two-droplet interaction. Therefore, the graph of OPGC versus mean droplet spacing $(S/d_0)_m$ for flame-spread simulation with considering two-droplet interaction shift to the right side from the graph of OPGC versus mean droplet spacing $(S/d_0)_m$ flame-spread simulation without considering two-droplet interaction, as shown in Fig. 4.3. This is because the local-flame-spread-limit distance with considering two–droplet interaction becomes larger. Thus, flame can continue to spread to the next unburned droplets.

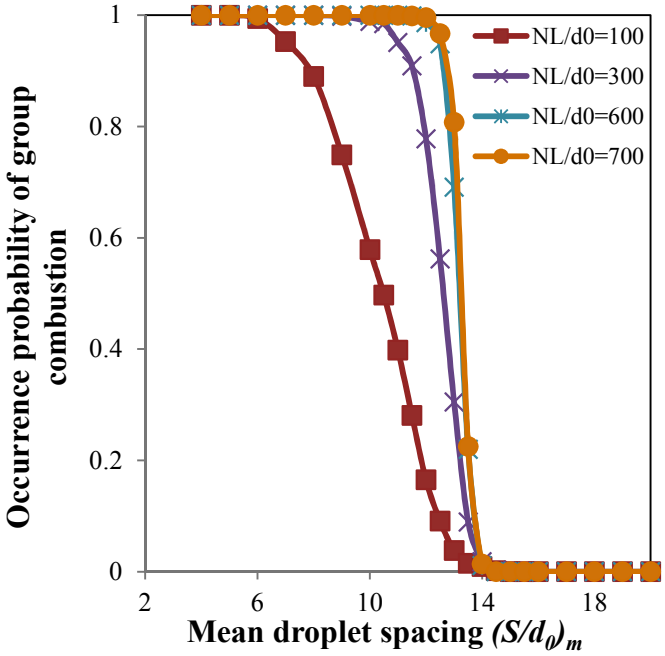

a. 2D droplet arrangement

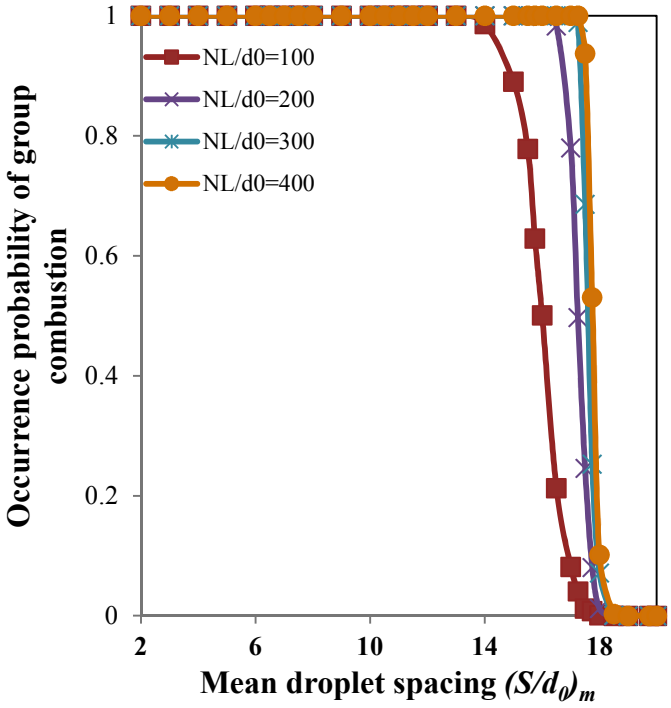

b. 3D droplet arrangement

Figure 4.2 Dependence of occurrence probability of group combustion (OPGC) on mean droplet spacing $(S/d_0)_m$ for $L/d_0 = 2$ and different lattice size (NL/d_0) flame-spread simulation with considering two-droplet interaction

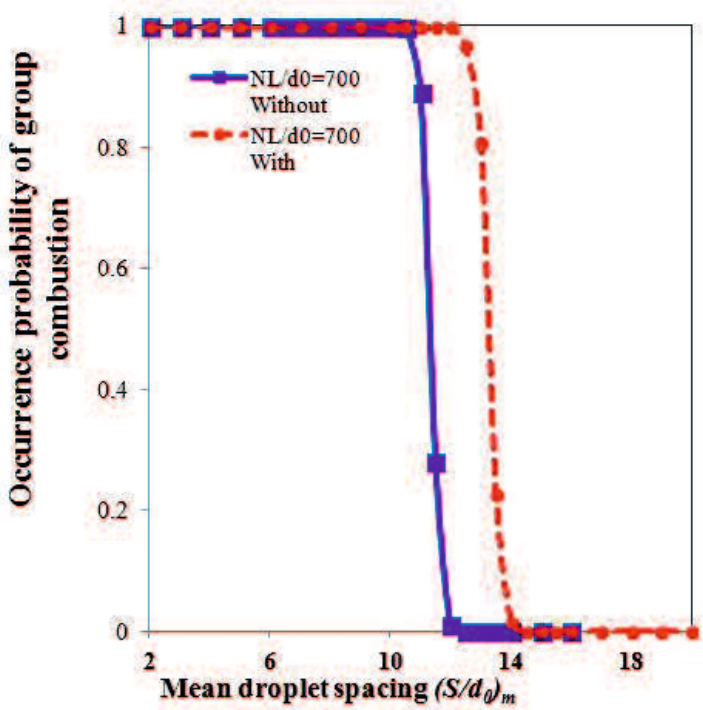

a. 2D droplet arrangement

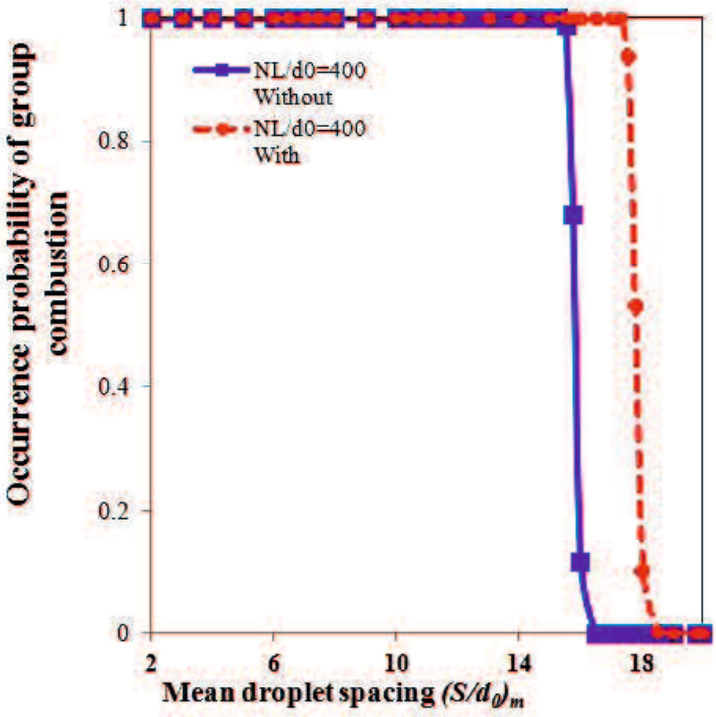

b. 3D droplet arrangement

Figure 4.3 The comparison of *OPGC* on mean droplet spacing $(S/d_0)_m$ between the flame-spread simulation without droplet interaction and with considering two-droplet interaction in 2D and 3D droplet arrangements

Same as the previous simulation, in order to predict the threshold value of $(S/d_0)_m$, we pay attention $(S/d_0)_m$ for 0.5 OPGC in which is defined as the critical mean droplet spacing $(S/d_0)_{critical}$. Figure 4.4 shows Dependences of critical mean droplet spacing $(S/d_0)_{critical}$ on lattice size NL/d_0 with considering two-droplet interaction at 2D and 3D droplet arrangements. This figure show that $(S/d_0)_{critical}$ increases with the increasing lattice size (NL/d_0) and also $(S/d_0)_{critical}$ decreases with decreasing lattice point interval (L/d_0).

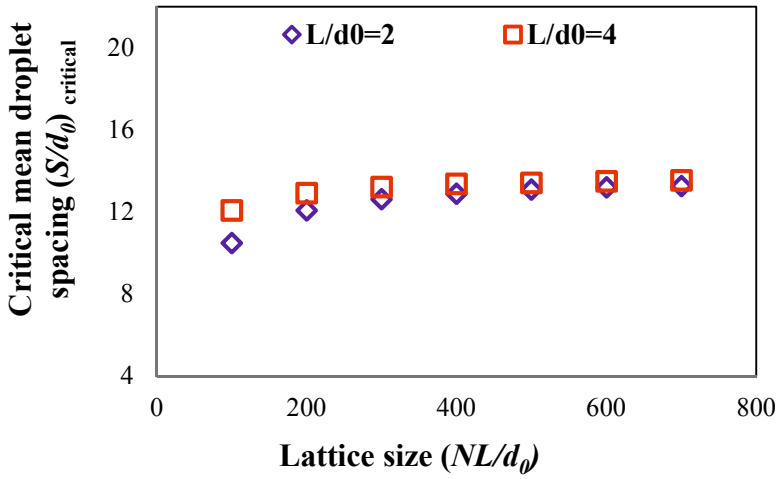

a. 2D droplet arrangement

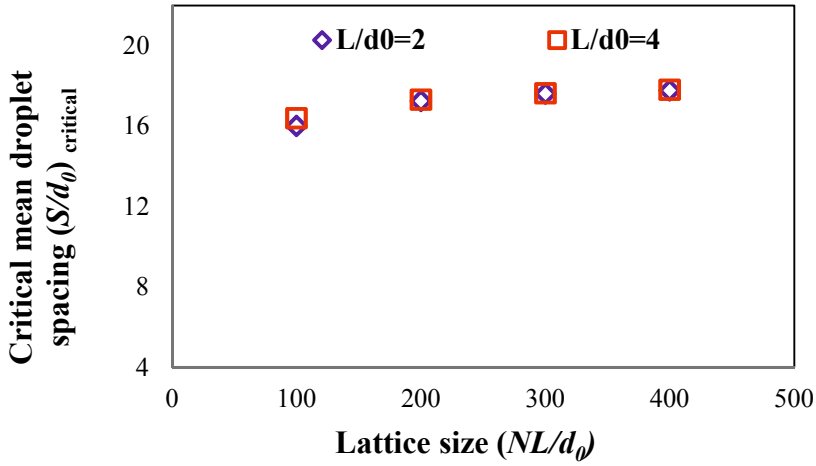

b. 3D droplet arrangement

Figure 4.4 Dependences of critical mean droplet spacing $(S/d_0)_{critical}$ on lattice size NL/d_0 with considering two-droplet interaction in 2D and 3D droplet arrangements.

Figure 4.2 and 4.3 shows that the threshold value of $(S/d_0)_m$ appears at lattice size (NL/d_0) = 700 for 2D droplet arrangement and NL/d_0 = 400 for 3D droplet arrangement. This is because at that position the graph of OPGC versus mean droplet spacing $(S/d_0)_m$ approach the step function. The lattice size ($NL/d0$) location of appearance of threshold value is similar as flame-spread simulation without considering two-droplet interaction However, the critical mean droplet spacing $(S/d_0)_{critical}$ of flame-spread simulation with considering two-droplet interaction is higher than that simulation without considering droplet interaction. The critical thresholds mean droplet spacing of flame-spread simulation considering two-droplet interaction is 13.3 for 2D droplet arrangement and 17.8 for 3D droplet arrangement. This means, when the flame spread with considering the effect of droplet interaction, the excitation of group combustion could be occurred in large of mean droplet spacing $(S/d_0)_m$ comparing without considering droplet interaction.

As shown in Fig. 4.5 when the lattice size (NL/d_0) is increased, the critical mean droplet spacing increases at the specific value of NL/d_0 and the increasing of $(S/d_0)_{critical}$ shown the constant tendency when the lattice size approach the threshold value. The flame-spread simulation without and with considering two-droplet interaction shown the similar phenomenon, but the critical mean droplet spacing $(S/d_0)_{critical}$ of flame-spread simulation with considering two-droplet interaction is greater than flame-spread simulation without considering two-droplet interaction.

Figure 4.5 also informed that the critical mean droplet spacing $(S/d_0)_{\text{critical}}$ with considering two-droplet interaction is higher than that without considering droplet interaction. If the critical mean droplet spacing $(S/d_0)_{\text{critical}}$ for NL/d_0 = 700 is compared in 2D droplet arrangement without considering droplet interaction, $(S/d_0)_{\text{critical}}$ is increased 1.943 by the two-droplet interaction. If $(S/d_0)_{\text{critical}}$ for NL/d_0 = 400 is compared in 3D droplet arrangement without considering droplet interaction, $(S/d_0)_{\text{critical}}$ is increased 1.938 by the two-droplet interaction. These results shows that the effect of droplet interaction on $(S/d_0)_{\text{critical}}$ is almost similar in both cases of 2D and 3D droplet arrangements.

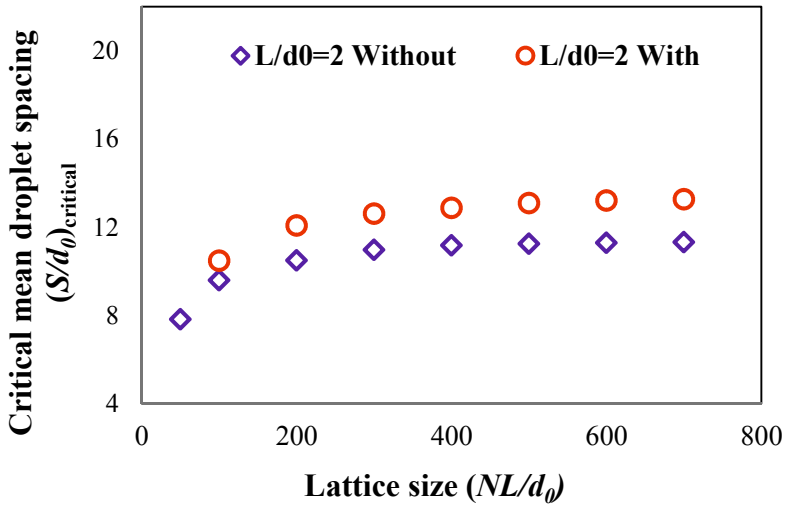

a. 2D droplet arrangement

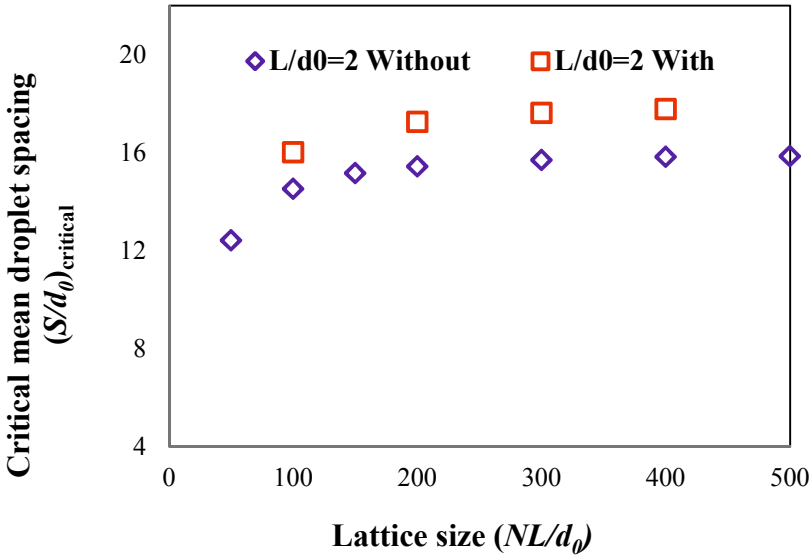

b. 3D droplet arrangement

Figure 4.5 Dependences of critical mean droplet spacing $(S/d_0)_{critical}$ on lattice size NL/d_0 without droplet interaction and with considering two-droplet interaction in 2D and 3D droplet arrangements

4.2 Flame-spread behavior near the critical threshold mean droplet spacing

When we used percolation approach, the location near the critical threshold mean droplet spacing is interesting to be explored. This is because the condition near the percolation threshold could be to guide understanding of real physical of flame-spread in large scale. The critical threshold mean droplet spacing separates the flame-spread behavior into group combustion is exited through flame spread and group combustion is never excited.

Figure 4.6 and 4.7 show examples of flame-spread distribution on the lattice, including the flame-spread ignition time for 2D droplet arrangement and 3D droplet arrangement near the critical mean droplet spacing $(S/d_0)_{critical}$. This figure shows that the group combustion occurs wherein the flame spread reaches all the sides of lattice at 2D droplet arrangement and all the surfaces of the lattice at 3D droplet arrangement. Even when the group combustion occurs, a portion of the droplet remains unburned. This behavior is relevant with the real condition of the spray combustion engine which is almost impossible to achieve the complete combustion or the incomplete combustion is much more common.

From the flame-spread ignition time history in Fig. 4.6 and 4.7, we can see that the flame doesn't spread straightly from bottom side or surface of lattice to the upper side or surface of lattice, but flame spreads in complicated paths. This behavior shows similarities with the real condition of flame-spread in fuel spray combustion engine.

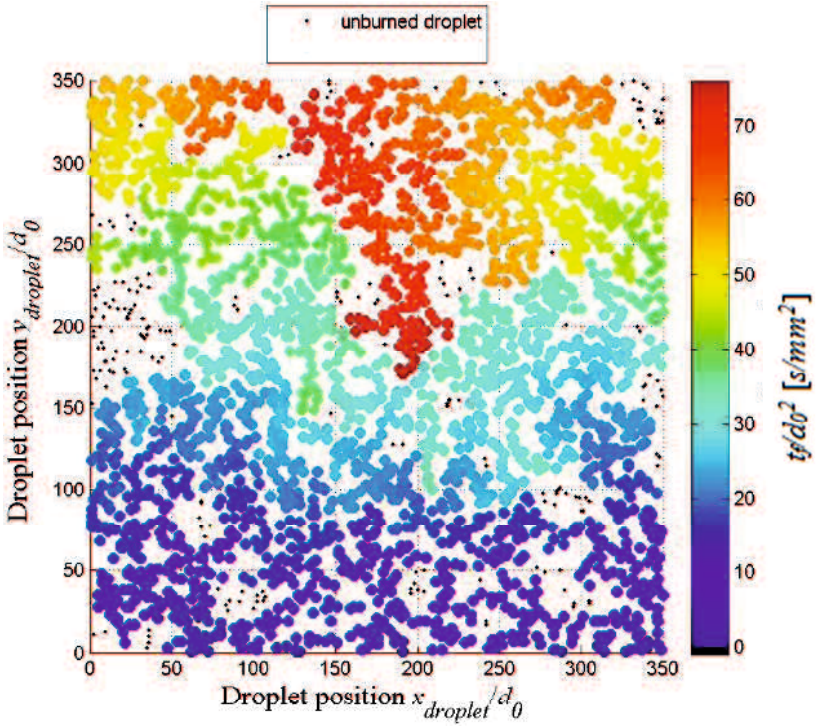

Figure 4.6 Flame-spread behaviors of ignition time at near critical threshold mean droplet spacing 2D droplet arrangement $(S/d_0)_{critical}$=13.3, NL/d_0 = 700 and L/d_0=2

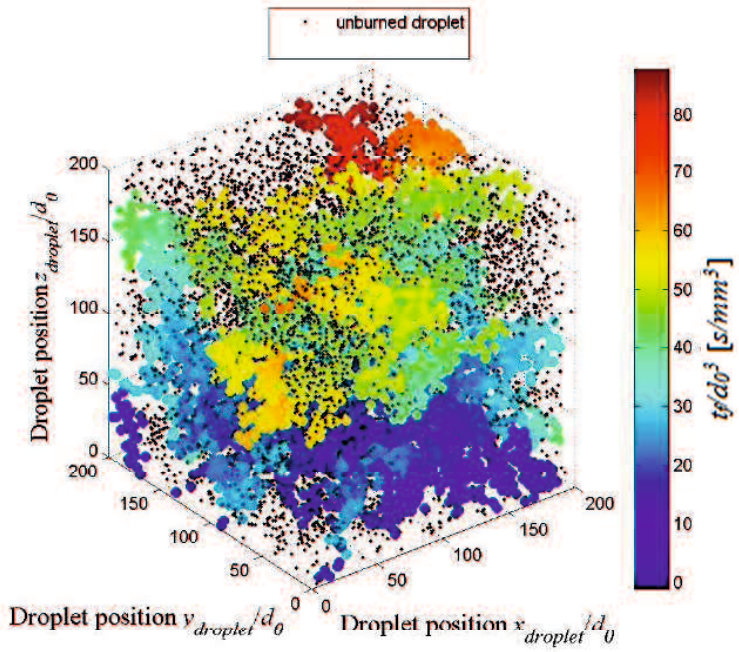

Figure 4.7 Flame-spread behaviors of ignition time at near critical threshold mean droplet spacing 3D droplet arrangement $(S/d_0)_{critical}$=17.7 , NL/d_0=400 and L/d_0=2

Figure 4.6 and 4.7 shows a portion of unburned droplet on the lattice even the group combustion excited. In order to understand the portion of unburned droplet, we have observed the ratio between the number of unburned droplet (M_{ub}) with lattice area $(NL)^2$ for 2D droplet arrangement or the ratio between the number of unburned droplet (M_{ub}) with lattice volume $(NL)^3$ for 3D droplet arrangement. Therefore, we have the behavior of unburned droplet for each droplet arrangement in each area (mm^2) or volume (mm^3).

Figure 4.8 shows the number of unburned droplet (M_{ub}/L^2) on the mean droplet spacing $(S/d_0)_m$ 2D droplet arrangement for $L/d_0 = 2$ and $NL/d_0 = 700$. From this figure, we can see that for $(S/d_0)_m < 8$ flame spread to all the droplets on the lattice or group combustion always occurs, there is no unburned droplet on the lattice. The number of unburned droplet (M_{ub}/L^2) appears start from $(S/d_0)_m = 8$ and increases with increasing mean droplet spacing. For $8 \leq (S/d_0)_m \leq 13.3$ the unburned droplet (M_{ub}/L^2) has a wide range of value. This is because for $8 \leq (S/d_0)_m \leq 13.3$ has two type of flame-spread i.e. flame can spread to all the side of lattice (group combustion occurs) and flame cannot spread to all the side of lattice (group combustion doesn't occurs). When the mean droplet spacing is increased after reach the critical mean droplet spacing $(S/d_0)_{critical}$, the number of unburned droplet (M_{ub}/L^2) shows the decreasing function. This is due to decreasing of the occurrences of group combustion on the lattice which has the large value of mean droplet spacing. Therefore, the number of unburned droplets attains maximum for the mean droplet spacing slightly greater than the critical mean droplet spacing.

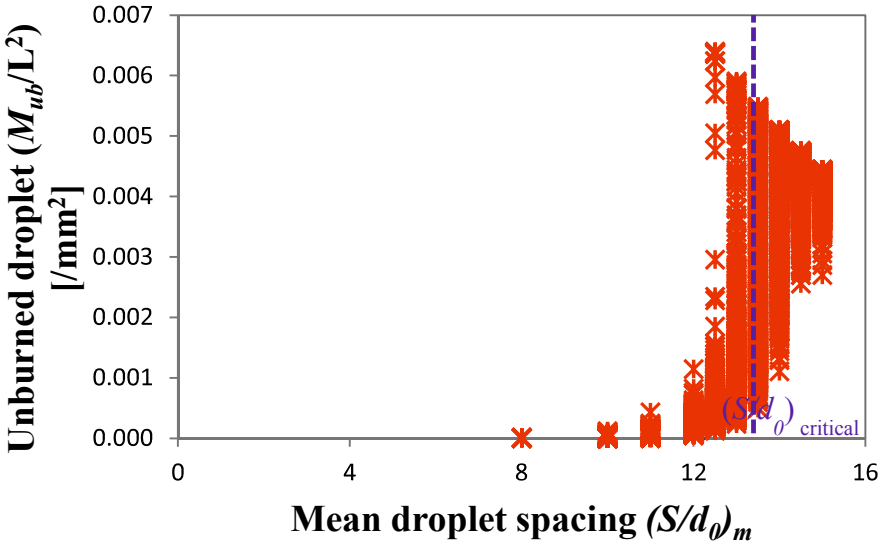

Figure 4.8 The unburned droplet on mean droplet spacing $(S/d_0)_m$ 2D droplet arrangement for L/d_0=2 and NL/d_0 = 700 flame-spread simulation with considering two-droplet interaction

From the comparison between Fig.3.13 and 4.8 we know that the unburned droplet region for flame-spread simulation with considering two-droplet interaction is lower than that flame-spread simulation without considering droplet interaction. These mean that if the flame-spread considering two-droplet interaction, the group combustion is exited even if the unburned droplet region is large.

In order to observes the effect of simulation with considering two-droplet interaction into flame-spread behavior, Fig. 4.9 and 4.10 shows the flame spread behavior for $(S/d_0)_m$ which is between $(S/d_0)_{\text{critical}}$ flame-spread without considering two-droplet interaction and $(S/d_0)_{critical}$ flame-spread with considering two-droplet interaction. This figure shows the comparison between flame-spread without considering droplet interaction and flame-spread with considering two-droplet interaction, wherein the simillar of droplet arrangement was simulated in role of flame-spread without considering droplet interaction and with considering two-droplet interaction. In order to get the detail discription of comparison of both

condition, we taken $(S/d_0)_m$ = 13 for 2D droplet arrangement and $(S/d_0)_m$ = 16.5 for 3D droplet arrangement.

When the mean droplet spacing $(S/d_0)_m$ greater than that $(S/d_0)_{critical}$, the flame-spread simulation without considering two-droplet interaction shown that flame spread in complicated path but flame-spread terminates on its way to the sides or surface of lattice (Fig. 4.9a and 4.10a). However, the flame-spread can reach all the sides or surface of lattice and after re-simulate with considering two-droplet interaction, the group combustion exited (Fig. 4.9b and 4.10b). When the droplet arrangement was simulated with considering two-droplet interaction the number unburned droplet region (M_{ub}/L^2) decreases and the group combustion exited. This is because, for droplets with small distance, the flame-spread limit distance $(S/d_0)_{limit}$ increases when the flame spread with considering two-droplet interaction.

From the comparison between flame-spread simulation without considering two-droplet interaction and with considering two-droplet interaction we know that interaction effect of two-adjacent burning droplets has big effect on the flame-spread behavior and group combustion excitation. This is due to the effect of local-flame spread limit distance, wherein the $(S/d_0)_{limit}$ at simulation with considering two-droplet interaction is higher than that at simulation without considering droplet interaction.

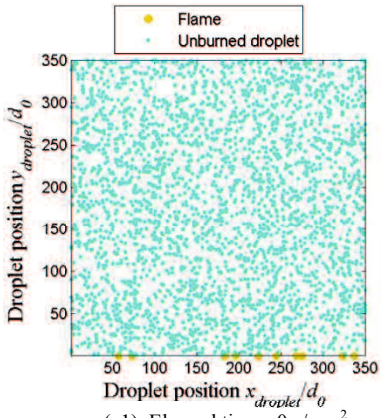

(a1). Elapsed time= 0 s/mm^2

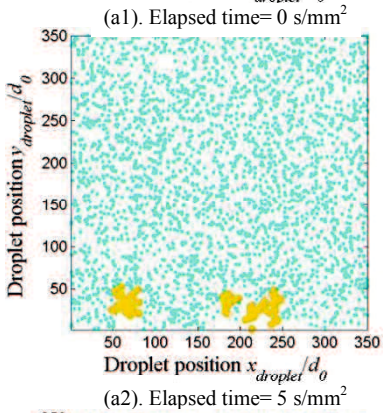

(a2). Elapsed time= 5 s/mm^2

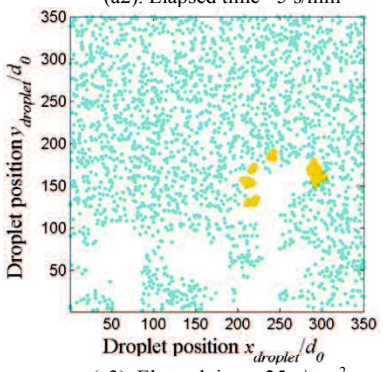

(a3). Elapsed time= 25 s/mm^2

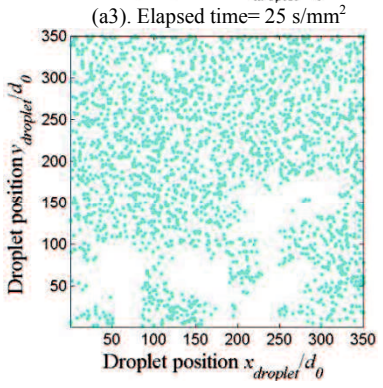

(a4). Elapsed time= 32 s/mm^2

a. Flame-spread simulation without considering droplet interaction

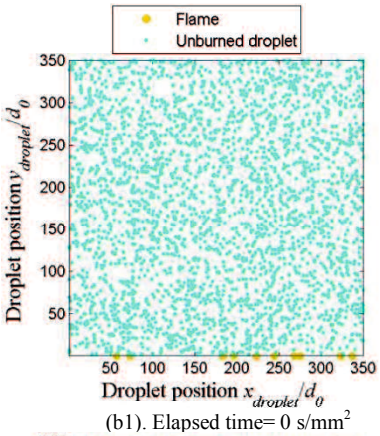

(b1). Elapsed time= 0 s/mm^2

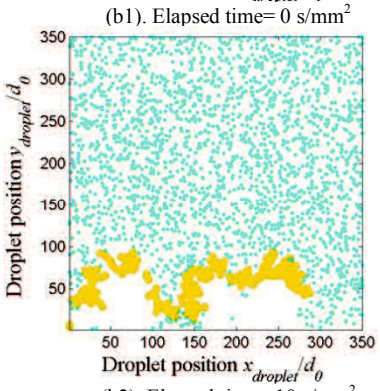

(b2). Elapsed time= 10 s/mm^2

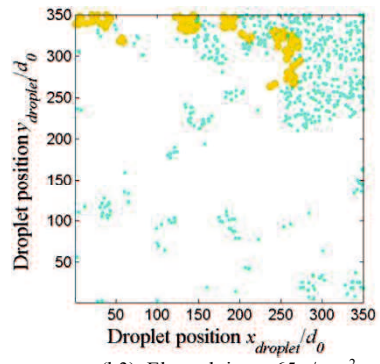

(b3). Elapsed time= 65 s/mm^2

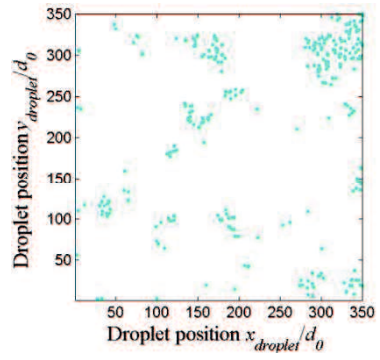

(b4). Elapsed time= 89 s/mm^2

b. Flame-spread simulation with considering two-droplet interaction

Figure 4.9 Flame-spread behavior in a 2-D droplet arrangement for $(S/d_0)_m$=13, which is between $(S/d_0)_{critical}$ without droplet interaction and $(S/d_0)_{critical}$ with two droplet interaction

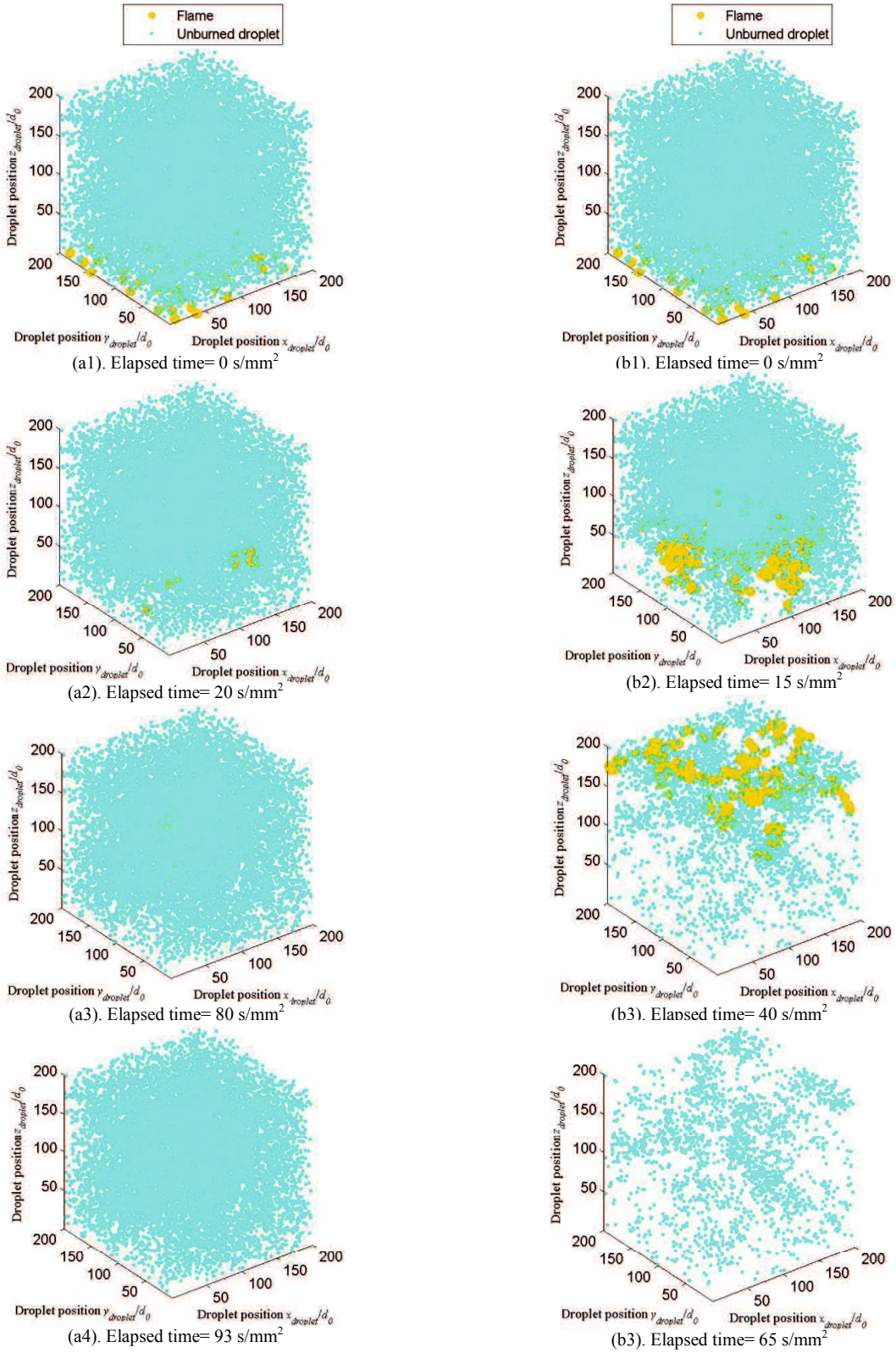

(a1). Elapsed time= 0 s/mm^2 (b1). Elapsed time= 0 s/mm^2

(a2). Elapsed time= 20 s/mm^2 (b2). Elapsed time= 15 s/mm^2

(a3). Elapsed time= 80 s/mm^2 (b3). Elapsed time= 40 s/mm^2

(a4). Elapsed time= 93 s/mm^2 (b3). Elapsed time= 65 s/mm^2

b. Flame-spread simulation without considering droplet interaction

a. Flame-spread simulation with considering two-droplet interaction

Figure 4.10 Flame-spread behavior in a 3-D droplet arrangement for $(S/d_0)_m$=16.5, which is between $(S/d_0)_{critical}$ without droplet interaction and $(S/d_0)_{critical}$ with two droplet interaction

4.3 Flame-spread rate

Figure 4.6 and 4.7 shows example of flame-spread behavior ignition time at near the critical mean droplet spacing for $L/d_0 = 2$, 2D droplet arrangement and 3D droplet arrangement. The flame-spread time from bottom side or bottom face to all sides or faces of lattice doesn't spread straightly but spread in complicated path. This section compares the ignition time of last burned droplet [s/mm^2] and flame-spread rate [mm^2/s] between flame-spread simulation at room temperature and high temperature as shown in Fig. 4.11 and 4.12.

When the mean droplet spacing $(S/d_0)_m$ is small enough, the ignition time of last burned and flame-spread rate are almost constant. However, as the $(S/d_0)_m$ increases, the ignition time of last burned droplet is increases and the flame-spread rate is decreases. The ignition time of the last burned droplet has a wide range of values, and the averaged of ignition time attains maximum around the critical mean droplet spacing. Therefore, this is showing the characteristic time of flame spread in randomly distributed droplet cloud. Thus, the flame spread rate over the droplet cloud also has a wide range of values around the critical mean droplet spacing and the flame-spread rate reaches minimum around the critical mean droplet spacing.

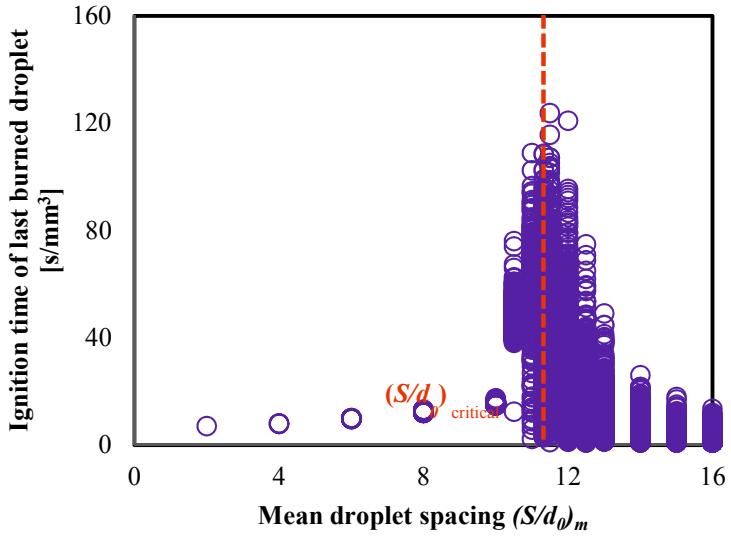

a. The ignition time of last burned droplet at normal pressure and room tempt. (300°K) without considering droplet interaction

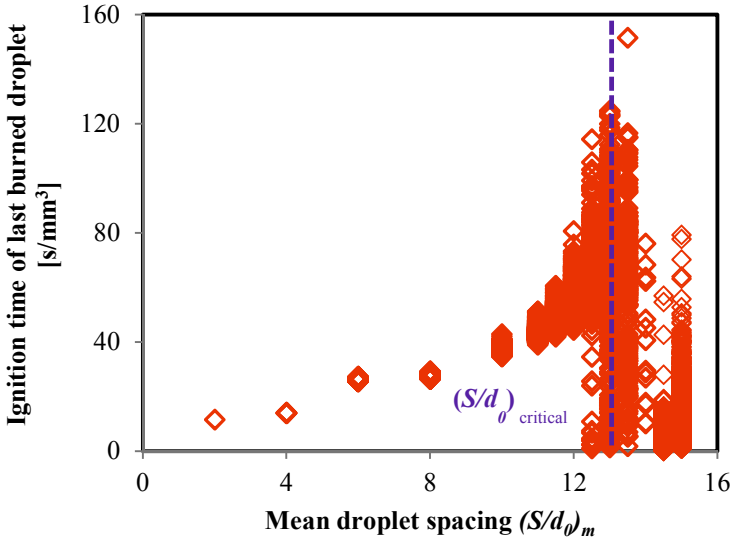

b. The ignition time of last burned droplet at normal pressure and room tempt. (300°K) with considering two-droplet interaction

Figure 4.11 The ignition time of last burned droplet on mean droplet spacing $(S/d_0)_m$ for flame-spread simulation without and with considering two-droplet interaction, 2D droplet arrangement

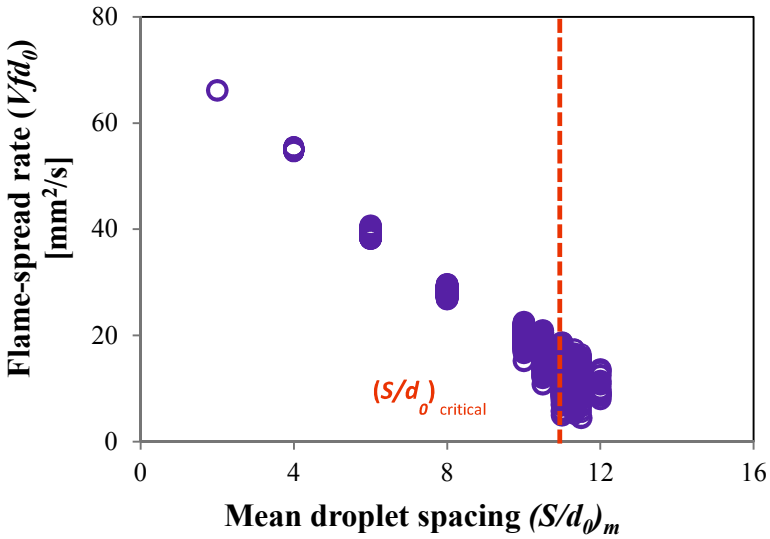

a. The flame-spread at normal pressure and room tempt. (300°K) without considering two-droplet interaction

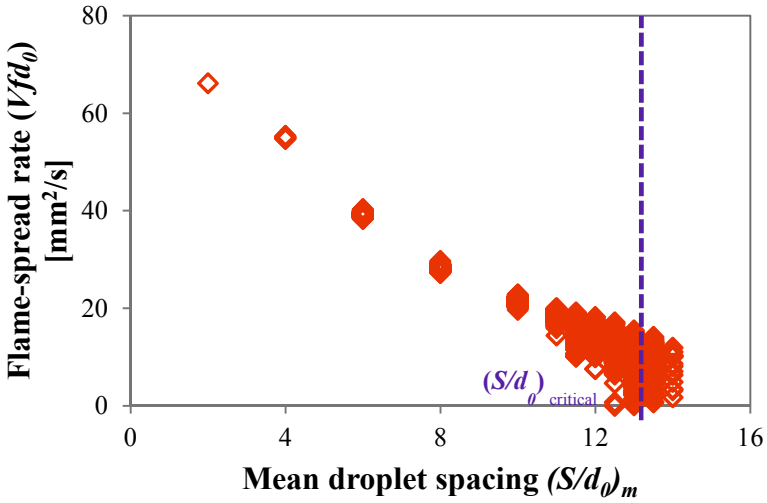

b. The flame-spread at normal pressure and room tempt. (300°K) with considering two-droplet interaction

Figure 4.13 The flame-spread rate on mean droplet spacing $(S/d_0)_m$ for flame-spread for flame-spread simulation without and with considering two-droplet interaction, 2D droplet arrangement

4.4 Summary

In this section we have discussed the comparison of flame-spread behavior without and with considering two-droplet interaction at normal pressure (101kPa) and room temperature (300K). We conclude that:

a. The interaction of two-adjacent burning droplet has big effect on the flame-spread behavior and group combustion excitation. Wherein the excitation of group combustion at flame-spread simulation with considering two-droplet interaction is greater than without considering two-droplet interaction. This is due to the effect of local-flame spread limit distance, wherein the $(S/d_0)_{limit}$ at flame-spread simulation with considering two-droplet interaction is higher than that without considering droplet interaction.

b. The critical mean droplets spacing $(S/d_0)_{\text{critical}}$ considering two-droplet interaction is greater than that without considering droplet interaction.

c. The effect of droplet interaction is almost similar in both cases of 2D and 3D droplet arrangements. In the case of 2D droplet arrangement, $(S/d_0)_{\text{critical}}$ is increased 1.9 by the droplet interaction and in the case of 3D droplet arrangement, $(S/d_0)_{\text{critical}}$ is increases 1.9.

d. The unburned droplet region for flame-spread simulation at lame-spread simulation with considering two-droplet interaction is lower than that lame-spread simulation without considering droplet interaction.

Chapter 5

Conclusions and Scope for Future Work

5.1 Conclusions

This study has simulated the flame-spread behavior in randomly distributed large-scale droplet clouds with a low-volatility fuel equal size droplets and group combustion excitation by using a percolation approach. This study created a percolation model based on so-called "Mode 3" flame-spread with paying attention to the flame-spread limit distance $(S/d_0)_{limit}$ which was obtained in microgravity experiment of flame-spread droplet array and droplet cloud element with n-decane as a fuel. The simulation applies a simple flame-spread rule that the flame can spread to droplets existing within the flame-spread limit distance $(S/d_0)_{limit}$, which varies with the flame-spread direction and droplet interaction. Therefore, the study is classified as follows: 1) Simulating flame-spread behavior of randomly distributed droplet clouds without considering droplet interaction. These simulations were created based on microgravity experimental results of evenly spaced droplet array. 2) Simulating flame-spread behavior of randomly distributed droplet clouds with considering two-droplet interaction. This simulation was created based on microgravity experiments of droplet-cloud elements.

The percolation theory describes macroscopic connection characteristics in randomly distributed particle cloud with near field connection rule. When the percolation theory is applied to fuel spray combustion, the droplet is characterized as the particle. The flame spread rule between droplets is characterized as the connection rule. Droplets are arranged at lattice points in two-dimensional (2D) lattice or three-dimensional (3D) lattice. The group combustion of droplet cloud is defined to appear if the flame starting from a side in 2D droplet arrangements and a face in 3D droplet arrangements reaches the other sides in 2D droplet arrangements and the other faces in 3D droplet arrangements. Mean droplet spacing $(S/d_0)_{\mathrm{m}}$ of droplet cloud, lattice size NL/d_0 and lattice point interval L/d_0

were varied in order to investigate their effects on the occurrence probability of group combustion (OPGC) and the flame-spread behavior in large-scale droplet clouds. $(S/d_0)_m$ for 0.5 OPGC is defined as the critical mean droplet spacing $(S/d_0)_{critical}$, which separates the droplet cloud into two groups if the lattice size becomes infinity; relatively dense droplet clouds in which the group combustion is excited through flame spread and dilute droplet clouds in which the group combustion is never excited.

The main conclusions of flame-spread simulation of randomly distributed droplet clouds without considering droplet interaction and with considering two-droplet interaction are as follows:

1. The occurrence probability of group combustion, OPGC, rapidly decreases around the critical mean droplet spacing $(S/d_0)_{critical}$ as the mean droplet spacing $(S/d_0)_m$ is increased. When the lattice size, NL/d_0, is increased, the OPGC graph approaches a step function in which OPGC is unity for $(S/d_0)_m$ less than the threshold value and zero for $(S/d_0)_m$ greater than the threshold value, and the critical mean droplet spacing $(S/d_0)_{critical}$ approaches the threshold value.
2. $(S/d_0)_{critical}$ is affected by the ambient temperature and pressure. $(S/d_0)_{critical}$ is greater at higher temperature and at lower pressure.
3. $(S/d_0)_{critical}$ in 3D droplet arrangement is greater than that in 2D droplet arrangement.
4. The $(S/d_0)_{critical}$ considering two-droplet interaction is higher than that without considering droplets interaction. The effect of two-droplet interaction on $(S/d_0)_{critical}$ in 2D droplet arrangements is almost similar to that in 3D droplet arrangements.
5. The ignition time of the last burned droplet has a wide range of values, and the averaged ignition time attains maximum around the critical mean droplet spacing, showing the characteristic time of flame spread in randomly distributed droplet cloud attains maximum. Thus, the flame spread rate over the droplet cloud also has a wide range of values around the critical mean droplet spacing.

6. Even when the group combustion occurs, a portion of the droplets remains unburned. The number of unburned droplets attains maximum for the mean droplet spacing slightly greater than the critical mean droplet spacing.

5.2 Scope for Future Work

While this dissertation has studied the simulation of flame-spread behavior of randomly distributed droplet clouds by using percolation approach without considering droplet interaction and with considering two-droplet interaction. There are many opportunities for extending the scope of this study. The followings present some of the scopes for future work:

a. In order to prove the simulation results, the experiment in large scale is necessary to be done. The experiments are going to be performed on the international space station in near future.

b. In this simulation we have simulated the flame-spread behavior and group combustion excitation by using the flame-spread limit of n-decane under negligible pre-vaporization condition. Therefore, for the future works it is necessary to simulate the flame-spread behavior with considering the pre-vaporization process.

c. In this simulation we assume that the droplet diameter is uniform or even droplet diameter. Therefore, for the future work it is important to simulate the flame-spread behavior in uneven droplet diameter.

References

Berkowitz, B. and Balberg, I., Percolation theory and its application to groundwater hydrology, Water Resources Research, Vol. 29, No.4 pp. 775-794, 1993.

Berkowitz, B. and Edwing, R.P., Percolation Theory and Network Modeling Applications in Soil Physics, Surveys in Geophysics, Vol. 19, No.1, pp. 23-72, 1998.

Broadbent, S.R. and Hammersley, J.M., Percolation processes, Mathematical Proceedings of the Cambridge Philosophical Society, Vol.53, No.3, pp. 629-641, 1957.

British Petroleum (BP), Digital libraries: BP annual report and form 20-F 2014, (online) available from <http://www.bp.com/content/dam/bp/pdf/investors/BP_Annual_Report_and_Form_20F_2014.pdf >, (accessed on 13 March 2015).

Chiu, H.H., Kim, H.Y. and Croke, E.J., Internal group combustion of liquid droplets, Proceedings of the Combustion Institute Vol. 19, No.1, pp. 971-980, 1982.

Faeth, G.M., Current status of droplet and liquid combustion, Progress in Energy and Combustion Science. Vol.3, No.4, pp. 191-224, 1977.

Hara, H. and Kumagai, S., The effect of initial diameter on free droplet combustion with spherical flame, Proceedings of the Combustion Institute, Vol.25, No.1, pp. 423-430, 1994.

Hunt, A.G., Percolation Theory for Flow in Porous Media, Springer, Berlin Heidelberg, 2005.

Imamura, O., Kubo, Y., Osaka, J., Sato, J., Tsue, M. and Kono, M., A study on single fuel droplets combustion in vertical direct current electric fields, Proceedings of the Combustion Institute, Vol. 30, No. 2, pp. 1949–1956, 2005.

Kato, S., Mizuno, H., Kobayashi, H. and Niioka, T., Experiment on Flame Spread of a Fuel Droplet Array in High-Pressure Ambience, JSME Int. J. B 41, pp. 322–330, 1998.

Kobayashi, H., Park, J. and Niioka, T., Microgravity Experiments on Flame Spread of an n-decane Droplet Array in A High-Pressure Environment, Proceedings of the Combustion Institute Vol. 29, pp. 2603-2610, 2002.

Kumagai, S. and Isoda, H., Combustion of Fuel Droplets in a Falling Chamber, Proceedings of the Sixth Symposium (International) on Combustion, Reinhold, N.Y., pp. 726-731, 1957.

Kumagi, S. and Isoda, H., New aspects of droplet combustion, Proceedings of the Combustion Institute, Vol. 7, No.1, pp. 523-531, 1958.

Kumagi, S., Sakai, T., Okajima, S. Combustion of free fuel droplets in a freely falling chamber, Proceedings of the Combustion Institute, Vol.13, No.1, pp. 779-785, 1971.

Law, C.K., Recent advances in droplet vaporization and combustion, Progress in Energy and Combustion Science, Vol.8, No.3, pp. 171-201, 1982.

Law, C.K. and Faeth, G.M., Opportunities and challenges of combustion in microgravity, Progress in Energy and Combustion Science. Vol.20, No.1, pp. 65-113, 1994.

Mikami, M., Kato, H., Sato, J. and Kono, M., Interactive Combustion of Two droplets in Microgravity, Proceedings of the Combustion Institute, Vol.25, No.1, pp. 431–438, 1994.

Mikami, M., Kono, M., Sato, J., and Dietrich, D.L., Interactive Effects In Two-droplet Combustion of Miscible Binary Fuel at High Pressure, Proceedings of the Combustion Institute, Vol.27, No.2, 2643–2649, 1998.

Mikami, M., Oyagi, H., Kojima, N., Wakashima, Y., Kikuchi, M., Yoda, S., Microgravity experiment on flame spread along fuel-droplet arrays at high temperature, Combustion and Flame, Vol. 146, No.3, pp. 391-406, 2006.

Mikami, M., Oyagi, H., Kojima, N., Kikuchi, M., Wakashima, Y. and Yoda, S., Microgravity experiment on flame spread along fuel-droplet array using a new droplet-generation technique, Combustion and Flame, Vol.141, No.3, pp. 241–252, 2005.

Mikami, M., Hirose, T., Watari, H., Seo, T., Moriue, O., and Kikuchi, M., Experimental study on flame spread of droplet-cloud elements with two-droplet interaction in microgravity, Proceedings of 25th European Conference on Liquid Atomization and Spray System (ILASS-Europe), 2013.

Mikami, M., Sano, N., Saputro, H., Watari, H. and Seo, T., Microgravity experiment of flame spread over droplets at low pressure, International Journal of Microgravity Science and Application, Vol.31, No.4, pp.172–178, 2014.

Miyasaka, K. and Law, C.K., Combustion of Strongly-Interacting Linear Droplet Arrays, Proceedings of the Combustion Institute, Vol. 18, pp. 283-292, 1981.

National Aeronautics and Space Administration (NASA), Digital libraries: NASA educational resources, (online) available from <http://www.nasa.gov/audience/foreducators/microgravity/multimedia/me-candleFlame.html#.VUfZZI6qqko>, (accessed on 3 March 2015).

Oyagi, H., Shigeno, H., Mikami, M., Kojima, N., Flame-spread probability and local interactive effect in randomly arranged fuel-droplet array in microgravity, Combustion and Flame, Vol. 156, No.4, pp. 763-770, 2009.

Sahimi, M., Applications of Percolation Theory, Taylor and Francis, 1994.

Sato, J., Tsue, M., Niwa, M. and Kono, M., Effects of Natural Convection on High-Pressure Droplet Combustion, Combustion and Flame, Vol. 82, No.2, pp. 142–150, 1990.

Sirignano, W.A., Advances in Droplet Array Combustion Theory and Modeling, Progress in Energy and Combustion Science, Vol.42, pp. 54-86, 2014.

Torquato, S. and Jiao, Y., Effect of dimensionality on the percolation threshold of overlapping nonspherical hyperparticles, Physical Review E, Vol. 87, No.2, pp. 1-39, 2013.

Umemura, A. and Takamori, S., Percolation theory for flame propagation in non- or less-volatile fuel spray: A conceptual analysis to group combustion excitation mechanism, Combustion and Flame, Vol. 141, No.4, pp. 336-349, 2005.

Williams, F.A., Droplet burning. In combustion experiments in zero-gravity laboratory, Progress in Aeronautics and Astronautics, Vol.73, 1981

Nomenclature

N	Number of lattice points on one side of lattice	[pcs]
M	Total droplet number in lattice	[pcs]
p	Occupation fraction	[-]
p_c	Percolation threshold	[-]
d_0	Initial droplet diameter	[mm]
L	Lattice point interval	[mm]
L/d_0	Lattice point interval	[-]
NL/d_0	Lattice size	[-]
$OPGC$	Occurrence probability of group combustion	[-]
S	Droplet spacing	[mm]
S/d_0	Droplet spacing	[-]
$(S/d_0)_m$	Mean droplet spacing	[-]
$(S/d_0)_{limit}$	Flame-spread limit distance	[-]
$(S/d_0)_{critical}$	Critical mean droplet spacing	[-]
t_f/d_0	flame-spread time	[s/mm^2]
$V_f d_0$	flame-spread rate	[mm^2/s]

Acknowledgements

In the name of Allah, the Most Gracious and the Most Merciful. Alhamdulillah, all praises to Allah for the strengths and His blessing in completing this thesis.

I am deeply grateful to my supervisor, Professor Masato Mikami, in Graduate School of Science and Engineering, Yamaguchi University, for his great inspiration, excellent guidance, deep thoughts and friendship during the course of my graduate studies. Without his consistent and helpful instruction, this thesis could not have reached its present form. Secondly, I would like to express my heartfelt gratitude to Associate Professor Takehiko Seo, in Graduate School of Science and Engineering, Yamaguchi University, who has helped me a lot in the past years.

This research was partly subsidized by JSPS KAKENHI Grant-in-Aid for Scientific Research (B) (24360350 and 15H04201).

Not forgotten, my appreciation to Ministry of Education and Culture of Republic of Indonesia, for his scholarship support through the Directorate of Higher Education Indonesia (DIKTI scholarship) cooperated with Sebelas Maret University.

I also would like to thanks to all members of Engine System Engineering Laboratory (ESEL), all Indonesian students, who gave me their help and time in discussing about anything and helping me work out my problems during my studies.

Lastly, very special thanks to my beloved parents, my dear wife, Laila Fitriana, my children, Razan Lauzai Muaddab and Rakan Lauzai Zuhair. Thanks for all the love, patience, prayers, and encouragement during the last three years.